UNITED STATES DEPARTMENT OF COMMERCE
DANIEL C. ROPER, Secretary
NATIONAL BUREAU OF STANDARDS
Lyman J. Briggs, Director

✦

# Journal of Research

## of the

## National Bureau of Standards

✦

Volume 19, Number 5
November 1937

[Published with approval of the Director of the Budget]

UNITED STATES
GOVERNMENT PRINTING OFFICE
WASHINGTON : 1937

For sale by the Superintendent of Documents, Washington, D. C. - - - - - - Price 25 cents
$2.50 per year on subscription

**The prices of the separate Research Papers appearing in this JOURNAL are given on the front cover page. If 100 or more copies of any separate are ordered, a discount of 25 percent is allowed. Those who desire copies of separate Research Papers should send their orders and remittances without delay to the Superintendent of Documents, U. S. Government Printing Office, Washington, D. C. This will aid him to determine the number of copies to be printed for sale. Research Papers are not printed from electrotypes, and usually no more reprints can be had when the first and only printing is exhausted.**

U. S. Department of Commerce National Bureau of Standards

RESEARCH PAPER RP1040

*Part of Journal of Research of the National Bureau of Standards, Volume 19, November 1937*

# IMPROVED CONTINUOUSLY VARIABLE SELF AND MUTUAL INDUCTOR

By Herbert B. Brooks and Arthur B. Lewis

**ABSTRACT**

The features to be desired in a continuously variable self and mutual inductor, and the extent to which a particular existing type of inductor meets these requirements are stated. The investigation here reported had as object the improvement of the design of this inductor.

Two new general theorems concerning a pair of mutually inductive coils are derived. They apply to coils of any form, capable of change of relative position. If the self inductance of the two coils in series has an upper value $L_u$ for a certain relative position and a lower value $L_l$ for a second relative position, and if either coil may be rewound with any desired number of turns without change of space factor, the first theorem states that the ratio $L_u/L_l$ will have its maximum value when the self inductances of the two coils are equal.

The second theorem relates to a quantity which is arbitrarily called the "characteristic time-constant" of the pair of coils for the given relative positions and is equal to $(L_u-L_l)/(R_1+R_2)$, where $R_1$ and $R_2$ are the resistances of the coils. This time-constant will have its maximum value when $R_1=R_2$.

When $L_1=L_2$ and $R_1=R_2$ the requirements for maximum $L_u/L_l$ and for maximum characteristic time-constant are satisfied. An added advantage of this set of conditions is that when the two coils are connected in parallel the value of the self inductance, for any given relative position of the coils, will be exactly one-fourth of the corresponding value for the series connection.

The procedure which was used in applying the new theorems to the design of an improved inductor and the performance of the finished instrument are given in detail.

## CONTENTS

| | | Page |
|---|---|---|
| I. | Introduction | 494 |
| | 1. Desirable features in a continuously variable inductor | 494 |
| | 2. Features of an existing type of continuously variable inductor | 494 |
| | 3. Features in which improvements were sought | 495 |
| II. | Theoretical basis for the improvements | 496 |
| | 1. Condition for optimum value of $L_u/L_l$ | 496 |
| | 2. Condition for optimum value of $(L_u-L_l)/(R_1+R_2)$ | 498 |
| | 3. Extension of range of self inductance downward by parallel connection of the two coil systems | 500 |
| III. | Basis of design of the improved inductor | 500 |
| | 1. Formula for the self inductance of a link-shaped coil | 500 |
| | 2. Relative dimensions of fixed coils and movable coils | 502 |
| | 3. Number of turns in each of the movable coils | 503 |
| | 4. Condition for equality of resistances of the two coil systems | 503 |
| | 5. Condition for equality of self inductances of the two coil systems | 504 |
| | 6. Calculation of the mutual inductance between the two coil systems | 507 |
| | 7. Experimental check of the linearity of the scale law | 509 |
| IV. | Design of coils for the new inductor | 511 |
| V. | Description of the new inductor | 513 |
| VI. | Performance of the new inductor | 513 |
| VII. | Conclusion | 515 |

# I. INTRODUCTION

## 1. DESIRABLE FEATURES IN A CONTINUOUSLY VARIABLE INDUCTOR

A satisfactory continuously variable self inductor should have (a) a large value of the ratio of the useful upper limiting value of self inductance $L_u$ to the useful lower limiting value $L_l$; (b) a large value of the useful upper limiting value of time-constant $L_u/R$ for the given mass of active material and the space occupied; (c) astaticism with respect to a uniform magnetic field produced by an external source; (d) a close approach to a linear scale law over nearly the whole scale; (e) a minimum dependence of the inductance on the frequency, over a considerable range of frequency. Because the continuous variation of the inductance is obtained by the relative motion of parts of the apparatus, with resulting wear, we may well add that the inductor should have (f) inherent compensation for the effect of wear of the bearing surfaces. Some of these requirements being antagonistic, the design of an inductor involves the inevitable compromises. For example, to satisfy requirements (a) and (b) it is necessary that the coils (or groups of coils) of which the relative motion effects the variation of inductance should be closely coupled at their extreme relative positions. This close coupling, however, introduces relatively large values of capacitance between turns, between layers, and between coils. The effective self inductance will therefore depend upon the frequency to a greater extent than would be the case in an inductor in which the individual turns and layers are more widely spaced and the individual coils are further apart, and which therefore will be inferior as regards requirements (a) and (b).

## 2. FEATURES OF AN EXISTING TYPE OF CONTINUOUSLY VARIABLE INDUCTOR

The variable self and mutual inductor devised by one of the authors[1] and F. C. Weaver is shown in cross section in figure 1. Figure 2 shows a plan view, to scale, of the two groups of link-shaped coils. This

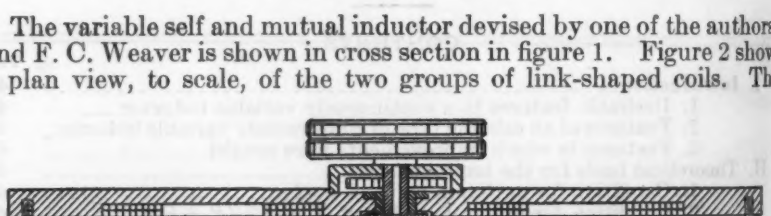

FIGURE 1.—*Cross-sectional view of variable self and mutual inductor.*

This illustration refers to the earlier form of variable inductor which it was the object of the present investigation to improve.

variable inductor meets requirements (a) and (b) by using interleaved groups of coils developed from Maxwell's circular coil of square cross section and maximum time-constant. It meets requirement (c) by having two like groups of fixed coils having opposite magnetic polarities and two like movable coils, also of opposite polarities. It meets

[1] H. B. Brooks and F. C. Weaver. BS Sci. Pap. **13**, 569 (1916-17) S290.

requirement (d) by having link-shaped coils of which the empirical proportions and relative positions are the result of extensive experiments. The interleaving which is necessary to meet requirements (a) and (b) also satisfies requirement (f) because a lowering of the movable-coil group as a result of wear of the step bearing increases the mutual inductance between the movable-coil group and the lower fixed coils by nearly the same amount that it decreases the mutual inductance between the movable-coil group and the upper fixed coils. This feature of construction also makes the inductance substantially inde-

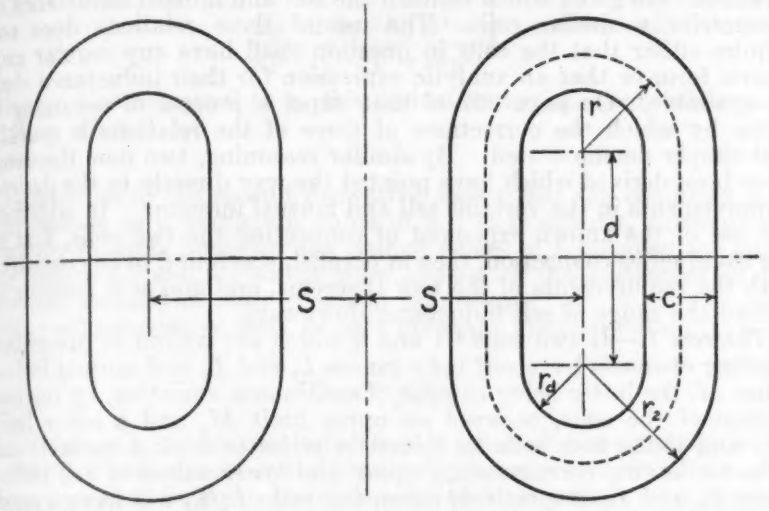


FIGURE 2.—*Plan view of the two groups of link-shaped coils used in the earlier form of variable inductor.*

pendent of warping of the movable plate, and is doubtless one of the principal reasons for the extensive use of inductors of this type during the 20 years since their introduction. Inductors of this type are preferably used on frequencies not exceeding 3,000 to 5,000 c/s, depending on the range of self inductance for which they are wound. Those for the higher ranges, having more turns per layer and more layers of wire, will show a greater change of inductance for a given change of frequency.

### 3. FEATURES IN WHICH IMPROVEMENTS WERE SOUGHT

A study of the question of possible improvements in the type of inductor just described led to the conclusion that requirements (c) to (f), inclusive, were probably satisfied as well as is possible without complication in construction. Urgent reasons, however, existed for an effort to meet requirements (a) and (b) to the greatest practicable extent.[2] As compared with adjustable rheostats, for example, these inductors are expensive, and, consequently, any improvement which will increase the ratio $L_u/L_l$ will reduce the number of inductors necessary for a given piece of work. Since the useful property of an

[2] Requirement (a) could be more fully met by a greater degree of interleaving of the fixed coils and the movable coils, but this would complicate and weaken the construction and increase the cost.

inductor is its inductance, and its undesirable (and often its limiting) property is its resistance, it was felt that any improvement in the time-constant would also be valuable.

## II. THEORETICAL BASIS FOR THE IMPROVEMENTS

### 1. CONDITION FOR OPTIMUM VALUE OF $L_u/L_l$

In a previous paper by one of the authors a number of general relations [3] are given which concern the self and mutual inductance of geometrically similar coils. The use of these relations does not require either that the coils in question shall have any regular geometric form or that an analytic expression for their inductance shall be available. On page 297 of that paper a process of reasoning is given by which the correctness of three of the relations is quickly and simply demonstrated. By similar reasoning, two new theorems have been derived which have pointed the way directly to the desired improvements in the variable self and mutual inductor. In addition, the use of the known expedient of connecting the two coils, first in the usual series connection, then in parallel, was found to be consistent with the requirements of the new theorems, and makes it possible to extend the range of self inductance downward.

*Theorem 1.*—If two coils [4] 1 and 2 which are wound in prescribed winding channels have self inductances $L_1$ and $L_2$ and mutual inductance $M$, the latter being capable of continuous variation, by relative motion of the coils, between an upper limit $M_u$ and a lower limit $M_l$; and if the two coils be joined in series to form a variable self inductor having corresponding upper and lower values of self inductance $L_u$ and $L_l$, respectively; then the ratio $L_u/L_l$ will have a maximum value when the channels are wound to make $L_1=L_2$.

In this theorem and in the one to follow it is assumed that the space factor of each coil is constant, regardless of the number of turns of wire in it, and hence that the time-constant of each coil is independent of the number of turns and depends solely on its geometric form, its absolute dimensions, the space factor, and the resistivity of the conducting material of the winding. The first theorem may be proved in the following manner:

The coupling coefficient $k$ is defined by the relation

$$k=M/(L_1L_2)^{\frac{1}{2}} \tag{1}$$

from which

$$M=k(L_1L_2)^{\frac{1}{2}} \tag{2}$$

For the two given limiting relative positions of the coils, denoted by the subscripts $u$ and $l$, the corresponding coefficients are $k_u$ and $k_l$. They depend on the geometry of the individual coils and their relative positions and are not altered by a change in the number of turns in either coil or in both coils if the change in the number of turns leaves unaltered the form of the coil and the distribution of the turns over its cross section.

---

[3] H. B. Brooks. BS J. Research 7, 296 (1931) RP342.

[4] Throughout this paper, for brevity, the word "coil" will be used to denote either a coil or a group of electrically and mechanically connected coils which function as a single coil.

If $L_2$ be denoted by $p^2L_1$, where $p^2$ is a coefficient as yet unknown, the ratio $L_u/L_l$, which may be denoted for brevity by $y$, may be written

$$y=\frac{L_1+p^2L_1+2k_upL_1}{L_1+p^2L_1+2k_lpL_1} \tag{3}$$

$$=\frac{1+p^2+2k_up}{1+p^2+2k_lp} \tag{4}$$

Differentiation gives the relation

$$\frac{dy}{dp}=\frac{2(k_l-k_u)(p^2-1)}{(1+p^2+2k_lp)^2} \tag{5}$$

Because $k_u$ is not equal to $k_l$, this derivative vanishes only when $p=1$, that is, when

$$L_1=L_2 \tag{6}$$

Examination of the second derivative shows that the condition $p=1$ corresponds to a maximum value of $y$. It is evident, furthermore, that the theorem holds for any pair of values of $L$ between the limiting values $L_u$ and $L_l$ which were chosen in the statement of the theorem because of their practical importance.

The substitution of $p=1$ in eq 4 gives the simple relation

$$y_{max}=\frac{1+k_u}{1+k_l} \tag{7}$$

If the change in the mutual inductance is accomplished either by rotating one coil 180° about a suitable axis of symmetry or by interchanging the connections between the coils so as to reverse their relative magnetic polarities, $k_l$ becomes $-k_u$ and eq 4 becomes

$$y'=\frac{1+p^2+2k_up}{1+p^2-2k_up} \tag{8}$$

which for the condition $L_1=L_2$, that is, $p=1$, assumes the simple form

$$y'_{max}=\frac{1+k_u}{1-k_u} \tag{9}$$

It is important to note that the closer the coupling between the coils the greater will be the relative loss in the ratio $L_u/L_l$ if the requirement that $L_1$ should be equal to $L_2$ is not fulfilled.

The requirement $L_1=L_2$ for $y_{max}$ imposes no restriction on the relative sizes of the two coils. It applies to any two winding channels, and requires only that the numbers of turns shall be such as to make the two self inductances equal. Consideration of eq 4 shows that a pair of coils, one large and having a relatively small number of turns, the other small and having a relatively large number of turns, would not constitute a good basis for the design of a variable inductor even if their inductances were equal because of the relatively small possible values of coupling coefficient. Theoretically, any pair of winding spaces, however dissimilar in their values of inductance for equal numbers of turns, could be wound to give any desired large value of self inductance of the pair of coils in series. Such an inductor might

be useful in cases where a relatively low time-constant is unobjectionable, but in general the design of any inductor should be such as to give the largest value of time-constant consistent with other requirements of the case. A study of this point led to the second general theorem.

## 2. CONDITION FOR OPTIMUM VALUE OF $(L_u-L_l)/(R_1+R_2)$

In a fixed standard of self inductance it is usually desirable that the resistance $R$ should be as low as possible in comparison with the inductance $L$, in other words, that the time-constant $\tau=L/R$ should be as large as possible, in order to minimize the weight and cost of the coil and the space occupied by it. For a variable inductor, several different values of time-constant may be defined, including the following:

$$\tau_u=L_u/(R_1+R_2) \tag{10}$$

$$\tau_l=L_l/(R_1+R_2) \tag{11}$$

and of course an infinite number of intermediate values for intermediate relative positions of the two coils. None of these, however, is suited for use as a criterion of the excellence of the design of a given system of coils and their relative positions. A characteristic which one strives to make as great as possible, however, is the ratio of the total change of self inductance $L_u-L_l$ to the resistance $R_1+R_2$ of the two coils in series. We may arbitrarily call this ratio the "characteristic time-constant" $\tau'$ of the set of coils; that is,

$$\tau'=(L_u-L_l)/(R_1+R_2) \tag{12}$$

The change $L_u-L_l$ defines the range of available values of self inductance, and is numerically equal to $2(M_u+M_l)$, where the $M$'s denote the values of mutual inductance for the limiting positions of the coils. An investigation to discover the conditions under which $\tau'$ will have a maximum value led to the second general theorem, as follows:

*Theorem 2.*—If two coils 1 and 2 which are wound in prescribed winding channels have self inductances $L_1$ and $L_2$, resistances $R_1$ and $R_2$, and mutual inductance $M$, the latter being capable of continuous variation, by relative motion of the coils, between an upper limit $M_u$ and a lower limit $M_l$; and if the two coils be joined in series to form a variable self inductor having corresponding upper and lower values of self inductance $L_u$ and $L_l$, respectively; then the characteristic time-constant $\tau'=(L_u-L_l)/(R_1+R_2)$ will have its maximum value when the channels are wound to make $R_1=R_2$.

It is assumed in this case, as in that of the first theorem, that the space factor of each of the coils is independent of the number of turns of wire in it, and hence that the time-constants $\tau_1$ and $\tau_2$ of the separate coils are also independent of the number of turns of wire in them. The theorem may be proved in the following manner:

The time-constants of the individual coils are

$$\tau_1=L_1/R_1$$
$$\tau_2=L_2/R_2 \tag{13}$$

from which

$$R_1 = L_1/\tau_1$$
$$R_2 = L_2/\tau_2 \tag{14}$$

and the characteristic time-constant of the system of coils, as defined, is

$$\tau' = (L_u - L_l)/\left(\frac{L_1}{\tau_1} + \frac{L_2}{\tau_2}\right) \tag{15}$$

If we denote $L_2$ by $p^2 L_1$, where $p^2$ is a coefficient as yet unknown, and the coupling coefficients for the two limiting positions by $k_u$ and $k_l$, eq 15 becomes

$$\tau' = \frac{L_1 + p^2 L_1 + 2k_u p L_1 - L_1 - p^2 L_1 - 2k_l p L_1}{\frac{L_1}{\tau_1} + \frac{p^2 L_1}{\tau_2}} \tag{16}$$

$$= \frac{2p(k_u - k_l)}{\frac{1}{\tau_1} + \frac{p^2}{\tau_2}} \tag{17}$$

The choice of definite winding channels and definite limiting positions of the coils, with the assumption that the space factor of each coil is independent of the size of wire in it, determines the values of $\tau_1$ and $\tau_2$ as well as of $k_u$ and $k_l$, leaving $p$ as the only independent variable in this equation. It remains to discover the value of $p$ for which $\tau'$ is a maximum. Differentiation of eq 17 gives

$$\frac{d\tau'}{dp} = 2(k_u - k_l)\frac{\frac{1}{\tau_1} - \frac{p^2}{\tau^2}}{\left(\frac{1}{\tau_1} + \frac{p^2}{\tau_2}\right)^2} \tag{18}$$

This vanishes only when

$$p^2 = \frac{\tau_2}{\tau_1} \tag{19}$$

that is, when

$$\frac{L_2}{L_1} = \frac{\tau_2}{\tau_1} = \frac{L_2}{R_2}\cdot\frac{R_1}{L_1} \tag{20}$$

that is, when

$$R_2 = R_1 \tag{21}$$

It should be noted that the separate attainment of each of the optimum conditions, $L_u/L_l$ a maximum, $(L_u - L_l)/(R_1 + R_2)$ a maximum, imposes no restrictions on the dimensions of either winding channel with respect to those of the other channel. This ceases to be true, however, when one requires that the system of coils shall satisfy *both* conditions; in which case

$$L_2 = L_1 \tag{22}$$
$$R_2 = R_1$$

and consequently

$$\tau_2 = \tau_1 = L_1/R_1 \tag{23}$$

To satisfy this condition, when the two coils are geometrically similar and their windings (of the same conducting material) have the same space factor, the two coils must have identical dimensions. If the coils are not geometrically similar, no simple general relation exists between their dimensions but it is obvious that in general the coils cannot differ greatly in size. It is also obvious that two coils differing greatly in size would have a relatively low value of coupling coefficient and therefore would be unsuitable also on this account for use as a variable self and mutual inductor.

### 3. EXTENSION OF RANGE OF SELF INDUCTANCE DOWNWARD BY PARALLEL CONNECTION OF THE TWO COIL SYSTEMS

When both of the preceding conditions for optimum values are satisfied, a third very desirable result immediately follows, provided the ratio of $L_u$ to $L_l$ is 4 or more. The usual connection of coils 1 and 2 in series gives a range of self inductance having upper and lower limits $L_u$ and $L_l$. The connection in parallel of two coils for which $L_1=L_2$ and $R_1=R_2$ in such a way that the instantaneous directions of the currents in the coils are the same as in the series connection, gives a range of self inductance having an upper limit $L_u/4$ and a lower limit $L_l/4$. For every relative position of the coils the inductance for the parallel connection will be exactly one-fourth of the corresponding value for the series connection. The range of self inductance is thus effectively from an upper limit $L_u$ to a lower limit $L_l/4$. The time-constant of the inductor, for any relative position of the coils, is the same for either method of connection.

If $L_u/L_l$ is less than 4, as may occur in variable inductors for frequencies high enough to intensify the effects of capacitance between coils and hence to require a greater separation of the coils, the full advantage of changing the connection from series to parallel cannot be realized because there will be a gap between the lower limit $L_l$ of the series arrangement and the upper limit $L_u/4$ of the parallel arrangement.

Inductors having the two coil systems equal in resistance and in inductance are regularly made by at least one American manufacturer. A similar method of extending the range of a variable inductor was used by Drysdale.[5] He made the movable system of two coils having equal self inductances and equal resistances; and similarly for the fixed system. This arrangement provides not only the two ranges of self inductance but also two ranges of mutual inductance, values for the lower range in each case being one-fourth of the corresponding values for the upper range.

## III. BASIS OF DESIGN OF THE IMPROVED INDUCTOR

### 1. FORMULA FOR THE SELF INDUCTANCE OF A LINK-SHAPED COIL

In designing link-shaped coils to meet the conditions laid down by the two theorems developed in section II it is necessary to use approximate formulas because no exact formula for the inductance of such

[5] Electrician 84, 108 (1920); H. Tinsley & Co. list 45 (April 1916).

coils is available. It is known, however, that to an accuracy of 1 or 2 percent the self inductance of a link-shaped coil of a given number of turns bears the same ratio to the self inductance of a circular coil having the same cross-sectional area, the same number of turns, and the same length of mean turn as the area inclosed by the mean turn of the link-shaped coil bears to the area inclosed by the mean turn of the circular coil.[6] For the coils used here this ratio is 0.83, so that we may take the self inductance of the link-shaped coil as equal to 0.83 times the self inductance of the equivalent circular coil, which latter is given conveniently and with sufficient accuracy by Maxwell's approximate formula.[7] We have, then, as an empirical formula which is sufficiently accurate for design purposes,

$$L_{\text{link}}=0.83\left[4\pi aN^2\left(-2+\log_e\frac{8a}{G}\right)\right] \tag{24}$$

where

$L_{\text{link}}$=self inductance of link-shaped coil in abhenries (millimicrohenries).

$a$=radius of the mean turn of the equivalent circular coil.
=length of the mean turn of the link-shaped coil, divided by $2\pi$.

$N$=number of turns.

$G$=geometric mean distance of the cross section of the winding channel.

It has been shown by Rosa and Grover[8] that

$$G=0.2235\ (b+c)\ \text{approximately} \tag{25}$$

where (see fig. 3)

$b$=axial depth of the coil.

$c$=radial width of the coil.[9]

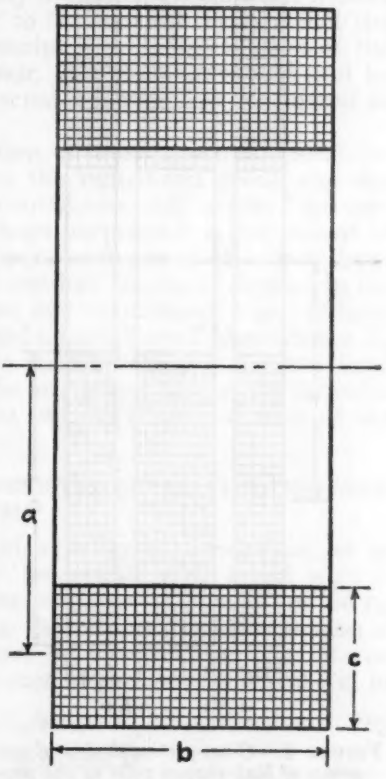


FIGURE 3.—*Cross-sectional view of circular coil of square cross section, to illustrate equation 25.*

[6] BS Sci. Pap. 13, 578 (1916-17) S290.
[7] Maxwell Elec. and Mag., 3d ed., 2, p. 345.
[8] BS Sci. Pap. 8, 168 (1916) S169.
[9] We have found, by actual computations by the two methods, that an equally good approximation to the inductance of a link-shaped coil can be obtained either by the use of eq 24 or by assuming that the inductance of the link-shaped coil is equal to the inductance of a rectangular coil of the same cross section and number of turns, the mean turn of the rectangular coil circumscribing the mean turn of the link-shaped coil. For the computation of the inductance of a rectangular coil we have used a formula given by Jeans, Math. Theory of Elec. and Mag., 5th ed., p. 446. While not as convenient for routine calculations as eq 24 given above, this rectangular formula is very useful in investigating the effects of various ratios of length to breadth, etc., on the inductance of a link-shaped coil.

## 2. RELATIVE DIMENSIONS OF FIXED COILS AND MOVABLE COILS

Figure 4 represents a cross-sectional view of two of the fixed coils and one of the movable coils of a variable inductor which consists of two coils which may be rotated between two equal pairs of fixed coils. It is obvious that if the self inductance of the two systems of coils is to have the optimum value for any given configuration, certain of their geometrical dimensions must be identical; that is, the fixed coils and the movable coils must be identical as to dimensions $c$, $r$, and $d$ (see fig. 2) and hence must have the same value of the equivalent radius $a$. As eq 24 indicates, the inductance of a coil is a function of the four variables, $N$, $a$, $b$, and $c$. In designing coils for a variable inductor we are at liberty to adjust these variables for one of the coil systems, say the movable system, almost at will. When the movable coils have been designed, however, the dimensions $a$ and $c$ for the fixed coils must be equal to the corresponding dimensions of the movable coils. We are therefore left with two variables, the axial depth $b_f$, of the fixed coil, and the number of turns, $N_f$, with which to satisfy the two conditions for optimum performance, namely, equality of inductance and equality of resistance.

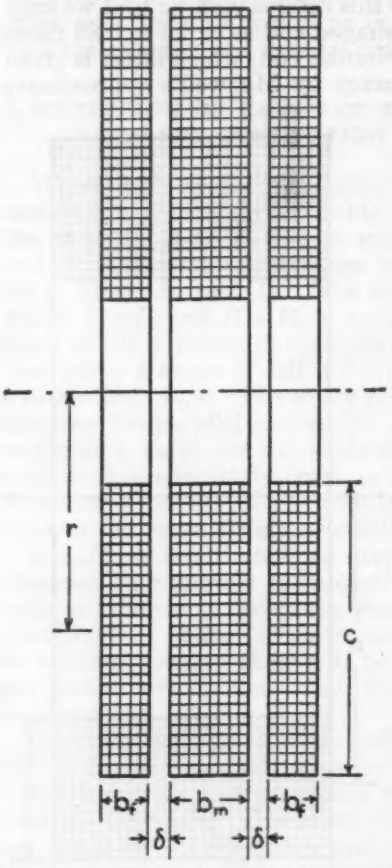


FIGURE 4.—*Cross-sectional view of one group of link-shaped coils of the proportions used in the improved inductor.*

The cross section is made by a plane whose trace is the horizontal center line in figure 2.

In designing an actual inductor we are not at liberty, however, to choose the dimensions even of the movable system entirely at will because the linearity of the scale law of an inductor constructed with link-shaped coils is very sensitive to the relative proportions of the coils.[10] It was felt desirable, therefore, that the relative proportions of the new coils should not depart too widely from those that had already been proved satisfactory. It was decided also that the movable coils of the new inductor should have substantially the same radius of mean turn and the same axial depth as the corresponding coils in inductors of the design then in commercial production.[11] Dimensions $d$, $r$, and $b_m$, see figures 2 and 4, were therefore left sub-

[10] BS Sci. Pap. 13, 572–575 (1916–17) S290.

[11] It should be noted that the absolute dimensions of the coils in the inductors as manufactured on the basis of the paper by Brooks and Weaver (BS Sci. Pap. 290) are not identical with those given in that article, in which, for example, $r$=36.8 mm. In the commercial model $r$=30.2 mm, and the other dimensions of the coils were such as to have relative proportions given in the paper.

stantially unchanged. It was proposed to increase the radial width, $c$, of the system by a slight amount, to be experimentally determined, to give a greater coupling coefficient between the fixed system and the movable system and consequently a greater range between $L_u$ and $L_l$.

### 3. NUMBER OF TURNS IN EACH OF THE MOVABLE COILS

With the equivalent radius $a$ and the dimension $b_m$ (fig. 4) fixed as has just been explained, and with provisional values chosen for $c$ and for the number of turns $N_m$ in one of the movable coils, we are in position to calculate $L_m$ with the aid of eq 24. Tentatively, therefore, each of the movable coils is completely determined. In what follows the subscripts $m$, $F$, and $f$ will refer to the movable system and the fixed system respectively. The subscript $f$ will refer to each of the separate fixed coils constituting a pair, and the subscript $F$ will be applied to a pair of fixed coils connected in series and considered as a unit.

With the coil systems in the position of maximum inductance the effect of mutual inductance between the right-hand group and the left-hand group of coils (see fig. 1) contributes only about 3 percent to the total self inductance. For design purposes it is convenient to neglect this contribution and to compute each group of coils to have a maximum self inductance equal to one-half the value desired in the complete inductor.[12] On this basis we have to consider a pair of fixed coils in series, of total resistance $R_F$, and a movable coil of resistance $R_m$ which is to be equal to $R_F$, while the inductance $L_F$ of the two fixed coils in series is to be equal to $L_m$, the self inductance of the movable coil. The symbol $L_f$ will denote the self inductance of each of the two fixed coils separately.

### 4. CONDITION FOR EQUALITY OF RESISTANCES OF THE TWO COIL SYSTEMS

Taking up first the requirement of equality of resistances, let us assume that the movable coil is to be wound with round wire of resistivity $\rho$. Let the diameter of the wire over the insulation be $x_m$, and the space factor be $s$; that is, $s$ is the ratio of the cross section of the conductor to the area of the square which circumscribes the wire over the insulation. Then the resistance of each movable coil will be

$$R_m = 2\pi a\rho(N_m/sx^2{}_m) \tag{26}$$

Also, the number of turns in the movable coil is

$$N_m = b_m c/x^2{}_m \tag{27}$$

from which

$$x_m = (b_m c/N_m)^{\frac{1}{2}} \tag{28}$$

and

$$R_m = 2\pi a\rho(N_m{}^2/sb_m c) \tag{29}$$

Similarly, the resistance of the two fixed coils in series is

$$R_F = 2\pi a\rho(2N_f{}^2/sb_f c) \tag{30}$$

in which $N_f$ is the number of turns in each of the two equal fixed coils.

[12] This true maximum value of self inductance, which is for the case of each movable coil coaxial with its fixed coils and with the magnetic fluxes additive, should be distinguished from the *useful* upper limit of self inductance $L_u$ above which the manner of variation of the inductance with angular position ceases to be approximately linear. In the inductor described later in this paper the ratio $L_u/L_l$ is about 8 percent lower than $L_{max}/L_{min}$. $L_u$, $L_l$, $L_{max}$, and $L_{min}$ refer to relative angular positions of the coils of 175, 5, 180, and 0°. This 8 percent difference should be taken into account in the design of inductors of this type.

It is assumed that the space factor $s$ is the same for all the coils. Then since the coils are to be wound so that $R_f = R_m$, it follows that

$$N_f = N_m(b_f/2b_m)^{\frac{1}{2}} \tag{31}$$

## 5. CONDITION FOR EQUALITY OF SELF INDUCTANCES OF THE TWO COIL SYSTEMS

The conditions for equality of the self inductances of the movable coil and of the pair of fixed coils are not determined so simply. The self inductance $L_F$ of the pair of fixed coils consists of the sum of the equal self inductances $L_f$ and $L_f$ of the separate coils plus twice the mutual inductance between them, and may be determined by the device of imagining an intermediate fictitious coil $\phi$, wound with wire of the same size (over the insulation) as that used for the two fixed coils and connected in series with them so as to form a coil (see fig. 5) whose cross section has a radial width $c$ and an axial depth equal to the sum of $b_m$, $2b_f$, and twice the axial clearance $\delta$ between the fixed coils and the movable coil. Let the self inductance of the fictitious coil be denoted by $L_\phi$. Let $L_{f,\phi,f}$ denote the self inductance of the large coil composed of the two fixed coils in series with the fictitious coil, and $L_{f,\phi}$ the self inductance of a coil composed of the fictitious coil and either of the two fixed coils. It may be shown [13] that the self inductance of the two fixed coils in series is

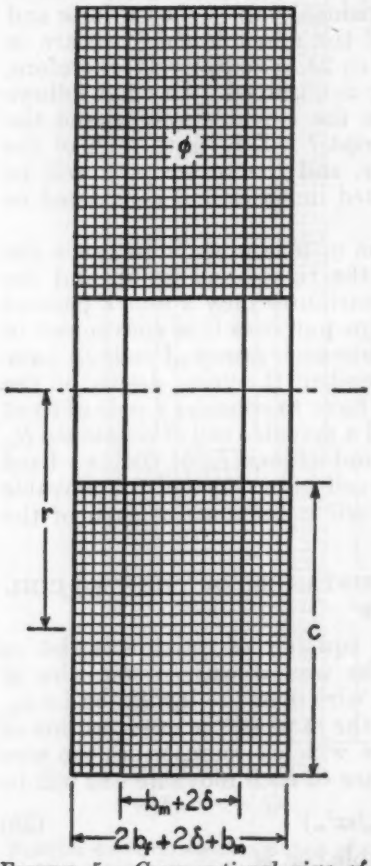


FIGURE 5.—*Cross-sectional view of two fixed coils and a fictitious coil* $\phi$.

The fictitious coil is assumed to fill completely the space between the fixed coils, and to have the same number of conductors per unit of area of cross section as the latter. The assumption of such a fictitious coil is a mathematical expedient to facilitate the computation of the mutual inductance between the fixed coils.

$$L_F = L_{f,\phi,f} + 2L_f + L_\phi - 2L_{f,\phi} \tag{32}$$

The four terms on the right in this expression are to be computed with the aid of eq 24.

In order that this formula shall apply, it is necessary to assume the same wire diameter over the insulation (and therefore the same number of turns per square centimeter of the cross section of the winding) for the fictitious coil as for the fixed coils. The number of turns in the fictitious coil (see fig. 5) will thus be

$$N_\phi = \frac{(b_m+2\delta)c}{b_f c} N_f = \frac{b_m+2\delta}{b_f} N_f \tag{33}$$

[13] BS Sci. Pap. 8, 41 (1912) S169.

We already have the relation

$$N_f = N_m(b_f/2b_m)^{\frac{1}{2}} \tag{31}$$

which, combined with eq 33, gives

$$N_\phi^2 = \frac{(b_m+2\delta)^2}{2b_f b_m}\cdot N_m^2 \tag{34}$$

The square of the number of turns in each fixed coil is

$$N_f^2 = \frac{b_f}{2b_m}\cdot N_m^2 \tag{35}$$

For the fictitious coil plus either fixed coil

$$N^2_{f,\phi} = \frac{(b_m+b_f+2\delta)^2}{2b_f b_m}\cdot N_m^2 \tag{36}$$

and for the fictitious coil plus both the fixed coils

$$N^2_{f,\phi,f} = \frac{(b_m+2b_f+2\delta)^2}{2b_f b_m}\cdot N_m^2 \tag{37}$$

We can now write the equations for the inductances of these various coils as follows, using eq 24:

$$L_m = K\left[-2+\log_e\frac{8a}{0.2235(b_m+c)}\right] \tag{38}$$

in which, for brevity, the symbol $K$ denotes the quantity $0.83\times 4\pi a N_m^2$. Similarly,

$$L_\phi = K\cdot\frac{(b_m+2\delta)^2}{2b_f b_m}\cdot\left[-2+\log_e\frac{8a}{0.2235(b_m+2\delta+c)}\right] \tag{39}$$

$$L_f = K\cdot\frac{b_f}{2b_m}\cdot\left[-2+\log_e\frac{8a}{0.2235(b_f+c)}\right] \tag{40}$$

$$L_{f,\phi} = K\cdot\frac{(b_m+b_f+2\delta)^2}{2b_f b_m}\cdot\left[-2+\log_e\frac{8a}{0.2235(b_m+b_f+2\delta+c)}\right] \tag{41}$$

$$L_{f,\phi,f} = K\cdot\frac{(b_m+2b_f+2\delta)^2}{2b_f b_m}\cdot\left[-2+\log_e\frac{8a}{0.2235(b_m+2b_f+2\delta+c)}\right] \tag{42}$$

Using these equations and eq 32, we are now able to set up explicitly an equation which expresses the condition that $L_x$ must equal $L_m$. After a little obvious rearrangement, this equation takes the form

$$\begin{aligned}K\Bigg[&\left(-2+\log_e\frac{8a}{0.2235(b_m+c)}\right)-\frac{b_f}{b_m}\cdot\left(-2+\log_e\frac{8a}{0.2235(b_f+c)}\right)\\&-\frac{(b_m+2b_f+2\delta)^2}{2b_f b_m}\cdot\left(-2+\log_e\frac{8a}{0.2235(b_m+2b_f+2\delta+c)}\right)\\&-\frac{(b_m+2\delta)^2}{2b_f b_m}\cdot\left(-2+\log_e\frac{8a}{0.2235(b_m+2\delta+c)}\right)\\&+\frac{(b_m+b_f+2\delta)^2}{b_f b_m}\cdot\left(-2+\log_e\frac{8a}{0.2235(b_m+b_f+2\delta+c)}\right)\Bigg]=0\end{aligned} \tag{43}$$

The quantity for which $K$ is an abbreviation cannot equal zero and hence may be ignored in solving this equation. Values having already been chosen for $a$, $b_m$, $c$, $N_m$, and $\delta$, the only unknown is $b_f$. The solution is most readily made by numerical substitution. Values of the quantity in brackets are computed for a series of values of $b_f$, after

which, by numerical or graphical interpolation, the value of $b_f$ is found for which the quantity in brackets equals zero. The procedure is tedious but straightforward, and it will now be shown that the range of values of $b_f$ to be tried is a narrow one.

In figure 6, (*a*) represents a cross section of the movable coil of $N_m$ turns and self inductance $L_m$; (*b*) represents the same coil divided in

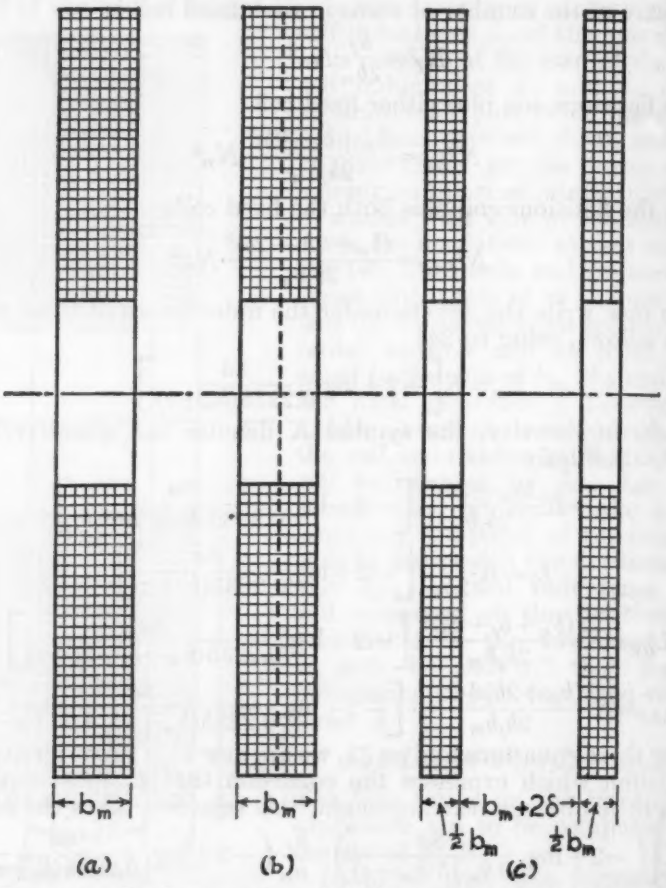


FIGURE 6.—*Development of a pair of fixed coils from a movable coil.*

In (*a*) is shown a cross section of a movable coil of the relative proportions used in the improved inductor. At (*b*) the movable coil is assumed to be divided into halves by a plane at right angles to the axis of the coil. At (*c*) these halves are shown as separated by the proper axial distance to admit placing between them, with suitable clearances, a movable coil of the form shown at (*a*). It is readily seen that the self inductance of the two halves in series and located as in (*c*) is less than the self inductance of the undivided coil as shown at (*a*). In the improved inductor the dimension marked $0.5b_m$ is increased to $0.6b_m$ and the coils are wound with more turns of somewhat larger wire.

halves by an imaginary plane normal to the axis of the coil; and (*c*) represents the halves separated axially by a distance $b_m+2\delta$ to constitute a pair of fixed coils. In either (*b*) or (*c*) the total self inductance of the halves (in series) is the sum of the two separate self inductances plus twice the mutual inductance between the halves. It is evident that the separation of the halves, in going from condition (*b*) to condition (*c*), reduces their mutual inductance and, therefore,

the total self inductance of the pair. Such a pair of fixed coils complies with the requirement that its resistance should be equal to that of the movable coil, but its inductance will be less than that of the movable coil. To bring this inductance up to the desired value, leaving $b_f$ unchanged, requires more turns of smaller wire. This, however, makes the resistance of the pair of fixed coils larger than that of the movable coil. It is evident that to make $L_F=L_m$ and also to keep $R_F=R_m$ we must make $b_f$ somewhat greater than $b_m/2$, in order that each fixed coil may have more than $N_m/2$ turns of wire suitably larger in cross section than that in the movable coil. In beginning the solution of eq 43 we may, therefore, substitute $b_m/2$ for $b_f$, after which the substitution of values successively larger by small increments will make the value of the quantity in brackets in eq 43 approach and pass through zero. The value of $b_f$ which makes this function zero, when substituted with $N_m$ and $b_m$ in eq 35, gives the number of turns $N_f$ in each of the pair of fixed coils. The diameter $x_f$ of the wire in these coils, over the insulation, is given by the formula, analogous to eq 28,

$$x_f=(b_f c/N_f)^{\frac{1}{2}} \tag{44}$$

The pair of fixed coils, wound with wire of this overall diameter having the same space factor $s$ as the wire in the movable coil, will satisfy both of the requirements, namely, $R_F=R_m$ and $L_F=L_m$.

The length of a mean turn being the same for the movable coil as for the fixed coils, and the resistance of the movable coil being equal to that of the pair of fixed coils, it follows that the corresponding values of resistance per unit length, $q_m$ and $q_f$, of the wires used, will have the simple relation

$$q_f/q_m=N_m/2N_f \tag{45}$$

Lest the impression should be given, however, that the fixed coils need to be of much larger wire than the movable coil and have an axial length $b_f$ considerably exceeding $b_m/2$, the following data are given at this place for the inductor designed by the authors in accordance with the procedure outlined in this paper. The value found from eq 43 for $b_f$ was 0.601 $b_m$, from which, by eq 31, $N_f=0.548\ N_m$. The value found for the cross section of the wire in the fixed coils, by eq 44, was 1.097 times that of the movable coil; in other words, with wire of a given size in the movable coil, even one gage number larger would be much too large for the fixed coils. This difficulty was met (as will be detailed later) by winding the greater part of each of the fixed coils with wire of the size used for the movable coil, and finishing with wire of the next larger gage size.

## 6. CALCULATION OF THE MUTUAL INDUCTANCE BETWEEN THE TWO COIL SYSTEMS

It remains to be seen whether the coil proportions as determined by the process above outlined are such as to give a sufficiently high value of coupling coefficient and hence of the related quantities, namely, the mutual inductance between the movable coil and the fixed coils, and the ratio $L_u/L_l$. This mutual inductance may be computed by the device (see fig. 7) of imagining a fictitious coil $\phi'$ wound so as to fill completely the small clearance between one of the fixed coils and the movable coil. The calculation must be made in two stages. In the

first stage it is assumed that a fictitious fixed coil $f'$ and the fictitious coil $\phi'$ are wound with wire of the same size [14] as that in the movable coil. It may be shown[15] that the mutual inductance between the left-hand fixed coil in figure 7 and the movable coil is given by the expression

$$M_{f',m}=\tfrac{1}{2}\cdot(L_{f',\phi',m}-L_{f',\phi'}-L_{\phi',m}+L_{\phi'}) \tag{46}$$

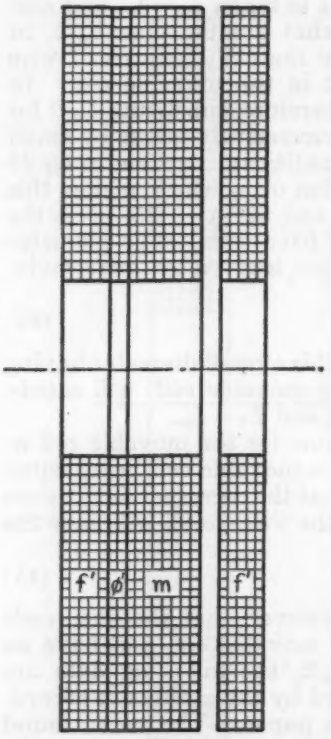


FIGURE 7.—*Cross-sectional view of group of link-shaped coils as used in the improved inductor, and a fictitious coil* $\phi'$.

The fictitious coil is assumed to fill completely the space between the coils adjacent to it, and to have the same number of conductors per unit of area of cross section as the latter. As in the case of figure 5, the assumption of such a fictitious coil facilitates the computation of the mutual inductance between the two coils adjacent to it.

in which the terms in parenthesis represent respectively the self inductances of the groups of coils indicated by the subscripts; thus $L_{\phi',m}$ denotes the self inductance of the fictitious coil and the movable coil in series as one coil. The four terms in eq 46 are to be calculated by means of eq 24. The value of mutual inductance $M_{f',m}$ so obtained is higher than the desired value $M_{f,m}$ for the fixed coil wound with the somewhat larger wire which must be used, and must be reduced in the ratio of the number of turns in the actual fixed coil to the number computed for the fictitious fixed coil; that is

$$M_{f,m}=\frac{N_m(b_f/2b_m)^{\frac{1}{2}}}{N_m(b_f/b_m)}\cdot M_{f',m}$$

$$=\left(\frac{b_m}{2b_f}\right)^{\frac{1}{2}}\cdot M_{f',m} \tag{47}$$

This is the mutual inductance between one of the fixed coils and the movable coil, and it must be doubled to obtain the mutual inductance between the pair of fixed coils and the movable coil. Referring to eq 1, and remembering that by design $L_r=L_m$, the coupling coefficient is seen to be

$$k=2M_{f,m}/L_r \tag{48}$$

If we change the connections so as to make the magnetic flux of the movable coil oppose that of the pair of fixed coils, the coupling coefficient $k$ will have the same numerical value but the opposite sign. The ratio of the maximum self inductance of the coil group to its minimum, by eq 9, is thus

$$\frac{L_{max}}{L_{min}}=\frac{1+k}{1-k} \tag{49}$$

[14] By "same size" for the present purpose is meant the same diameter over the insulation. The significant thing here is that the number of turns per unit area of cross section of the winding shall be the same for all the coils involved in this kind of calculation.

[15] BS Sci. Pap. 8, 41 (1912) S169; 18, 469 (1922) S455.

This ratio should be, say 10 percent greater than the desired value of $L_u/L_1$. If it is not as large as desired, and if the clearance $\delta$ cannot be reduced, the only remedy is to use coils which are wider radially and shorter axially than those assumed. That is, with a given value of $a$, one must start with a movable coil having a larger value of $c$ and a smaller value of $b_m$. The method is essentially one of trial and error.

## 7. EXPERIMENTAL CHECK OF THE LINEARITY OF THE SCALE LAW

Coil proportions and wire sizes having been determined for which $L_m=L_r$ and $R_m=R_r$, and for which the coupling coefficient has a sufficiently high value, it remains to be determined whether these coils can be used to form an inductor having a sufficiently good approximation to a linear scale law. This question must be answered by experiment. It is known that the linearity of the scale law is a function of the ratio $S/r$ (see fig. 2). This matter was checked, in the design of the inductor to be described below, in the following manner.

Trial fixed coils and movable coils having the desired proportions were wound of copper strip of widths to give one turn per layer. These coils were mounted in a temporary wooden frame which permitted the dimension $S$ to be varied. The scale law for this temporary instrument was then determined for a number of values of the radius $S$. The results of three such runs are shown in figure 8, in which the inductance scales of the various runs have been arbitrarily displaced vertically with respect to each other. Curves $A$ and $C$ represent conditions when the ratio $S/r$ was respectively 2 percent greater and 4 percent less than its optimum value. Curve $B$ represents the condition when $S/r$ was within 1 percent of its optimum value. In these curves the circles represent the observed points and the solid lines represent the least-square straight lines which have been drawn, using all the experimental points between the 7.5° point and the 172.5° point, inclusive. It is obvious that curve $B$ represents a better scale law than either of the other two. In order to have a more objective basis for judging the linearity of the scale law, the curve of figure 9 was drawn. A number of curves similar to those of figure 8 were drawn, corresponding to a number of values of the ratio $S/r$. For each of these curves the least-square deviation, $\epsilon$, of the observed points from the corresponding straight line was computed. The magnitude of $\epsilon$ was taken to be a measure of the departure from linearity of the scale law under the given conditions. In figure 9 this quantity, $\epsilon$, is plotted against the ratio $S/r$ and is expressed as a fraction of a scale division, each scale division being 7.5° long. It is seen that $\epsilon$ goes through a decided minimum between the values of $S/r$ of 2.24 and 2.26, a result which closely confirms the corresponding result of Brooks and Weaver.[16]

[16] BS Sci. Pap. 12, 575 (1916–17) S290. The ratio designated as $F/r$ in this earlier paper corresponds to that which is called $S/r$ in the present paper.

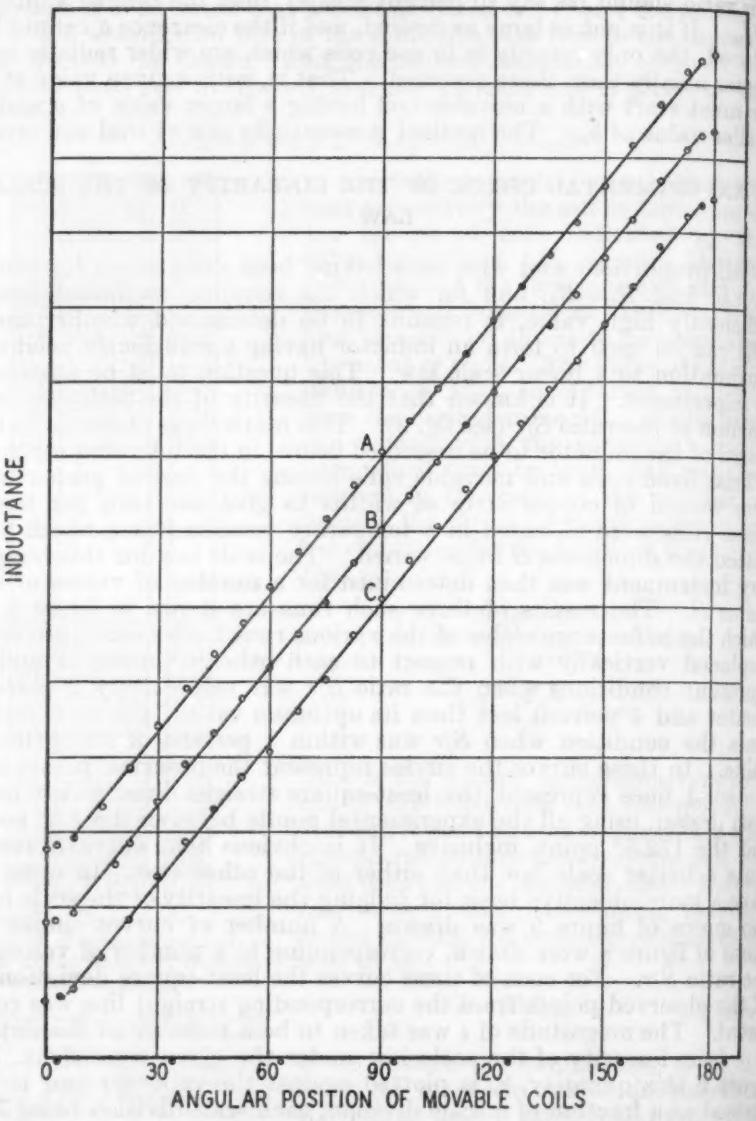


FIGURE 8.—*Curves showing the manner of variation of self inductance with relative angular position of fixed coils and movable coil, as affected by the relative spacing S/r of the two groups of coils.*

(See fig. 2 for the significance of $S$ and $r$.)

In the case of curves $A$ and $C$ the ratio $S/r$ was respectively 2 percent greater and 4 percent less than its optimum value. In the case of curve $B$ this ratio was within 1 percent of its optimum value, namely, 2.25. See also figure 9.

The deviations from linearity, shown by the plotted points, are characteristic of systems of coils of the given form, and are not the result of errors in the measurements. Furthermore, it may readily be seen that the slope of all curves of this kind must become zero for the angular positions 0 and 180°.

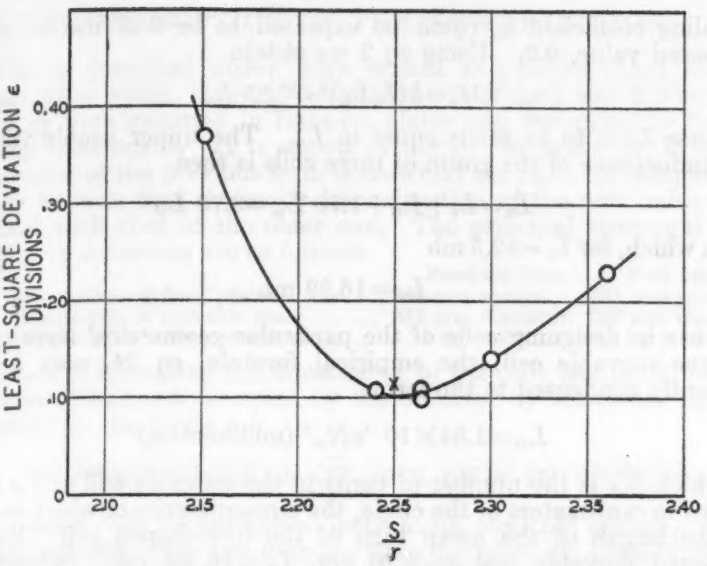


FIGURE 9.—*Curve showing the least-square deviation from linearity of curves similar to those in figure 8, as a function of the relative spacing S/r of the two groups of coils.*

The points plotted as circles were determined by measurements on the experimental inductor with coils wound with copper strip. The point marked *x* relates to the improved inductor, with wire coils, shown at the left in figure 10.

## IV. DESIGN OF COILS FOR THE NEW INDUCTOR

It was proposed to construct a variable inductor to have a ratio $L_u/L_l$ of at least 10. Because $L_{max}$ is somewhat greater than $L_u$, and $L_{min}$ somewhat smaller than $L_l$, $L_{max}/L_{min}$ would need to be at least 11. To provide a liberal allowance to cover unavoidable inaccuracies in winding the coils, failure to match exactly the inductances of the fixed system and the movable system, etc., coil proportions were determined, in the manner above outlined, which gave a calculated coupling coefficient of 0.9 at the point of maximum mutual inductance. By eq 7 this value of coupling coefficient would give $L_{max}/L_{min}=19$.

Referring to figure 2, a value of $r=3.14$ cm was chosen as a basic dimension, in terms of which the other significant dimensions were found to be as follows:

$$c=1.24r;\ d=2.06r;\ S=2.25r;\ b_m=0.318r;\ b_f=0.191r.$$

The separation which we planned to have between each fixed coil and the movable coil was 0.08 cm (1/32 inch).

The desired maximum usable value of self inductance, $L_u$, was 125 mh. For simplicity it was assumed initially that we had to design one movable coil and a pair of fixed coils to give a maximum usable value of 62.5 mh. Measurements made on the experimental copper-strip inductor indicated that the maximum usable value of the

coupling coefficient $k_u$ could be expected to be 0.85 instead of the proposed value, 0.9. Using eq 2 we obtain

$$M_u=k(L_rL_m)^{\frac{1}{2}}=0.85\ L_m$$

because $L_r$ is to be made equal to $L_m$. The upper usable value of self inductance of the group of three coils is then

$$L_u=L_r+L_m+1.70\ L_m=3.70\ L_m$$

from which, for $L_u=62.5$ mh

$$L_m=16.89 \text{ mh}$$

For use in designing coils of the particular geometrical form chosen for the movable coil, the empirical formula, eq 24, may be conveniently condensed to the form

$$L_m=1.84\times10^{-5}aN_m^2 \text{ (millihenries)} \tag{50}$$

in which $N_m$ is the number of turns in the movable coil and $a$ is the radius in centimeters of the circle, the circumference of which is equal to the length of the mean turn of the link-shaped coil. For the proposed movable coil $a=5.20$ cm, $L_m=16.89$ mh. Substituting these values in the preceding formula, we get

$$N_m=420$$

Using eq 31 we have, since $b_f/b_m=0.601$,

$$N_f=230$$

The cross-sectional area of the movable coil is $10\times39=390$ mm$^2$, from which the area of the square circumscribing the insulated wire must be $390/420=0.929$ mm$^2$, and hence the diameter of the insulated wire is 0.964 mm. Number 20 AWG [17] silk-enamel wire is enough smaller than this to allow for unavoidable irregularities of winding, and was used for the movable coil. The resistance per meter of no. 20 copper wire at 25° C is 0.034 ohm$=q_m$. By eq 45, the resistance per meter of the wire to be used for the fixed coils should be

$$\begin{aligned} q_f&=N_mq_m/2N_f \\ &=(420\times0.034)/460 \\ &=0.0391 \text{ ohm/meter.} \end{aligned}$$

This value calls for a wire having a cross-sectional area only 15 percent larger than no. 20. The next larger gage size, no. 19,[18] has a cross-sectional area 1.26 times that of no. 20. To avoid the necessity for drawing and insulating wire of a nonstandard intermediate size, each fixed coil was wound with no. 19 and no. 20 wires, with silk-enamel insulation, in such proportions as to fill the given cross section for winding and to have the desired resistance and number of turns. Each fixed coil was accordingly wound with 77 turns of no. 20 wire and 38 turns of no. 19.

[17] The diameter of no. 20 AWG bare wire is 0.032 in. (0.81 mm). The diameter over the insulation (enamel and one wrapping of silk) is 0.0363 in. (0.92 mm).

[18] The diameter of no. 19 AWG bare wire is 0.036 in. (0.91 mm). The diameter over the insulation (enamel and one wrapping of silk) is 0.0403 in. (1.02 mm).

## V. DESCRIPTION OF THE NEW INDUCTOR

Coils as described above were wound and impregnated at this Bureau, after which, through the cooperation of the Leeds & Northrup Co., they were mounted in Bakelite plates and assembled to form a working instrument. It is shown at the left in figure 10, in which an inductor of the previous form is shown at the right for comparison. It may be seen that the general construction of the new inductor is identical with that of the older one. The principal structural data for the two inductors are as follows:

| | Previous form | New form |
|---|---|---|
| Dimensions of fixed plates | 245 mm square | 281 mm square |
| Dimensions of movable plate | 262 mm diameter | 298 mm diameter |
| Weight of inductor, complete | 4.35 kg (9.6 lb) | 6.6 kg (14.6 lb). |

The effect of increasing the dimension $c$ of the coils (see fig. 2) is thus to increase the space occupied by the inductor by the factor 1.3 and its weight by the factor 1.5.

## VI. PERFORMANCE OF THE NEW INDUCTOR

As measured in the completed instrument, the fixed system and the movable system of the new inductor have the following characteristics:

Inductance of four fixed coils in series = 35.10 mh.
Inductance of two movable coils in series = 35.57 mh.
Difference in inductance = 1.3 percent.

Resistance of four fixed coils in series = 9.52 ohms.
Resistance of two movable coils in series = 9.62 ohms.
Difference in resistance = 1.0+ percent.

$$L_{max} = 130.0_7 \text{ mh.}$$

$$L_{min} = 11.2_6 \text{ mh.}$$

These differences in inductance and reistance seem to indicate that there should have been a slightly greater proportion of no. 20 wire and hence more turns in the fixed coils. The values of $L_{max}$ and $L_{min}$ indicate a coupling coefficient at the positions of maximum and minimum inductance of 0.84, which is smaller than the value 0.9 predicted by calculation. This lower value is not the result of inaccuracy in the calculation but arises chiefly from the fact that in this experimental model the clearances between the coils are greater than we had planned to use. Study of the problem from the manufacturing standpoint will be necessary to determine the permissible amount of clearance in inductors as produced commercially.

The edge of the disk which carries the movable coils in the new inductor is graduated from 0 to 360° in 0.5° divisions. This kind of graduation was convenient for this experimental inductor but would not necessarily be applied to inductors manufactured for sale. The fiducial mark is so located on the upper (stationary) plate that the readings 90 and 270° correspond to zero mutual inductance between the two coil systems, and hence the points 0 and 180° correspond to the minimum and the maximum values respectively of the self inductance.

The plotted points of figure 11 show the self inductance of the new inductor, in the series connection, as a function of the relative position of the two coil systems. To bring out the close approach to linearity,

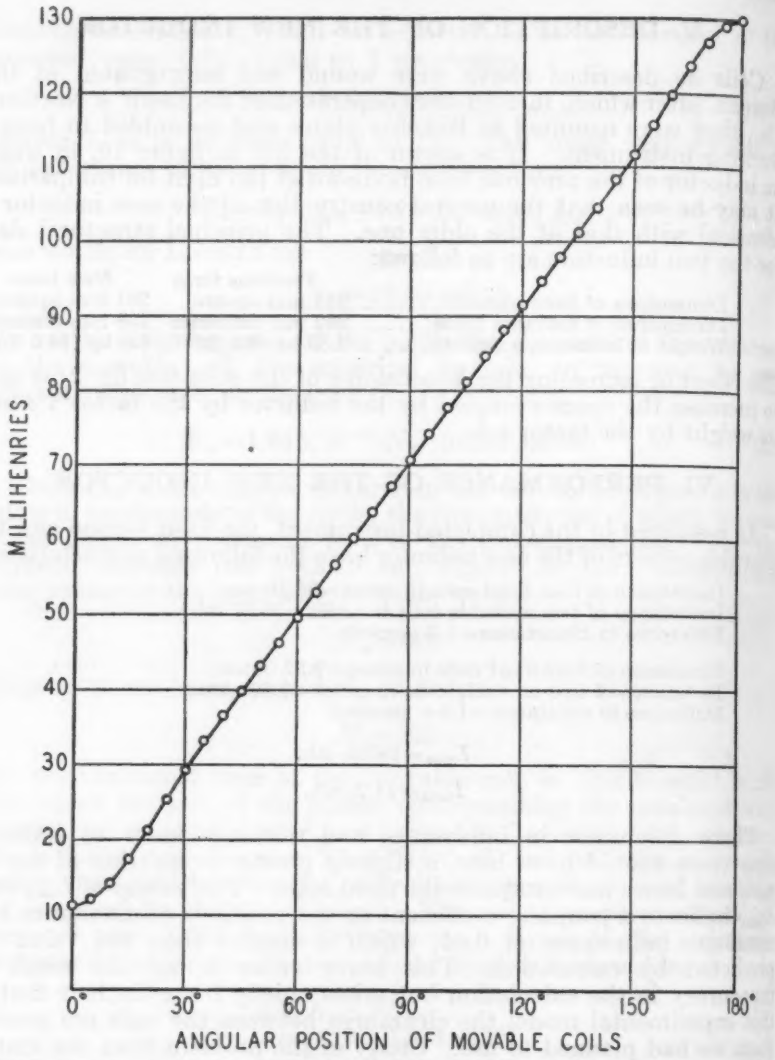


FIGURE 11.—*Curve showing the self inductance of the improved inductor as a function of the relative angular position of the movable coils with respect to the fixed coils.*

the part of the curve for abscissas from 30 to 150°, inclusive, has been determined by the method of least squares as the straight line which most nearly fits the observed points. The approach to linearity is seen to be very good. Below 30° and above 150° the rate of change in the slope is gradual enough to make it feasible to subdivide the scale down to 5° and up to 175°. The plotted points are those corresponding to bridge measurements in which the frequency of the current was 60 c/s. Measurements at 1,000 c/s were also made for the angular positions 5, 30, 60, 90, 120, 150, and 175°. The measured values of inductance for this higher frequency exceeded those made at the lower frequency by 0.00 to 0.11 mh; in other words, by amounts comparable

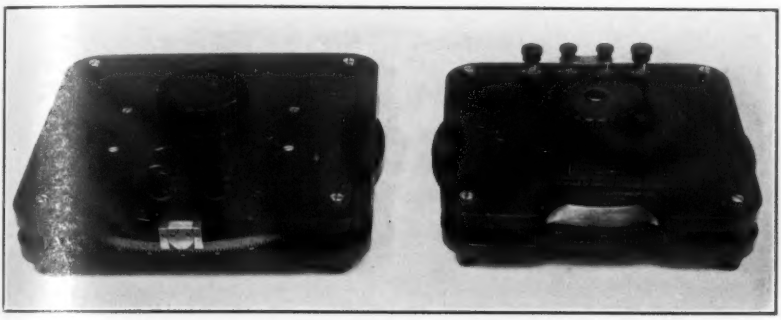

FIGURE 10.—*The improved inductor (at the left) and the older form.*

The latter is graduated to read directly in millihenries. The new inductor, being an experimental model, has a scale of angular degrees.

UNIV. OF MICH.

with those which might be caused by errors of 0.0 to 0.15° in setting the movable disk to a specified angular position with respect to the fixed coils. For practical purposes the effect of the change from 60 to 1,000 c/s may therefore be considered inappreciable.

Additional bridge measurements of the inductance, at the above-mentioned seven angular positions of the movable coils, were made at 60 and 1,000 c/s with the fixed system of coils in parallel with the movable system. The results, given in table 1, show that the change to the parallel connection reduces the inductance to one-fourth of the corresponding value for the series connection, within an amount which is less than the probable error of the bridge measurements. The last column gives the computed differences in inductance which arise from the fact that the inductance and the resistance of the movable system of coils are not exactly equal to those of the fixed system. These differences are far below the probable errors of the bridge measurements and the differences in inductance which would result from the inevitable small errors of setting the relative angular position of the two coil systems.

TABLE 1.—*Measured self inductance of improved variable inductor in series connection and in parallel connection*

| Scale setting | Coils in series | $\frac{L_{series}}{4}$ | Coils in parallel | Observed difference | Computed difference |
|---|---|---|---|---|---|
| *Degrees* | mh | mh | mh | mh | mh |
| 0 | 11.26 | | | | |
| 5 | 12.04 | 3.01 | 3.00 | 0.01 | $0.00_0$ |
| 30 | 29.37 | 7.34 | 7.33 | .01 | $.00_0$ |
| 60 | 49.66 | 12.42− | 12.41 | .01− | $.00_1$ |
| 90 | 70.69 | 17.67 | 17.67 | .00 | $.00_1$ |
| 120 | 91.52 | 22.88 | 22.87 | .01 | $.00_1$ |
| 150 | 111.79 | 27.95 | 27.94+ | .01− | $.00_2$ |
| 175 | 129.32 | 32.33 | 32.30 | .03 | $.00_5$ |
| 180 | 130.07 | | | | |

Inspection of the curve of figure 11 shows that the scale law of the new inductor is sufficiently linear to be considered usable over the range 5 to 175°. From table 1 it appears that for these limiting positions $L_u/L_l$=129.32/12.04=10.7. The time-constant of the new inductor, for the 175° position of the coil systems, is 6.7 milliseconds. The use of a molded plate for supporting the movable coils, which would be feasible and economical for inductors in regular production, would probably permit a reduction of the clearances, and in consequence, a somewhat higher value of $L_u/L_l$ and of the time-constant.

## VII. CONCLUSION

The approach to linearity of the self inductance of the new inductor, as a function of the relative position of the coils, is as good as that of the older inductor. The ratio $L_u/L_l$ in the new inductor is 10.7, as compared with 7.4 for the older model. The time-constant of the new inductor, for the upper limiting value of the self inductance, is 6.7 milliseconds as compared with 4.5 milliseconds for the older instrument. This increase in time-constant, however, has been obtained at the expense of an almost equal relative increase in the weight of the inductor. If it should be found feasible, in manufacture, to reduce

the clearances to more nearly the values aimed at in the design, this reduction will increase both $L_u/L_l$ and the time-constant without any increase in the weight.

---

The writers express their appreciation to Dr. Frederick W. Grover for valuable suggestions during their study of the problem; for his careful reading of the manuscript and his suggestions for its improvement. They are grateful to the Leeds and Northrup Co. for the construction of the framework of the instrument and the mounting of the coils, and to Miss C. M. Sparks for the very careful series of measurements which forms the basis of table 1 and of figure 11.

WASHINGTON, September 8, 1937.

U. S. DEPARTMENT OF COMMERCE NATIONAL BUREAU OF STANDARDS

RESEARCH PAPER RP1041

*Part of Journal of Research of the National Bureau of Standards, Volume 19, November 1937*

# EFFECT OF WAVE FORM UPON THE PERFORMANCE OF CURRENT TRANSFORMERS

By John H. Park

ABSTRACT

The effects of changing the wave form of the primary current from sinusoidal to peaked or flat top (20-percent third harmonic) upon the ratio and the phase angle of several current transformers and upon the performance of a Silsbee current-transformer testing set were determined experimentally. Definitions of the ratio and the phase angle of a current transformer under nonsinusoidal conditions of current were derived in terms of the ratios of transformation and the shifts in phase angle of the fundamental and of the harmonic components of the primary current due to transformation.

CONTENTS

| | Page |
|---|---|
| I. Introduction | 517 |
| II. Definitions of ratio and phase angle for nonsinusoidal conditions | 518 |
| 1. Ratio | 518 |
| 2. Phase angle | 519 |
| III. Apparatus and procedure | 523 |
| IV. Results and conclusions | 525 |

## 1. INTRODUCTION

Commercial measurements of electric power and energy, in circuits carrying alternating currents of large magnitude, are invariably made by the use of current transformers which supply, to the measuring instruments proper, secondary currents which are replicas on a reduced scale of the corresponding currents in the primary circuit. In important installations, the proportionality factor or "ratio" of the transformer is obtained by an experimental comparison between the transformer in question and a standard transformer of known ratio. This comparison is usually made in the testing laboratory of the utility company concerned, and the standard transformer in turn is tested at suitable intervals by some absolute method, usually in a standardizing laboratory, such as that of the National Bureau of Standards.

It is obvious that the accuracy of the final results would be affected if the conditions under which either the working or the standard transformer is operated were allowed to differ to a significant extent from the conditions under which either transformer was tested. With ordinary care such conditions as frequency and secondary burden can be readily reproduced with sufficient fidelity, and the effect of changes in these conditions decreases in general with an increase in the current to be measured, and hence with the commercial importance of the measurement. The variations in ratio and phase angle of a current transformer resulting from changes in the geometrical configuration

of its primary circuit have been investigated and the results published.[1] While these variations are negligible in multiturn transformers of low current rating, they tend to increase as the rated primary current increases and if accurate results are desired in the measurements of large alternating currents it becomes necessary to test the current transformer involved, with the same arrangement of primary circuit as will be used when the transformer is in operation.

The effect of variations in the wave form of the current being measured on the ratio and phase angle of a current transformer has received very little consideration since an investigation by Agnew[2] from which he concluded that the effect was negligible for commercial wave forms. Agnew's investigation, however, was limited to transformers of low primary-current rating, and since the measurement of alternating currents of from 500 to 4,000 amperes has become quite common in recent years it was decided that an investigation of the effect of wave form upon the ratio and the phase angle of current transformers of this range was desirable.

## II. DEFINITIONS OF RATIO AND PHASE ANGLE FOR NONSINUSOIDAL CURRENTS

The ratio and phase angle of a current transformer, as measured by a majority of the methods now in use, give the relation between the fundamental components of the primary and the secondary currents. Unless the current being measured is nearly sinusoidal, this relation may not be the most useful one obtainable. Therefore, it becomes necessary in this investigation to measure not only the ratio and the phase angle between the fundamental components of the primary and the secondary currents, but also the ratios and the phase angles between the harmonic components of the primary current and the corresponding harmonic components of the secondary current. In order to express the results of this work in terms of quantities which are really important in the use of the current transformer, definitions of the ratio and the phase angle of a current transformer were derived in terms of the measured quantities.

### 1. RATIO

In defining the ratio of a current transformer for use in measurements of nonsinusoidal currents it will be assumed that the current to be measured contains an indefinite number of odd harmonics and that its instantaneous value can be represented by the equation

$$i_1 = I_m[\sin \omega t + k_3 \sin (3\omega t + \lambda_3) + k_5 (\sin 5\omega t + \lambda_5) + \cdots] \quad (1)$$

If $Nc_1$, $Nc_3$, $Nc_5$, $\cdots$ denote the ratios in which the fundamental and the 3d, 5th, $\cdots$ harmonic components of the primary current are transformed and if $\beta_1$, $\beta_3$, $\beta_5$, $\cdots$ denote the corresponding phase angles, the instantaneous value of the secondary current of the transformer can be represented by

$$i_2 = \frac{I_m}{N}\left[\frac{1}{c_1}\sin(\omega t + \beta_1) + \frac{k_3}{c_3}\sin(3\omega t + \lambda_3 + \beta_3) + \frac{k_5}{c_5}\sin(5\omega t + \lambda_5 + \beta_5) + \cdots\right] \quad (2)$$

[1] John H. Park. *Accuracy of high-range current transformers.* J. Research NBS **14**, 367 (1935) RP775.
[2] *A study of the current transformer with particular reference to iron losses.* Bul. BS **7**, 470 (1911) S164.

The constant $N$ is the nominal ratio of the current transformer and the $c$'s are ratio correction factors, i. e., the factors by which the nominal ratio must be multiplied to obtain the true ratios.

The usually accepted definition of the ratio of a current transformer is the ratio of the effective or rms value of primary current to the effective or rms value of secondary current. With this definition as a basis the ratio for nonsinusoidal currents is to be expressed in terms of the ratios of the fundamental and the harmonic components. From eq 1 and 2 the effective values of the primary current and the secondary current are

$$I_1=\frac{I_m}{\sqrt{2}}(1+k_3^2+k_5^2+\cdots)^{\frac{1}{2}} \tag{3}$$

and

$$I_2=\frac{I_m}{N\sqrt{2}}\left(\frac{1}{c_1^2}+\frac{k_3^2}{c_3^2}+\frac{k_5^2}{c_5^2}+\cdots\right)^{\frac{1}{2}} \tag{4}$$

If the ratio of effective values is denoted by $Nc_e$, where, as before, $N$ is the nominal ratio, and $c_e$ is the ratio correction factor,

$$Nc_e=\frac{I_1}{I_2}=N\left(\frac{1+k_3^2+k_5^2+\cdots}{\frac{1}{c_1^2}+\frac{k_3^2}{c_3^2}+\frac{k_5^2}{c_5^2}+\cdots}\right)^{\frac{1}{2}} \tag{5}$$

Performing the indicated division within the parenthesis, and neglecting terms such as $\left(1-\frac{c_1^2}{c_n^2}\right)k_n^4$ in the fourth and higher powers of $k_n$

$$c_e=c_1\left[1+\left(1-\frac{c_1^2}{c_3^2}\right)k_3^2+\left(1-\frac{c_1^2}{c_5^2}\right)k_5^2+\cdots\right]^{\frac{1}{2}} \tag{6}$$

It will be assumed here that $k_n \leqq 0.2$. Thus, the terms in $k^2$ will be quite small, and since each one of the $c$'s is nearly unity, eq 6 becomes

$$c_e=c_1[1+(c_3-c_1)k_3^2+(c_5-c_1)k_5^2+\cdots] \tag{7}$$

Equation 7 is in convenient form for computing the ratio of the effective primary current to the effective secondary current from the ratios of transformation for the fundamental and the harmonic components. It may be noted that unless the ratios for the harmonic components are considerably different from the ratio for the fundamental, the ratio of the effective primary current to the effective secondary current is very nearly the same as the ratio of transformation for the fundamental component.

## 2. PHASE ANGLE

The phase angle of a current transformer for currents of sinusoidal wave form is customarily defined as the angle between the primary-current vector and the secondary-current vector reversed. This definition cannot be used for nonsinusoidal currents since they cannot be represented by single vectors.

The phase angle of a current transformer is of importance only when power or energy is to be measured. For either of these measurements, with nonsinusoidal wave forms, a definition of phase angle must take account not only of the current but also of the load circuit and hence of the voltage across the load. If a primary current as represented by eq 1 is assumed to flow through a load circuit of resistance $R$ and inductance $L$, the instantaneous voltage across this circuit is

$$e_1=I_m\Big[(R^2+\omega^2L^2)^{\frac{1}{2}}\sin\Big(\omega t+\tan^{-1}\frac{\omega L}{R}\Big)+$$

$$k_3(R^2+9\omega^2L^2)^{\frac{1}{2}}\sin\Big(3\omega t+\lambda_3+\tan^{-1}\frac{3\omega L}{R}\Big)+$$

$$k_5(R^2+25\omega^2L^2)^{\frac{1}{2}}\sin\Big(5\omega t+\lambda_5+\tan^{-1}\frac{5\omega L}{R}\Big)+\ldots.\Big] \quad (8)$$

The effective value of this voltage is

$$E_1=\frac{I_m}{\sqrt{2}}[R^2+\omega^2L^2+k_3^2(R^2+9\omega^2L^2)+k_5^2(R^2+25\omega^2L^2)+\ldots.]^{\frac{1}{2}} \quad (9)$$

Since the current in this circuit is $i_1$ (see eq 1) and the voltage across it is $e_1$ (see eq 8), the apparent power is

$$U_1=E_1I_1=\frac{I_m^2}{2}\{[1+k_3^2+k_5^2+\ldots.][R^2+\omega^2L^2$$

$$+k_3^2(R^2+9\omega^2L^2)+k_5^2(R^2+25\omega^2L^2)+\ldots.]\}^{\frac{1}{2}} \quad (10)$$

For brevity let

$$\theta_1=\tan^{-1}\frac{\omega L}{R},\ \theta_3=\tan^{-1}\frac{3\omega L}{R},\ \theta_5=\tan^{-1}\frac{5\omega L}{R}\ \ldots.$$

The active power in this circuit may then be expressed by

$$P_1=\frac{I_m^2}{2}[(R^2+\omega^2L^2)^{\frac{1}{2}}\cos\theta_1+k_3^2(R^2+9\omega^2L^2)^{\frac{1}{2}}\cos\theta_3$$

$$+k_5^2(R^2+25\omega^2L^2)^{\frac{1}{2}}\cos\theta_5+\ldots.] \quad (11)$$

If a hypothetical circuit whose current is $i_2$ (see eq 2) and voltage $e_1$ (see eq 8) is considered, its apparent power would be

$$U_2=E_1I_2=\frac{I_m^2}{2N}\Big\{\Big[\frac{1}{c_1^2}+\frac{k_3^2}{c_3^2}+\frac{k_5^2}{c_5^2}+\ldots.\Big][R^2+\omega^2L^2$$

$$+k_3^2(R^2+9\omega^2L^2)+k_5^2(R^2+25\omega^2L^2)+\ldots.]\Big\}^{\frac{1}{2}} \quad (12)$$

The active power in this hypothetical circuit would be

$$P_2=\frac{I_m^2}{2N}\Big[\frac{(R^2+\omega^2L^2)^{\frac{1}{2}}}{c_1}\cos(\theta_1-\beta_1)+k_3^2\frac{(R^2+9\omega^2L^2)^{\frac{1}{2}}}{c_3}\cos(\theta_3-\beta_3)$$

$$+k_5^2\frac{(R^2+25\omega^2L^2)^{\frac{1}{2}}}{c_5}\cos(\theta_5-\beta_5)+\ldots.\Big] \quad (13)$$

By referring to the first parts of eq 10 and 12, and recalling that $I_1=Nc_eI_2$, it can be seen that

$$U_1=Nc_eU_2 \tag{14}$$

The ratio of active power to apparent power can be represented by the cosine of some angle $\phi$, i. e.,

$$\frac{P_1}{U_1}=\cos\phi_1 \text{ and } \frac{P_2}{U_2}=\cos\phi_2 \tag{15}$$

By substituting the values of $U_1$ and $U_2$ obtained from eq 15 in eq 14

$$P_1=Nc_eP_2\frac{\cos\phi_1}{\cos\phi_2} \tag{16}$$

Equation 16 is a formula for the active power of the load circuit in terms of (a) the power $P_2$, measured with a wattmeter which has current $i_2$ flowing through its current circuit and voltage $e_1$ applied across its potential circuit; (b) the ratio, $Nc_e$, of the current transformer used in transforming $i_1$ to $i_2$; and (c) another factor, $\cos\phi_1/\cos\phi_2$, involving the phase angle of this current transformer and the power factor of the load circuit. Under sinusoidal conditions this last factor would be $1/(\cos\beta+\tan\gamma\sin\beta)$, where $\beta$ is the phase angle of the current transformer and $\cos\gamma$ is the power factor of the load circuit. The following arbitrary equation

$$\frac{\cos\phi_1}{\cos\phi_2}=\frac{1}{\cos\beta+\tan\gamma\sin\beta} \tag{17}$$

can be set up and if a value of $\beta$ in terms of $\beta_1, \beta_2, \beta_3, \cdots c_1, c_3, c_5, \cdots$ can be found which satisfies this equation, then this value of $\beta$ can be used as the definition of the phase angle of a current transformer under nonsinusoidal conditions. The main advantage of this definition is that the phase angle so defined can be correctly used in the customary formula for power when a current transformer is used in conjunction with a wattmeter for power measurements.

The first step in solving eq 17 is to obtain a value for $\cos\phi_2/\cos\phi_1$ by referring to eq 15 and substituting the values of $U_1$, $P_1$, $U_2$, and $P_2$ given in eq 10 to 13. After simplifying, this relation becomes

$$\frac{\cos\phi_2}{\cos\phi_1}=\frac{\left(\cos\beta_1+k_3^2\frac{c_1}{c_3}\cos\beta_3+k_5^2\frac{c_1}{c_5}\cos\beta_5+\cdots\right)+\tan\theta_1\left(\sin\beta_1+3k_3^2\frac{c_1}{c_3}\sin\beta_3+5k_5^2\frac{c_1}{c_5}\sin\beta_5+\cdots\right)}{\left[(1+k_3^2+k_5^2+\cdots)^{\frac{1}{2}}\left(1+k_3^2\frac{c_1^2}{c_3^2}+k_5^2\frac{c_1^2}{c_5^2}+\cdots\right)^{\frac{1}{2}}\right]} \tag{18}$$

The denominator of the right-hand side of eq 18 may be replaced by the following series, which is a sufficiently close approximation if $k_n\leqq 0.2$

$$1+k_3^2\frac{c_1}{c_3}+k_5^2\frac{c_1}{c_5}+\cdots$$

Making this substitution and performing the indicated division gives a value for $\cos \phi_2/\cos \phi_1$, which, when placed in eq 17, gives

$$\cos \beta+\tan \gamma \sin \beta=\cos \beta_1+\frac{k_3^2\frac{c_1}{c_3}(\cos \beta_3-\cos \beta_1)+k_5^2\frac{c_1}{c_5}(\cos \beta_5-\cos \beta_1)+\ldots.}{1+k_3^2\frac{c_1}{c_3}+k_5^2\frac{c_1}{c_5}+\ldots.}$$

$$+\tan \theta_1\left[\sin \beta_1+\frac{k_3^2\frac{c_1}{c_3}(3 \sin \beta_3-\sin \beta_1)+k_5^2\frac{c_1}{c_5}(5 \sin \beta_5-\sin \beta_1)+\ldots.}{1+k_3^2\frac{c_1}{c_3}+k_5^2\frac{c_1}{c_5}+\ldots.}\right] \quad (19)$$

Under sinusoidal conditions, $\gamma$ is defined as the angle between the voltage and the current. By defining $\gamma$ under nonsinusoidal conditions as the angle between the fundamental components of the voltage and the current, $\tan \gamma$ is made equal to $\tan \theta_1$.

For nearly all commercial current transformers $\beta_n \leqq 120$ minutes. For such small angles $\sin \beta_n$ can be replaced by $\beta_n$ and $\cos \beta_n$ by $1-\beta_n^2/2$ and eq 19 becomes

$$1-\frac{\beta^2}{2}+\tan \theta_1(\beta)=1-\frac{\beta_1^2}{2}+\frac{k_3^2\frac{c_1}{c_3}\left(\frac{\beta_1^2-\beta_3^2}{2}\right)+k_5^2\frac{c_1}{c_5}\left(\frac{\beta_1^2-\beta_5^2}{2}\right)+\ldots.}{1+k_3^2\frac{c_1}{c_3}+k_5^2\frac{c_1}{c_5}\ldots.}$$

$$+\tan \theta_1\left[\beta_1+\frac{k_3^2\frac{c_1}{c_3}(3\beta_3-\beta_1)+k_5^2\frac{c_1}{c_5}(5\beta_5-\beta_1)+\ldots.}{1+k_3^2\frac{c_1}{c_3}+k_5^2\frac{c_1}{c_5}+\ldots.}\right] \quad (20)$$

For nearly all commercial current transformers $\beta-\beta_1 \leqq 15$ minutes and $\beta_1-\beta_n \leqq 60$ minutes, and since $k_n \leqq 0.2$ the following maximum values can be set for certain terms in the above equation:

$$\frac{\beta^2-\beta_1^2}{2} \leqq 0.00012$$

$$\frac{k_3^2\frac{c^1}{c_3}\left(\frac{\beta_1^2-\beta_3^2}{2}\right)+k_5^2\frac{c_1}{c_5}\left(\frac{\beta_1^2-\beta_5^2}{2}\right)+\ldots.}{1+k_3^2\frac{c_1}{c_3}+k_5^2\frac{c_1}{c_5}+\ldots.} \leqq 0.00006$$

Equation 20 now becomes

$$1+\tan \theta_1(\beta)=1+\tan \theta_1\left[\beta_1+\frac{k_3^2\frac{c_1}{c_3}(3\beta_3-\beta_1)+k_5^2\frac{c_1}{c_5}(5\beta_5-\beta_1)+\ldots.}{1+k_3^2\frac{c_1}{c_3}+k_5^2\frac{c_1}{c_5}+\ldots.}\right]+\delta \quad (21)$$

where $\delta \leqq 0.00018$, i. e., the maximum error introduced by neglecting $\delta$ is less than 0.02 percent. For nearly all measurements of power or energy, this error is negligible and eq 21 becomes

$$\beta=\beta_1+\frac{k_3\frac{c_1}{c_3}(3\beta_3-\beta_1)+k_5\frac{c_1}{c_5}(5\beta_5-\beta_1)+\ldots.}{1+k_3\frac{c_1}{c_3}+k_5\frac{c_1}{c_5}+\ldots.} \tag{22}$$

Equation 22 is a definition of the phase angle of a current transformer for nonsinusoidal currents in terms of the ratios and the phase angles of transformation for the fundamental and for the harmonic components of the current being measured. The approximations used in deriving eq 22 hold true for all of the transformers tested during this investigation except two which were intentionally of poor design. For these two transformers the maximum error introduced by the approximations was less than 0.04 percent.

## III. APPARATUS AND PROCEDURE

The apparatus [3] regularly employed at the National Bureau of Standards in testing current transformers was used in the experimental work of this investigation. For the usual measurements with this apparatus the detector is a single vibration galvanometer which is sensitive only to the fundamental frequency of the current being used. During the present investigation the current wave form was varied from the sinusoidal by the introduction of a third harmonic. It was therefore necessary to provide an alternate detector sensitive to the third harmonic. This was the only addition to the apparatus regularly employed in testing current transformers.

The source of the current used in the experimental work consisted of two revolving-field alternating-current generators mounted on the same shaft with a direct-current motor which was supplied from a storage battery. The rated frequencies of the generators were 60 and 180 cycles per second, respectively. The terminal voltages of the 60-cycle and the 180-cycle generators contained not more than 2 and 5 percent, respectively, of any harmonic under the conditions of load used for this investigation. The stator of the 180-cycle generator was mounted in such a way that it could be rotated with respect to the stator of the 60-cycle generator through 180 electrical degrees of the 60-cycle generator.

Three different wave forms of primary current were used in the experimental work: (a) sinusoidal; (b) peaked, consisting of the fundamental plus a 20 percent third harmonic, the positive crest of the fundamental coinciding with a positive crest of the harmonic; (c) flat top, consisting of the fundamental plus a 20 percent third harmonic, the positive crest of the fundamental coinciding with a negative crest of the harmonic (see fig. 1 for sketches of these three wave forms). The sinusoidal wave form was obtained by using the 60-cycle generator only. The nonsinusoidal wave forms were obtained by connecting the stators of the two generators in series. The amplitude and phase of the third harmonic were adjusted by varying the field excita-

[3] For a complete description of this apparatus, see BS J. Research 11, 93 (1933) RP580.

tion of the 180-cycle generator and the angular position of its stator. The amplitude of the third harmonic was measured with a wattmeter whose current coils were connected in the secondary circuit of the transformer being tested and whose voltage circuit was connected to an independent 180-cycle source whose phase relation with respect to the test supply could be controlled. This phase relation was adjusted to give maximum deflection on the wattmeter. By using this maximum value of watts and the known value of 180-cycle voltage impressed on the voltage circuit of the wattmeter, the rms value of the 180-cycle component of current in the secondary circuit of the current transformer was computed. The phase relation between the third harmonic and the fundamental was observed by viewing the wave form of the secondary current on a galvanometer-type oscillograph.

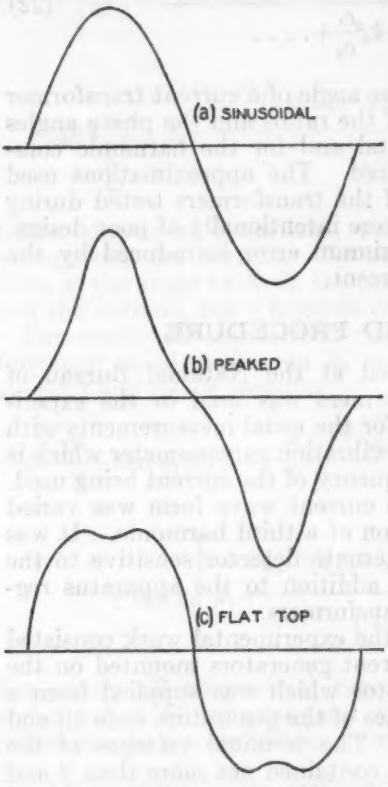


FIGURE 1.—*Drawings of the three wave forms used in the experimental work.*

Waves (b) and (c) each consisted of the fundamental, plus a 20-percent third harmonic.

The procedure in determining the effect of changing the current wave form upon the ratios and the phase angles of current transformers was first to measure the ratio and the phase angle of the transformer in the customary manner at six values of secondary current, using a current of sinusoidal wave form. Then another set of measurements was made with all conditions duplicated except that a current of peaked wave form was used. In this second set of measurements two values of ratio and phase angle were obtained for each setting of the secondary current, one being the ratio and phase angle between the fundamental components of the primary current and the secondary current and the other between the third harmonic components. These values were obtained using the 60-cycle and the 180-cycle vibration galvanometers, respectively. A third set of measurements was next made in the same manner as the second set except that a current of flat-top wave form was used. The ratios and the phase angles of the current transformer for nonsinusoidal currents were computed from the ratios and phase angles for the fundamental and for the third harmonic by means of eq 7 and 22, respectively. This procedure was duplicated for each transformer tested and for some transformers it was repeated using a different arrangement of primary leads.

Since the Silsbee current-transformer testing set is a well-known and widely used apparatus for comparing the ratios and phase angles of two transformers of the same nominal ratio, it was deemed ad-

visable to check the performance of one of these sets, using a non-sinusoidal current. Two transformers of the same nominal ratio were chosen and their ratios and phase angles were first measured by the absolute method as described above for the three different wave forms. Then the ratios and phase angles of these transformers were compared by means of a Silsbee testing set, using in succession currents of each of the three wave forms used in the absolute measurements. The results of this test indicate how nearly sinusoidal the current should be in order to obtain a given accuracy of measurement when using one of these testing sets.

## IV. RESULTS AND CONCLUSIONS

Seven current transformers, having various core shapes and arrangements of windings and primary current ratings up to 2,000 amperes, were tested according to the procedure just outlined. The results on a few of these transformers were chosen as being sufficient to indicate

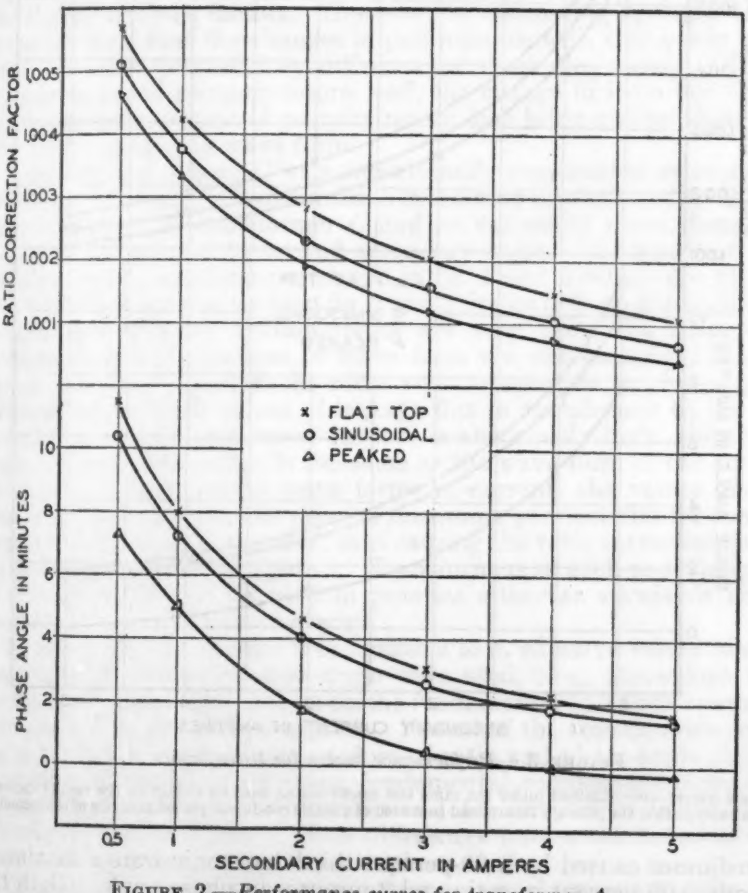


FIGURE 2.—*Performance curves for transformer A.*

Nominal ratio 2000:5. Burden 0.4 ohm and 310 microhenries. Frequency 60 cycles per second. Rectangular-shaped core with two secondary coils of 200 turns each on opposite legs of the core. Primary circuit consisting of a single straight conductor through the center of the core window and four return leads uniformly spaced around the central conductor.

the magnitude of changes in ratio and phase angle when the wave form departs from the sinusoidal. These results are shown by the curves of figures 2 to 5.

The results on transformer *A*, shown in figure 2, were chosen as being typical of commercial current transformers of good design for large currents. The distortion of a sine wave caused by the introduction of a 20-percent third harmonic can easily be detected by visual observation of the wave on an oscillograph. With distortions of this magnitude, it is even possible to estimate the magnitude and phase relation of the harmonic by visual observation (see fig. 1). However, as shown by the curves of figure 2, the changes in performance of this

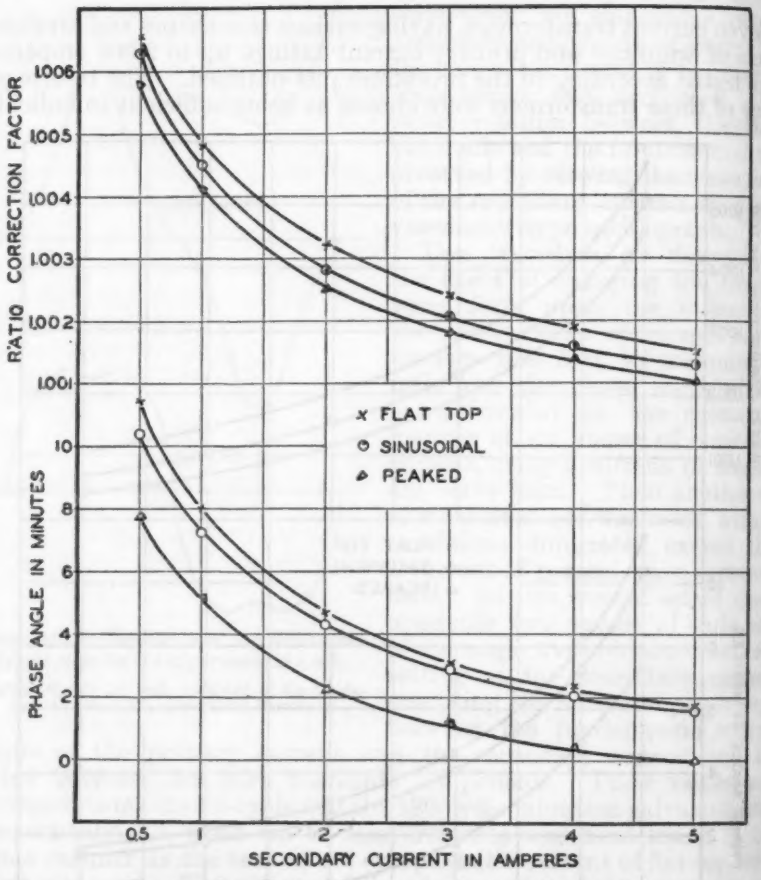


FIGURE 3.—*Performance curves for transformer A.*

These curves were obtained under the same test conditions as used for obtaining the results shown in figure 2 except that the primary return lead consisted of a single conductor placed near one of the secondary coils.

transformer caused by a 20-percent third harmonic were a maximum of only 0.05 percent in ratio and 2 minutes in phase angle. Both the ratio and the phase angle are greater for a flat-top wave form than for a sinusoidal wave form and less for a peaked wave form. These results may be accounted for by the following reasoning. The wave

form of the primary current and the secondary current of a well-designed current transformer is essentially the same as the wave form of the voltage induced in the windings by the core flux. If this wave form is changed from sinusoidal to peaked, keeping the effective value constant, the average value will be less. A lower value of average induced voltage requires a lower maximum value of core flux and less exciting ampere-turns, thus decreasing the ratio and the phase angle. If the wave form is changed from sinusoidal to flat top the effect will be the opposite.

The results shown in figure 3 were obtained from the same transformer and under the same test conditions as the results shown in figure 2, except that the primary return lead was arranged in such a way as to produce a large value of primary leakage flux in one leg of the core. Under these conditions the performance [4] of a current transformer involves a number of factors which are not readily predictable, and changing the wave form further complicates the predictability of these factors. However, by comparing figures 2 and 3 it can be seen that the changes in performance with changes in wave form are only very slightly different for these two widely different arrangements of primary return lead, the change in ratio due to the change in arrangement of primary return lead being greater than that due to the change in wave form.

Transformers *B* and *C* were intentionally constructed as examples of very poor design. Transformer *B* had a very low value of secondary ampere-turns and transformer *C* had an extremely nonuniform distribution of primary turns and secondary turns. The results of the tests on these transformers (shown in fig. 4 and 5 which are plotted to a much less open scale than fig. 2 and 3) indicate that, although their general performance characteristics are very poor, the changes in performance with changes in wave form are not excessive, being a maximum of 0.2 percent in ratio and 20 minutes in phase angle. Because of the high values of leakage flux in transformer *C*, the flux density in certain sections of its core is abnormally high. Since the wave form of leakage flux is the same as the wave form of the current producing it, for peaked wave forms of current, the values of core flux density go beyond the point of maximum permeability for secondary currents above 3 amperes, thus causing the ratio correction factor to increase, as shown in figure 5. Transformers of such poor design as *B* and *C* would not be used in practice either as standards or for measurements of power or energy.

In all of the results shown in figures 2 to 5, effective values of ratio correction factor and phase angle were used, i. e., the values were computed from measurements on the fundamental and third-harmonic component by use of eq 7 and 22. For all of the transformers tested except *B* and *C*, the effective values of ratio and phase angle differed from the values obtained using fundamental components only, by a maximum of 0.01 percent in ratio and 1.5 minutes in phase angle. For transformers *B* and *C* these differences were a maximum of 0.13 percent in ratio and 12 minutes in phase angle.

The ratios and phase angles of two commercial current transformers (nominal ratio 100:5) of good design were compared by means of a Silsbee current-transformer testing set, using each of the three different wave forms of primary current used in the previous tests. It was

[4] See pages 370 and 371 of J. Research NBS 14 (1935) RP775.

found that the results using the testing set (to the limits of its accuracy) agreed with the results obtained by the absolute method.

The detector of a Silsbee testing set consists of a separately excited galvanometer. Its moving coil is connected in the detector circuit. Its fixed coil is supplied by an external circuit whose frequency and (for this investigation) wave form are the same as those of the supply voltage being used for the transformer testing. A phase-shifting

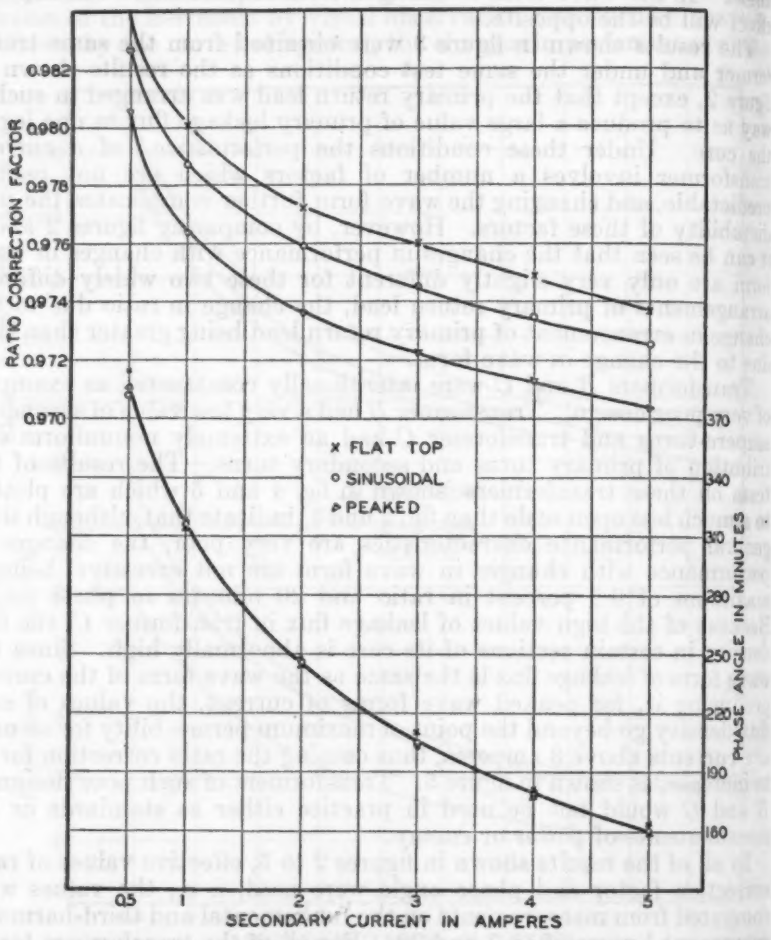


FIGURE 4.—*Performance curves for transformer B.*

Nominal ratio 50:5. Burden 0.16 ohm. Rectangular-shaped core with 38 secondary turns uniformly distributed around it. Four primary turns, one around each leg of the core.

transformer in the supply circuit for the galvanometer excitation serves as a means of adjusting the phase relation between the exciting current and the primary current of the transformers being tested. A balance is obtained by adjusting alternately the ratio and the phase-angle dials of the testing set while the phase-shifting transformer is set for each alternate adjustment to give sensitivity for the quantity indicated by the dial being adjusted.

A balance obtained by means of such a detector may reasonably be expected to depend not only upon the relation between the fundamental components of the currents being compared but also, at least to a slight extent, upon any harmonic components present in these currents. Since the phase relation between the fundamental and the harmonic components may be quite different for the galvanometer exciting current than for the current being detected, the extent of the

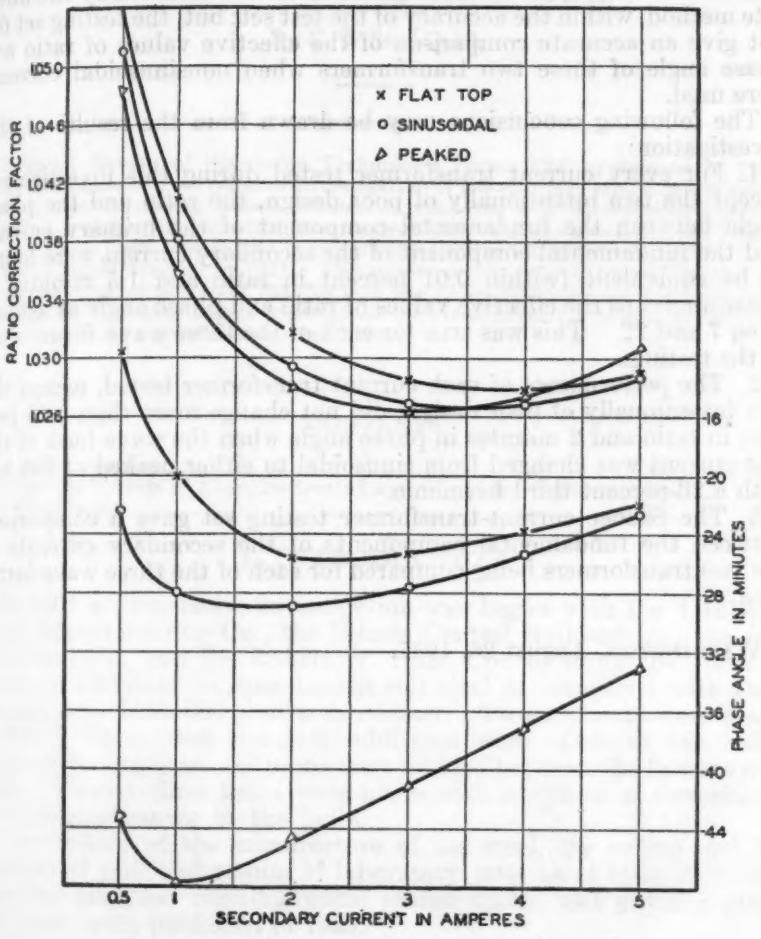


FIGURE 5.—*Performance curves for transformer C.*

Nominal ratio 100:5. Burden 0.4 ohm and 310 microhenries. Rectangular-shaped core with one secondary coil of 200 turns around one leg of the core. Primary circuit consisted of 10 turns on opposite leg of the core.

effect of the harmonic components on the detector balance cannot readily be derived. It was decided that the magnitude of such an effect could be measured experimentally more readily than it could be calculated theoretically.

For the two commercial current transformers of good design whose performance characteristics were compared by the use of a Silsbee testing set, the differences between the effective values of ratio and

phase angle and the values obtained using fundamental components only were too small to discriminate which of the two types of values was being indicated by the testing set.

In order to determine this, transformer *C*, the one of poor design referred to above, was compared with a transformer of good design by use of the testing set. The results showed that the testing set gave a comparison of the ratios and phase angles of the fundamental components of the currents, which agreed with that obtained by the absolute method, within the accuracy of the test set; but, the testing set did not give an accurate comparison of the effective values of ratio and phase angle of these two transformers when nonsinusoidal currents were used.

The following conclusions may be drawn from the results of this investigation:

1. For every current transformer tested during this investigation except the two intentionally of poor design, the ratio and the phase angle between the fundamental component of the primary current and the fundamental component of the secondary current were found to be equivalent (within 0.01 percent in ratio and 1.5 minutes in phase angle) to the effective values of ratio and phase angle as defined in eq 7 and 22. This was true for each of the three wave forms used in the testing.

2. The performance of each current transformer tested, except the two intentionally of poor design, did not change more than 0.05 percent in ratio and 2 minutes in phase angle when the wave form of the test current was changed from sinusoidal to either peaked or flat top with a 20-percent third harmonic.

3. The Silsbee current-transformer testing set gave a comparison between the fundamental components of the secondary currents of the two transformers being compared for each of the three wave forms used.

WASHINGTON, August 26, 1937.

U. S. Department of Commerce National Bureau of Standards

RESEARCH PAPER RP1042

*Part of Journal of Research of the National Bureau of Standards, Volume 19, November 1937*

# SERVICE-TEST RESULTS OF TITANIUM-TREATED AND SILICON-TREATED STEEL RAILS

By G. Willard Quick

ABSTRACT

National Bureau of Standards Technologic Paper T241, published in 1923, gives the results of a cooperative investigation of the effects of titanium treatment on the properties of open-hearth rail steel as compared with those of silicon-treated rail steel. Rails from the titanium-treated heats and from comparison silicon-treated heats were laid in the tracks of the Illinois Central Railroad Co. (now Illinois Central System) in 1921. The service results reported for these rails are given in this paper and show that for rails laid in heavy-traffic territory, a slightly larger percentage of titanium-treated rails remained in service after 15 years than of the comparison or silicon-treated rails.

CONTENTS

| | Page |
|---|---|
| I. Introduction | 531 |
| II. Service records of titanium-treated and silicon-treated steel rails | 532 |
| III. Summary | 533 |

## I. INTRODUCTION

In 1921 a cooperative investigation was begun with the Titanium Alloy Manufacturing Co., the Illinois Central Railroad Co., the Illinois Steel Co., and the Robert W. Hunt Co., to study the effect of titanium additions in open-hearth rail steel as compared with steel treated with ferrosilicon as a deoxidizer. Twenty heats were made to which ferrocarbon-titanium additions were made in the ladle, while ferromanganese additions were divided between the furnace and ladle. Twenty-three heats were made with additions of ferrosilicon and ferromanganese in the ladle.

Descriptions of the manufacture of the steel, the rolling and inspection of rails and results of laboratory tests on *A* rails, including chemical analyses, metallographic examinations, and physical-property tests, were published in 1923.[1]

The laboratory tests showed that the top ends of the *A*-rails from titanium-treated steel ingots were much less segregated than the top ends of *A*-rails from silicon-treated steel ingots. It was found, however, that piping, as shown by inspection of the top ends of the *A*-rails, was more prevalent in the titanium-treated than in the silicon-treated steel. As a whole, there was not as much improvement in mechanical properties from titanium treatment as might be expected from the decreased segregation, and the improvement in the steel

[1] George K. Burgess and G. Willard Quick. *A comparison of the deoxidation effects of titanium and silicon on the properties of rail steel.* Tech. Pap. BS 17, 581 (1922-24) T241.

was confined largely to the upper portion of the ingot, the effects disappearing before the *B*-rail was reached. The results of the investigation were summarized in Technologic Paper 241 as follows:

1. A higher percentage of piped rails come from titanium- than from silicon-treated rails, but the time of teeming affects the number of pipes. The greatest number of pipes were in rails from steel treated with the smaller amount of ferrocarbon-titanium per ton, and variations in the amount above this did not seem to affect the pipe.

2. The titanium-treated rails were harder to break and showed more uniform fractures in the drop test than those treated with ferrosilicon.

3. The titanium additions compared with the silicon additions had a marked effect in reducing the segregation of carbon at the top of the ingot. This improvement was approximately proportional to the titanium additions, but the effect falls off rapidly at the bottom ends of the *A*-rails.

4. Nitrogen determined by the Allen method decreases as the residual titanium in the steel increases. This indicates that less nitrogen is combined with iron and manganese, not that the nitrogen has been eliminated, but that it probably is combined with titanium or silicon.

5. The addition of from 8 to 10 pounds of ferrocarbon-titanium per ton causes an immediate and appreciable drop in the amount of oxides reducible by carbon, while for additions of more than this amount the oxides reducible by carbon are entirely lacking.

6. Titanium treatment is shown by sulphur prints to lessen segregation of sulphur, particularly in the drop-test pieces, and in samples from the top ends of the *A*-rails, where this segregation is most prevalent in the silicon-treated rails. This condition was checked by etching specimens in boiling hydrochloric acid, which showed streaks in many of the silicon-treated pieces, whereas the pieces treated with titanium remained practically free from streaks.

7. Rail sections from the top of the ingots from titanium-treated heats were more uniform in hardness than those from similar positions in silicon-treated heats. This effect had entirely disappeared at the bottom of the ingot.

8. The results of tensile, impact, and endurance tests did not show as much improvement from titanium treatment as was expected from the decreased segregation. There was somewhat more uniformity in mechanical properties at the top ends of *A*-rails from titanium- than from silicon-treated heats. At the bottom ends of *A*-rails not much improvement was shown by titanium treatment.

9. Steel treated with from 8 to 10 pounds of ferrocarbon-titanium per ton retains about 19 percent of the titanium and steel treated with from 10 to 13 pounds, about 33 percent, whereas the silicon-treated steel retains about 81 percent of the silicon. The smaller amount of titanium remaining in the steel treated with from 8 to 10 pounds of ferrocarbon-titanium per ton is retained in the form of violet inclusions, perhaps of titanium oxide and some of a lower nitrogen compound of titanium, and for treatments with larger amounts much more titanium is retained as similar violet inclusions, and, in addition, in the form of orange inclusions, probably a higher nitrogen compound of titanium.

10. In the titanium-treated steel the sulphide inclusions were more broken up and scattered than in the silicon-treated steel, and this effect is dependent upon the retention of titanium in the steel.

## II. SERVICE RECORDS OF TITANIUM-TREATED AND SILICON-TREATED STEEL RAILS

According to the program of the investigation, 1,000 tons each of the titanium-treated and the silicon-treated steels, from the heats described in Technologic Paper 241, were laid in the tracks of the Illinois Central Railroad in 1921. The rails were 90 lb 33 ft ARA section 9020.

All of the titanium-treated rails were laid in groups in heavy traffic, whereas only half of the silicon-treated rails were laid in heavy traffic, the other half in intermediate traffic. Recently, at the request of the National Bureau of Standards, A. F. Blaess, Chief Engineer, Illinois Central System (formerly Illinois Central Railroad

Co.) furnished a report on the service of these rails over a period of 15 years. Service records on rails from 20 other titanium-treated heats and on rails from 92 other untreated heats, (not treated with titanium) over a period of 16 years, were also supplied. The complete report follows:

15.38 track miles of this rail (titanium treated) were laid in 1920 and 1921; 6.71 track miles of it have been removed for various reasons, mainly worn out on curves and removed in regular rail program.

Transverse fissures in titanium-treated rail and ordinary untreated of the same rollings compared:

| Treatment | Date rolled | Mill | Weight and section | Number of heats | Transverse-fissure rails |
|---|---|---|---|---|---|
| Titanium treated * | 2-1920 | Gary | 90-ARA-A | 20 | 7 |
| Untreated * | 2-1920 | do | 90-ARA-A | 92 | 177 |
| Titanium treated | 2-1921 | do | 90-ARA-A | 20 | 0 |
| Untreated | 2-1921 | do | 90-ARA-A | 23 | 8 |

* These heats are additional to those described in Technologic Paper 241.

Comparison on basis of per 100 track miles (laid) per year:

Titanium treated ..... 3.5 transverse-fissure rails.
Untreated ..... 25.1 transverse-fissure rails.

Records were not kept separately of other kinds of rail failures, but no difference was noted. Both the treated and untreated rail have some corrugation and measurements of contours show very little difference in amount of wear.

In the 92 heats of untreated rail rolled in 1920, 27 heats have been entirely without transverse fissures, and the test can hardly be regarded as conclusive as to the effect of the titanium treatment.

For the rails rolled in 1921 (Tech. Pap. 241), from titanium-treated and silicon-treated heats, the following additional data were furnished:

| | *Track miles* |
|---|---|
| Titanium treated rail rolled and laid in groups at several locations in heavy-traffic territory | 7.76 |
| Remaining in track at original locations | 3.69 |
| Untreated rail from same rolling laid in 1921 in groups at several locations, one-half tonnage in heavy-traffic territory and one-half in intermediate-traffic territory | 8.9 |
| Remaining in track at original locations, one-third in heavy-traffic territory and two-thirds in intermediate-traffic territory | 4.75 |

According to the report quoted above, 52.5 percent of the titanium-treated rails, described in Technologic Paper 241, were removed for various reasons between 1921 and 1936, whereas during the same period, 64.5 percent of the untreated rails laid in heavy traffic were removed for various reasons.

## III. SUMMARY

1. To supplement laboratory studies, service tests of titanium-treated open-hearth steel rails and comparison silicon-treated steel rails, all prepared under careful supervision, were started in 1921, the rails being placed in the regular service lines of the Illinois Central Railroad Co.

2. Up to date, no transverse fissures have been reported in the rails from the 20 heats of titanium-treated steel and 8 transverse fissures in the comparison rails from the 23 heats of silicon-treated

steel. However, in rails purchased independently by the Illinois Central Railroad Co. and installed a year previously, 1920, in similar service, 7 transverse fissures have been reported up to date in the rails from 20 heats of titanium-treated steel and 177 transverse fissures in comparison rails from 92 heats of steel not treated with titanium.

3. During 15 years of service in heavy traffic, 52.5 percent of the titanium-treated rails were removed for various reasons, whereas 64.5 percent of the comparison silicon-treated rails were removed during the same period.

WASHINGTON, August 12, 1937.

U. S. Department of Commerce National Bureau of Standards

RESEARCH PAPER RP1043

*Part of Journal of Research of the National Bureau of Standards, Volume 19, November 1937*

# STRESS-STRAIN CHARACTERISTICS OF WOOL AS RELATED TO ITS CHEMICAL CONSTITUTION

By Arnold M. Sookne and Milton Harris [1]

**ABSTRACT**

An apparatus for studying the extensibility of single wool fibers is described. Data on the effects of the tanning (quinone), dyeing, and deamination processes, and of neutral salts on the extensibility of wool fibers are reported. The results indicate that the extensibility of the wool fibers is governed, for the most part, by factors which influence the swelling or hydration of the protein. Salt linkages of the type which might be formed by an attraction between the free amino and carboxyl groups in wool do not appreciably contribute to the physical stability of the fiber in aqueous solutions.

CONTENTS

| | Page |
|---|---|
| I. Introduction | 535 |
| II. Description of apparatus and method | 536 |
| III. Results and discussion | 539 |
| 1. Effect of tanning | 539 |
| 2. Effect of dyeing with acid dyes | 541 |
| 3. Effect of deamination | 542 |
| 4. Effect of neutral salts | 545 |
| IV. Relation of swelling to the extensibility of wool | 546 |
| V. Summary | 547 |
| VI. References | 549 |

## I. INTRODUCTION

The classical view of protein structure, based on the work of Emil Fischer and his contemporaries, is that the protein molecule is a polypeptide composed of a series of amino acids united through their carboxyl and amino groups. These earlier workers focused their attention on the isolation and identification of the protein constituents and obtained large amounts of information which supported this view. Their work was of great importance in protein chemistry, but from the standpoint of protein structure, and more especially, the structure of protein fibers, it proved of limited value until recently, when it was augmented by physical-chemical methods and X-ray studies.

The more recent advances in the X-ray studies of wool and similar materials have been made by Astbury and his collaborators [1] [2], whose investigations indicate that the fiber consists of long-chain molecules (polypeptides) which lie parallel to the fiber axis and which are held together by a variety of cross-linkages of the covalent and electrovalent types. That most of the covalent cross linkages in wool

[1] Research Associates at the National Bureau of Standards, representing the American Association of Textile Chemists and Colorists. This work was aided by grants from the Textile Foundation, Inc., and the Chemical Foundation, Inc.

[2] Numbers in brackets indicate literature references at the end of this paper.

are those of the disulfide groups of the amino acid, cystine, is at the present time generally accepted. On the other hand, little is known about the nature of the electrovalent forces.

As a result of a number of studies, principally on the changes in the extensibility of wool brought about by various treatments of the fiber, Speakman and Hirst [2] postulated the existence of electrovalent linkages between the free acid groups of the glutamic and aspartic acids and the free basic groups of the arginine, lysine, and histidine constituents of the polypeptides in wool, which they termed salt linkages. Presumably the attractive forces between the oppositely charged $R–COO^{-+}$ and $R–NH^{+}$ ions are reduced by water and for this reason the wool fiber is more easily stretched in water than in dry air. Similarly, they postulated that since acids and alkalies would depress the ionization of the free acid and basic groups which make up the salt linkage, they would increase the ease of stretching to an even greater extent.

The presence of salt linkages in various proteins has been suggested by different investigators and there appears to be some evidence for their existence. The question has arisen therefore as to whether salt linkages, formed by the attraction between the free amino and carboxyl groups, contribute appreciably to the physical strength of the wool fibers.

The results of studies on the extensibility of wool fibers are reported here for the purpose of further elucidating the nature of the electrovalent linkages in wool. In addition, some of the data have been applied to an interpretation of the tanning, dyeing, and deamination of wool.

## II. DESCRIPTION OF APPARATUS AND METHOD

The stretching of wool under load has been extensively investigated by Harrison [3], Karger and Schmid [4], Shorter [5], Astbury and Woods [6] and especially by Speakman [2, 7]. The general procedure has been to determine the load-elongation curves of fibers under various conditions. This procedure has been followed in the present work. The method employed is relatively simple and requires little equipment that is not generally available.

A sample of domestic wool was purified by successive extractions with alcohol and ether, followed by washing with water at about 40° C. The fibers were for the most part nonmedullated and were fairly uniform in width along the 4-cm length used in this work, the average width as measured at 20 places being about 35 microns. Before measuring the fiber width, each end of the fiber was attached to a platinum-iridium hook, weighing about 0.35 g, with asphalt (dissolved in chloroform) as the binding material. The measurements of the widths of the fibers were made in a room at 21° C and 65-percent relative humidity), using a projection microscope equipped with a heat filter, and giving a magnification of about 700 diameters. Duplicate determinations of the effective diameter of the same fiber checked to within 1 percent. In addition to this method for the direct determination of fiber width, the fibers were calibrated by a reextension method, described later in this section.

The fibers were always soaked for 24 hours at 21° C in the solutions in which they were to be stretched. Loads were applied to the fibers

and the extension was measured with the analytical balance and auxiliary equipment shown in figure 1. A fiber, *E*, of known length was attached to the left side of the balance beam, and the pointer of the balance was brought to the zero position by adding weights on the left-hand pan to counterbalance the rubber pad *G*. The lower hook on the fiber was then attached to the glass hook sealed to the bottom of the 250-ml Erlenmeyer flask *D* resting on the movable platform *F*.[3] Flask *D* contained enough of a given solution to assure complete immersion of the fiber during elongation. The load was applied by the addition of steel balls, each weighing $0.4392 \pm .0004$ g, to a sponge-rubber pad on the right-hand balance pan. The rubber pad contained small holes, each of which held one steel ball. The application of this stress causes an elongation of the fiber and a consequent leftward displacement of the pointer of the balance. By lowering platform *F*,

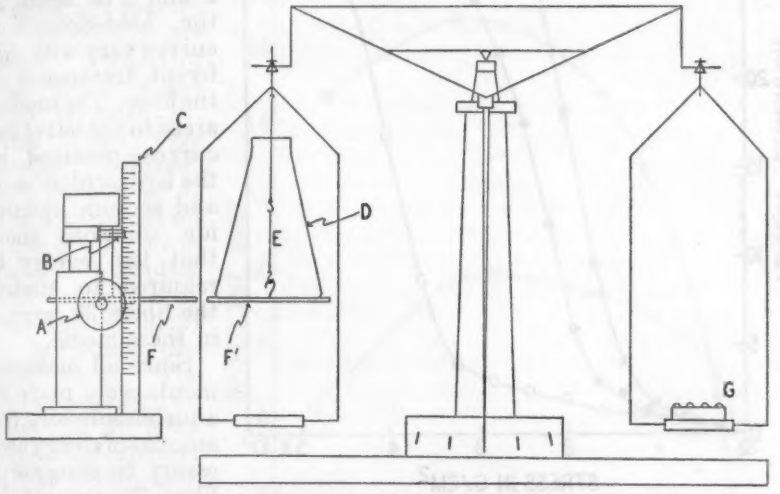


FIGURE 1.—*Apparatus for determining the load-elongation curves of single wool fibers.*

using thumbscrew *A*, the pointer was returned to the zero position, and the extent of vertical displacement was read on the scale *C* by the index *B*. Elongation was read in this manner to 0.1 mm. The balls were added at 30-second intervals, and readings of elongation were made 15 seconds after the addition of each ball. The rate of applying stress for the fibers studied was approximately $1 \times 10^5$ g/cm$^2$ min. The length at zero load was obtained by extrapolation, correcting for the weight of the lower hook. All load-elongation measurements were made at 21° C.

The method described above has several advantages in addition to its simplicity. The regular lowering of the platform maintains the fiber in an effectively vertical position, which assures application of the full apparent stress. The platform may be allowed to remain in position long enough to make an unhurried reading of the scale. Although the loading process is a discontinuous one, which at first sight appears to be a disadvantage, the reproducibility of the measurements and the sensitivity of the method show this type of loading to be satisfactory for the determination of the load-elongation curves.

[3] During operation, platform *F* is in position *F'*.

A typical load-elongation curve obtained with this apparatus for an untreated wool fiber in equilibrium with water at 21° C is shown in figure 2, curve 1. Speakman [7] has shown that such curves are most reproducible up to an elongation of 30 percent and that the area to the left of the curve, representing the amount of energy necessary to produce a given elongation, is a sensitive measure of changes in fiber extensibility. When the fibers are stretched beyond 30 percent, permanent alterations in their extensibility may occur.

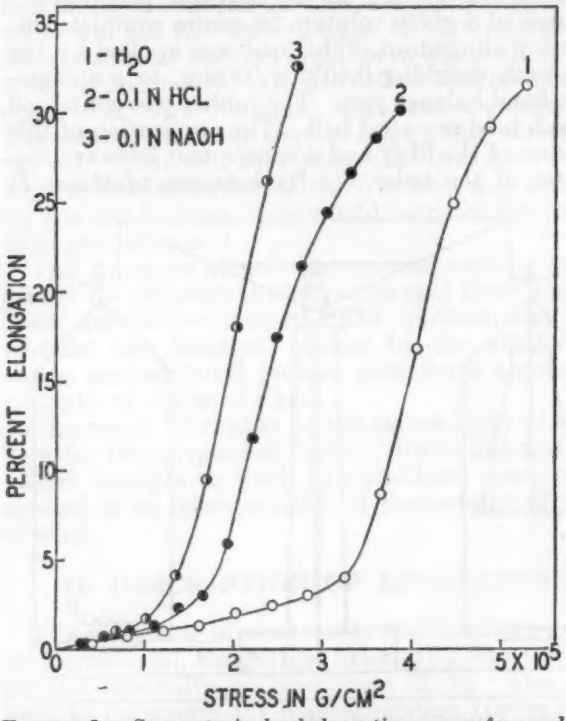


FIGURE 2.—*Stress-strain load-elongation curves for wool fibers immersed in water, and in acid and alkaline solutions.*

As shown in curves 2 and 3 of figure 2, the load-elongation curves vary with different treatments of the fiber. The smaller areas to the left of the curves obtained in the hydrochloric acid and sodium hydroxide solutions show that less energy is required to stretch the fibers 30 percent in these media.

Since all measurements were made in aqueous solutions, the amount of energy necessary to elongate a fiber 30 percent in distilled water (approximately pH 5.8) was taken as a standard. Comparison of the extensibilities of fibers in various solutions was facilitated by calculating the "30-percent index", which is defined as the ratio of the energy required to elongate a treated or untreated fiber 30 percent in a given medium to the energy which should be required to elongate the untreated fiber 30 percent in distilled water. Comparison of data by this method was limited to experiments in which the general shape of the curves was similar to that for an untreated fiber in distilled water.

It has been shown by Speakman [6] that fibers elongated 30 percent or less, after a 24-hour period of rest without load, will give load-elongation curves very nearly identical with the original curves. That the fibers used in this investigation possess this ability was demonstrated by reextending in distilled water, five individual fibers which 24 hours previously had been elongated 30 percent in distilled water. The mean value of their 30 percent indices was 0.996. Wherever possible, the fibers used in the present work were first extended 30 percent in distilled water and then allowed to rest without load for 24 hours. They were then reextended or subjected to some treatment

and reextended in a given medium. This procedure eliminated the necessity of measuring the cross-sectional area used to calculate the energies to a unit cross-sectional area. Fibers to be reextended by this method are referred to as "calibrated" fibers in this paper.

## III. RESULTS AND DISCUSSION

### 1. EFFECT OF TANNING

Much has been written about tanning and there are many different views as to the nature of tanning processes. However, it is generally accepted that the principal effect of tanning is to decrease the swelling of proteins in aqueous media. In tanning collagen to prepare leather, it has been shown [8] that the acid-combining capacity is appreciably reduced. Tanning appears to affect wool similarly. Wool fibers were treated (refluxed) for 3 days at 50° C with a saturated solution of quinone in about 50% alcohol, after which they were washed for 24 hr. in running distilled water. The quinone-tanned wool had an acid-combining capacity of 0.39 millimole/g, as compared to 0.80 millimole/g for the untreated fibers, which indicates that about half of the basic groups in wool reacted with the quinone.

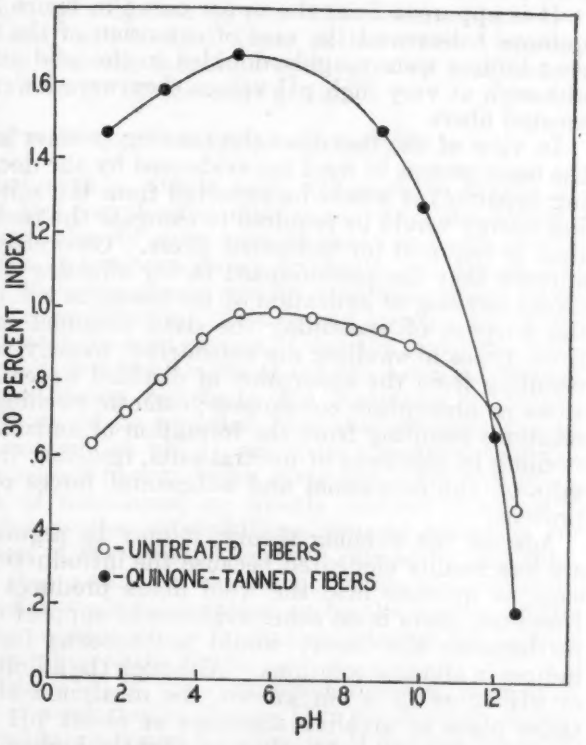


FIGURE 3.—*Effect of tanning with quinone on the extensibilities of wool fibers in solutions of different* pH.

Determinations of the 30-percent indices of untreated and quinone-tanned fibers in solutions having pH values ranging from about 1 to 12 are shown in figure 3. The curve for the untreated wool is similar to that obtained by Speakman and Hirst, which exhibits a region of maximum stability between about pH 5 and 7, a region of linear decrease in the 30-percent indices from pH 5 to 1 and a region above about pH 10 in which the 30-percent index decreases rapidly with increasing pH. The maximum region is somewhat smaller than that obtained by Speakman and Hirst in unbuffered solutions but very similar to that obtained by them using acids and alkalies in 0.2 *N* solutions of sodium chloride. Buffer solutions, prepared according to

Clark [9] were used in the present work, which probably accounts for the similarity of the shape of the curve obtained in the present work with that obtained in the presence of dilute solutions of sodium chloride.

The decrease in the 30-percent index of untreated wool in the acid solutions is practically reversible, since reextension of the fibers in distilled water after thorough washing yielded 30-percent indices of more than 0.98. Above pH 8, however, the degree of recovery of the fibers decreases with increasing pH. The 30-percent index of fibers extended in 0.1 *N* sodium hydroxide, washed, and reextended in distilled water was only 0.59. This is in agreement with the known susceptibility of the fibers to chemical degradation in the more-alkaline solutions.

It is apparent from the upper curve in figure 3 that tanning with quinone [4] decreases the ease of extension of the fibers. The 30-percent indices were roughly doubled in the acid and neutral solutions, although at very high pH values they were lower than those for untreated fibers.

In view of the fact that the tanning process has blocked many of the basic groups in wool (as evidenced by the decreased acid-combining capacity) it would be expected from the salt-linkage theory that less energy would be required to elongate the tanned fibers 30 percent than is required for untreated fibers. Obviously, this is not so. It appears that the predominant factor affecting the extensibility may be the swelling or hydration of the fibers, as will be shown later. For the purpose of explaining the data obtained in the present work, three types of swelling are considered; namely, imbibitional swelling resulting from the absorption of distilled water by wool to form solvates or absorption compounds; osmotic swelling, in acid or alkaline solutions resulting from the formation of ionizable protein salts; and swelling in solutions of neutral salts, resulting from the effect of the salts on the cohesional and adhesional forces of the water and the protein.

Against the swelling theory, it may be argued that tanned fibers are less readily elongated because the introduction of large molecules such as quinone into the wool fibers produces new cross linkages. However, there is no other evidence in support of such a theory and furthermore the theory would not account for the low 30-percent indices in alkaline solutions. Although the affinity of wool for quinone at pH 12 or 13 is not known, the maximum absorption of quinone takes place in alkaline solutions at about pH 8 to 11 [10], and it hardly seems probable that at slightly higher pH values the wool would lose all of its affinity for the quinone. A more probable mechanism for the behavior of the tanned fibers is that, in acid solution, less acid is bound by the tanned fibers than by untreated fibers and there is accordingly less osmotic swelling, whereas in alkaline solution, the carboxyl groups, which presumably are unaffected by the quinone are capable of binding as much alkali as untreated fibers. Thus the normal swelling would take place in alkaline solution in addition to the chemical degradation which is known to occur under these conditions.

[4] As indicated by alkali-solubility determinations, no significant amount of oxidation has occurred during treatment with quinone.

It is interesting to note that the decrease in 30-percent index for the tanned fibers from pH 5 to about pH 1 is about half that for the untreated fibers between the same pH values. The fact that the tanned wool used for these experiments had only about one-half of the acid-combining capacity of the untreated wool is evidence that the extensibility of the fibers in this pH region is proportional to the amount of acid combined, as previously noted by Speakman and Stott [11]. This immediately suggests that at least two effects result from the tanning of wool with quinone; namely, the reaction of a portion of the basic groups with the quinone, which decreases the acid-combining capacity, thus decreasing the Donnan effect (osmotic swelling) in acid solutions, and the reaction of wool with quinone in a manner which decreases the swelling that occurs in water alone (imbibitional swelling), as indicated by the difference in 30-percent indices of the untreated and tanned fibers in the neutral region. This is also in keeping with the fact that wool takes up much more quinone than is accounted for by the basic groups.

### 2. EFFECT OF DYEING WITH ACID DYES

The dyeing of wool with a simple acid dye such as orange II appears to involve a less complicated mechanism than the tanning process. Although wool absorbs more quinone than can be accounted for by the basic groups, it has been shown by Smith and Harris [12] that it absorbs only 1 molecule of acid dye for each basic group when the dyeing is carried to equilibrium. The dyeing appears to be the result of the interaction of the acid groups of the dye molecules with the basic groups in wool, but the nature of the wool-dye compound is not known. If the dyeing results in the formation of highly ionized compounds, it would be expected that the extensibilities of the dyed fibers, for example at pH 1, would be approximately the same as those of untreated fibers at the same pH. On the other hand, the formation of nonionized or weakly ionized compounds would appreciably change the extensibilities in acid solutions by decreasing that portion of the osmotic swelling caused by the acid. It seemed, therefore, that a study of the extensibilities of completely dyed fibers [5] would offer some information as to the nature of the wool-acid dye complex in addition to further elucidating the factors which affect the extensibility of the fibers.

Single fibers were calibrated by the reextension method, then dyed for 20 hours at 50° C in a solution of Orange II in 0.1 *N* hydrochloric acid. (The stock-solution contained 5 millimoles of dye per liter and sufficient solution was used to assure an excess of dye. It has been shown [12] that under these conditions, wool absorbs about 0.8 millimole of dye per gram.) The fibers were washed in running distilled water for one hour and then allowed to remain in buffer solutions for 24 hours, after which they were reextended. The results given in table 1 show that the extensibilities of the completely dyed fibers in acid solutions are very similar to those of untreated fibers in distilled water. The basic groups not only appear to be blocked by the dye molecules, but they are at the same time rendered practically inactive.

[5] Fibers dyed under such conditions that all of the basic groups have reacted with dye molecules [12].

TABLE 1.—*Comparison between the 30-percent indices at different* pH *values of untreated wool fibers and fibers dyed to equilibrium with orange II, when extended in buffer solutions of different* pH *values*

| pH | 30-percent index | |
|---|---|---|
| | Dyed fibers | Untreated fibers |
| 1.42 | 1.01 | 0.66 |
| 2.98 | 1.01 | .81 |
| 4.95 | 0.99 | .98 |
| 6.90 | .88 | .99 |

In other words, when untreated wool is put in acid solutions, heteropolar compounds of wool and acid are formed, which facilitate extension of the fibers (by increasing osmotic swelling), whereas, when completely dyed, the wool and dye appear to form compounds which approach homopolar compounds in their behavior.

Unfortunately, the 30-percent indices of the dyed fibers could not be determined in alkaline solutions because of the reversal of the dyeing process. The somewhat low 30-percent index for the dyed fibers in solutions at pH 6.9 indicates a shift in stability to the more acid region.

### 3. EFFECT OF DEAMINATION [6]

It would appear on first sight that the influence of the basic groups on the extensibility of wool could best be studied by comparing the properties of untreated and deaminated fibers. This would have the obvious advantage of eliminating the introduction into wool of new molecules, such as occurs in the tanning and dyeing processes. As will be shown later, however, the action of nitrous acid on wool is not limited to the amino groups, and as a result the value of this method of attack is somewhat questionable.

The deamination process has been frequently used by various investigators for the purpose of studying the role of the amino groups in wool. An investigation of the effect of nitrous acid on wool revealed two principal weaknesses in this method, namely, that it is impossible to completely deaminate wool in a reasonable length of time, and that the state of the sulfur of the cystine in wool is altered during deamination.

It has been shown [13, 14] that deaminated proteins retain a considerable portion of their acid-combining capacities, even after prolonged treatment with nitrous acid. Experimental results indicate that there is a sudden drop in acid-combining capacity after a very short treatment with nitrous acid, followed by a very slow decrease in the acid-combining capacities during the continued treatment. This is in agreement with the results of Rutherford, Harris, and Smith [15], who studied the rates of evolution of nitrogen from various proteins during treatment with nitrous acid and found that there is a primary reaction with a rapid rate of evolution of nitrogen, followed by a secondary reaction with a very much slower evolution of nitrogen.

[6] In the present paper, deamination refers only to removal of amino groups with nitrous acid and has no quantitative significance as to the extent or completeness or their removal.

The effect of the deamination process on the state of the sulfur in wool practically precludes the making of rigorous comparisons between the untreated and deaminated fibers. Harris and Smith [16] have recently shown that during treatment with oxidizing agents, the disulfide sulfur appears to be changed to higher states of oxidation, the existence of oxidation derivatives being indicated by four different methods. Nitrous acid is an active oxidizing agent and, as such, should also be capable of at least partial oxidation of the sulfur in wool. That oxidation does occur during deamination is indicated by three [7] of the methods used by Harris and Smith. The deaminated wool gave a negative lead acetate test,[8] and showed increasing alkali-solubilities and decreasing cystine contents with increasing time of deamination.

In view of these apparent difficulties, it was necessary to reinvestigate the extensibility of deaminated fibers from the standpoint of the different reactions which may occur during deamination. Wool fibers were treated for different lengths of time at 20° C with a solution of nitrous acid (one volume of glacial acetic acid to four volumes of a solution containing 30 g of sodium nitrite in 100 ml of water), the ratio of solution to wool being approximately 500 to 1. The fibers were thoroughly washed in running distilled water and their 30-percent indices in solutions of different pH values determined. The results are recorded in table 2.

From the foregoing discussion on the reactions of wool with nitrous acid, at least two effects of the deamination process on the extensibility of wool fibers may be expected, namely, an increase in 30-percent index in acid solutions caused by a reduction in osmotic swelling resulting from loss of amino groups and corresponding acid-binding capacity, and a decrease in 30-percent index caused by oxidation of the disulfide groups and the subsequent weakening of the bonds between the disulfide sulfur atoms. The latter effect should increase with increasing pH, since it has been shown by Lavine [17] and Toennies [18] that the stability of the intermediate oxidation derivatives of cystine decreases with increasing pH.

TABLE 2.—*The 30-percent indices of wool fibers which have been deaminated for different lengths of time with nitrous acid*

| Duration of treatment with $HNO_2$ | 30-percent indices | | | |
|---|---|---|---|---|
| | pH 1.1 | pH 4.0 | pH 7.0 | pH 12.0 |
| *Hours* | | | | |
| 0 | 0.66 | 0.93 | 0.98 | 0.76 |
| 3 | .72 | .85 | .75 | .48 |
| 24 | .73 | .85 | .73 | .39 |
| 48 | .74 | .84 | .68 | .29 |
| 96 | .74 | .84 | .64 | .28 |
| 192 | .72 | .80 | .62 | .21 |

An examination of the data in table 2 shows that the results of these experiments are in agreement with the above-mentioned postulates. The 30-percent indices of all of the deaminated fibers are

[7] The fourth method, namely, reduction with hydrochloric acid-potassium iodide solutions, could not be used because of interference from what appeared to be nitroso derivaties formed during deamination.

[8] Samples of wool were prepared for this test by deamination at 0 to 5° C to prevent excessive yellowing of the wool.

greater at pH 1.1 than are those of the untreated fibers. At this pH, the inhibition of osmotic swelling resulting from loss of amino groups (the acid-combining capacity of the deaminated fibers is roughly half of that for untreated fibers) is the predominant factor, the partially oxidized disulfide groups being moderately stable at this pH. At pH 4 the 30-percent indices are slightly lower than for the untreated fibers. Since the number of basic groups in the deaminated wool is far greater than the number of moles of acid bound by wool at pH 4, it is to be expected that there should be very little difference between the osmotic swelling of the treated and untreated fibers. However, at this pH the instability of the oxidized sulfur groups becomes appreciable [17], thus accounting for the lowering of the 30-percent indices of the deaminated fibers. At the higher pH values, the differences become even more pronounced since the instability of the oxidized sulfur groups increases rapidly in alkaline solutions. The effects of the prolonged treatments with nitrous acid are especially noticeable at pH 7 and above. Fibers deaminated for 48 hours or longer and stretched in solutions at pH 12 no longer gave load-elongation curves similar to those for untreated fibers.

According to Speakman and Stott [13], "the resistance of wool fibers to extension is less in acid solution than in water, owing to the rupture of salt linkages between peptide chains. Similarly, deaminated fibers are less resistant to extension in water than untreated fibers, the reduction in the resistance to extension being dependent on the extent of deamination.—*A critical test for complete deamination is to be found in the fact that completely deaminated fibers should be no more difficult to stretch in water than in hydrochloric acid solution at pH 1.*" [Italics ours.] In addition, Speakman and Stott presented data which presumably indicated that the load-extension curve of completely deaminated fibers in distilled water and at pH 1 are almost identical.

The results of the present investigation show that the extensibilities of deaminated fibers cannot be used as a measure of the completeness of deamination. Deaminated fibers were found to be more resistant to extension in a solution of pH 1.1 than untreated fibers in spite of the apparent attack on the sulphur groups, which indicates that the main effect at this pH is the lowering of the osmotic swelling by reducing the amount of acid bound by the wool. The ease of extension of the deaminated fibers in neutral solution (pH 7.0) increases relatively rapidly with increasing duration of deamination, whereas at pH 1.1 the fibers at first become slightly more difficult and then slightly easier to stretch. In other words, the extensibilities of deaminated fibers in solutions of pH 1 and pH 7 are not the same nor are the changes which are produced in the ease of extension in the two solutions, the result of the same reaction. It follows then that complete deamination cannot be defined in terms of the extensibility of wool. It appears that Speakman and Stott's [13] conclusion that wool fibers may be "completely deaminated" by 50 hours' treatment with the Van Slyke reagent was the result of a coincidence in which they obtained practically identical load-elongation curves for a deaminated fiber in distilled water and at pH 1. As was previously pointed out, the 30-percent indices for deaminated fibers at pH 1.1 are almost constant, while those obtained at pH 7 decrease with increasing duration of treatment with nitrous acid. It should be noted that extend-

ing strongly deaminated fibers more than once is a questionable procedure and as a result at least three fibers, previously calibrated and then deaminated, were used for each determination shown in table 2.

### 4. EFFECT OF NEUTRAL SALTS

In addition to the effect produced by acids and alkalies, neutral salts also may have a marked influence on the swelling of wool. Actually, there are salts which depress swelling as well as salts which increase it, the former producing what is commonly known as "salting out" and the latter, "salting in" or "peptization". The relative effect of various salts was first investigated by Hofmeister [19], who arranged the salts in an order corresponding to their effect on the proteins.

Whereas an insoluble protein such as wool may swell in distilled water by an imbibition process and in acids or alkalies by osmotic forces resulting from salt formation, the mechanism by which salts influence the swelling has not been satisfactorily explained. It appears, as suggested by Gibson and Kincaid [20] that the salts influence the structure of water by strengthening or weakening the electrostatic bonds which hold the molecules of water together. There is also the possibility that the salts influence the forces of cohesion in the protein. It would be expected, then, that when the cohesional forces between the water molecules become relatively greater than the adhesional forces between the protein and water, depression of swelling ("salting-out") will take place. Similarly, when the adhesional forces between water and protein are relatively greater, increased swelling ("salting-in") will result.

Since the pH of solutions of most of the neutral salts lies within the pH stability range for wool, and since the free amino and carboxyl groups should not be attacked by the salts, the investigation of the effect of various neutral salts offered another approach to the study of the nature of the forces involved in the extension of the fibers. Accordingly, calibrated fibers were soaked for 24 hours in 1 *N* solutions of various potassium salts and then extended in the same solutions. When the data were arranged in order of decreasing 30-percent indices, as shown in table 3, it was found that the anions of the salts were arranged in an order corresponding to their ability to increase the swelling of proteins [19].

TABLE 3.—*Effect of normal solutions of various potassium salts on the extensibility of wool fibers*

| Solution | 30-percent index |
|---|---|
| 1 *N* $K_2SO_4$ | 1.03 |
| 1 *N* $KOOCCH_3$ | 1.02 |
| 1 *N* KCl | 1.01 |
| 1 *N* KBr | 0.97 |
| 1 *N* KI | .90 |
| 1 *N* KCNS | .83 |

That the salts influenced the swelling of the wool fibers was corroborated by measuring the change in the diameters of fibers immersed in 1 *N* solutions of potassium bromide and potassium thiocyanate.

The method employed was similar to that described by Speakman and Stott [11] and consisted essentially in the mounting of 5 fibers on a glass slide marked with 10 lines, 1 mm apart so that the fibers and lines crossed each other at right angles. The ends of the fibers were sealed to the glass with asphalt so that the slide and fibers could be immersed in any liquid under consideration. The fiber widths were determined microscopically on both sides of the intersections of the fibers and the lines, so that 100 measurements were made on each slide. All the experiments were conducted in a room kept at 21° C. The widths were first determined after soaking in distilled water for 24 hours and after 24 hours in the desired reagent. By this method, it was found that the average widths of the wool fiber increased 0.2 percent in 1 *N* potassium bromide, and 1.0 percent in 1 *N* potassium thiocyanate solutions over what they were in distilled water.

Speakman and Hirst [2] investigated the stretching of wool in 0.2 *N* solutions of sodium chloride containing varying amounts of hydrochloric acid, with the idea of studying the action of acids on wool in the absence of swelling. From their results they concluded that "the fact that swelling can be reduced without interfering with the action of acid in facilitating fiber-extension, is a confirmation of the view that swelling is not the primary cause of a reduced resistance to extension." However, actual measurements of fiber diameters indicate that in 0.1 *N* hydrochloric acid solutions the amount of sodium chloride they used reduces the swelling obtained with acid alone by only about 25 percent. If, however, a 0.1 *N* solution of hydrochloric acid saturated with sodium chloride is used, not only does the osmotic swelling produced by the acid appear to be eliminated but there also appears to be a contraction in fiber width. Consistent with this is the fact that wool fibers are more difficult to elongate in such a solution than in water, the 30-percent index for the fibers being 1.10. The acid-combining capacity of wool in a 0.1 *N* solution of hydrochloric acid, saturated with sodium chloride is 1.12 [9] millimoles of acid per gram of wool, which indicates that any existing salt linkages would have been broken and on the basis of the salt-linkage theory, the fiber should have been easier to stretch.

## IV. RELATION OF SWELLING TO THE EXTENSIBILITY OF WOOL

Although it has been shown that the extensibility of a fiber is qualitatively influenced by the factors which affect the swelling of the wool, it is not to be expected that the ease of elongation will be directly proportional to the degree of swelling. That there is a relationship for a specific type of swelling is shown in table 3 and in figure 4. The data for the latter are those of Speakman [2, 11] and his collaborators. The curve indicates a relationship between the ease of elongation and the osmotic swelling. However, when the effects of osmotic swelling and swelling produced by a "salting-in" salt on the extensibilities of the fibers are compared, somewhat different results are obtained. The 30-percent indices of fibers stretched in a hydrochloric acid solution of pH 2.9 and in a 5 *N* solution of

[9] This is not strictly comparable to the value of 0.80 obtained for 0.1 *N* HCl alone, in which no correction is made for swelling. Reduction of swelling by the NaCl gives a higher apparent value for the acid-combining capacity. In addition, the hydrogen ion activity of the solutions is greatly changed by the NaCl [21].

lithium bromide are 0.81 and 0.82, respectively. The average increase in the fiber diameter in the acid solution as compared to water was 1.8 percent and in the lithium bromide solution, 3.1 percent. A possible explanation for such differences may be found in a consideration of the electrovalent linkages in the wool molecule. As was previously pointed out, the fiber appears to consist of long-chain polypeptides held together by a variety of cross linkages of the covalent and electrovalent types. The valence forces vary according to the type of linkage. The electrovalent forces, however, are of essentially two types; Coulomb forces which vary inversely as the

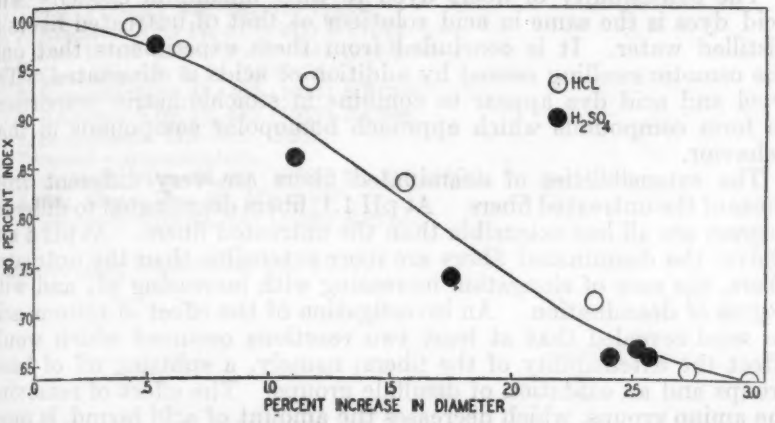


FIGURE 4.—*Relation between extensibility and swelling of wool fibers in acid solutions of different concentrations.*

Data from Speakman [2, 11].

square of the distance and Van der Waal's forces which vary inversely as the sixth and higher powers of the distance. It is obvious, then, that the extensibility of the fiber should depend on the relative proportions of the various types of forces which are affected in the different types of swelling. In other words, a given amount of swelling which involves a relatively high proportion of Coulomb forces should produce a less extensible fiber than a similar amount of swelling involving a higher proportion of Van der Waal's forces.

## V. SUMMARY

The results of this investigation indicate that salt linkages of the type which might be formed by an attraction between the free amino and carboxyl groups in wool do not appreciably contribute to the physical stability of the fiber in aqueous solutions. It appears that the extensibility of wool fibers in aqueous solutions is governed, for the most part, by factors which influence the swelling or hydration of the wool. For the purpose of explaining the data obtained in the present work, three types of swelling are considered, namely, imbibitional swelling resulting from the absorption of distilled water by wool to form solvates or adsorption compounds; osmotic swelling, in acid or alkaline solutions resulting from the formation of ionizable protein salts; and swelling in solutions of neutral salts, resulting from

the effect of the salts on the cohesional and adhesional forces of the water and the protein.

Tanning with quinone appears to decrease the ease of extension of the fibers (except in strongly alkaline solutions) by decreasing the swelling of the wool. The experimental data suggest that part of the effect results from blocking some of the basic groups and reducing some of the osmotic swelling, while the remainder of the effect is caused by a decrease in imbibitional swelling. The results are consistent with the fact that proteins take up more tanning materials than can be accounted for by the basic groups.

The extensibility of fibers dyed to their maximum capacity with acid dyes is the same in acid solutions as that of untreated fibers in distilled water. It is concluded from these experiments that only the osmotic swelling caused by addition of acids is eliminated. The wool and acid dye appear to combine in stoichiometric proportions to form compounds which approach homopolar compounds in their behavior.

The extensibilities of deaminated fibers are very different from those of the untreated fibers. At pH 1.1, fibers deaminated to different degrees are all less extensible than the untreated fibers. At pH 4 and above, the deaminated fibers are more extensible than the untreated fibers, the ease of elongation increasing with increasing pH and with degree of deamination. An investigation of the effect of nitrous acid on wool revealed that at least two reactions occurred which would affect the extensibility of the fibers; namely, a splitting off of basic groups and an oxidation of disulfide groups. The effect of removing the amino groups, which decreases the amount of acid bound, is most pronounced when the fibers are extended in the strongly acid solutions. The osmotic swelling is decreased and this results in a decreased extensibility. This effect becomes less pronounced as the pH of the solutions with which the wool is in contact increases. On the other hand, the effect on the sulfur is at a minimum in the more acid solutions but becomes more pronounced as the pH increases. The net effect then, is a combination of the two reactions.

Neutral salts increase the ease of elongation of the fibers in an order corresponding to their abilities to increase the swelling of proteins. 0.2 *N* solutions of sodium chloride cause only a relatively small decrease in the osmotic swelling produced by hydrochloric acid. However, saturated solutions of this salt not only appear to eliminate the osmotic swelling produced by 0.1 *N* hydrochloric acid but also actually produce a contraction in the fiber. In spite of the fact that in such a system the wool takes up more acid than wool in acid solutions without sodium chloride, the fibers in contact with the acid-salt solution are more difficult to stretch than untreated fibers in water alone.

Although the extensibility of the fiber is modified by the factors which affect the swelling of wool, it is not necessarily directly proportional to the degree of swelling. In general, it appears to depend on the relative proportion of the different electrovalent cross linkages which are affected in each type of swelling.

## VI. REFERENCES

[1] J. Textile Inst. **27,** p281 (1936).
[2] Trans. Faraday Soc. **29,** 148 (1933).
[3] Proc. Roy. Soc. A. **94,** 460 (1918).
[4] Z. tech. Physik **6,** 124 (1925).
[5] J. Textile Inst. **15,** T207 (1924).
[6] Phil. Trans. Roy Soc. London A. **232,** 333 (1933).
[7] J. Textile Inst. **17,** T457 (1926); **18,** T431 (1927); Proc. Roy. Soc. B**103,** 377 (1928).
[8] Ind. Eng. Chem. **18,** 84 (1926).
[9] The Determination of Hydrogen Ions (Williams and Wilkins Co., p. 75, 1920).
[10] Ind. Eng. Chem. **16,** 925 (1924).
[11] Trans. Faraday Soc. **30,** 539 (1934).
[12] J. Research NBS **19,** 81 (1937) RP1012.
[13] J. Soc. Dyers Colourists **50,** 341 (1934).
[14] J. Gen. Physiol. **6,** 94 (1923–24)
[15] J. Research NBS **19,** 467 (1937) RP1038.
[16] J. Research NBS **18,** 623 (1937) RP998.
[17] J. Biol. Chem. **113,** 583 (1936).
[18] Personal communication.
[19] Arch. expt. Path. **25,** 13 (1888); **28,** 219 (1891).
[20] J. Am. Chem. Soc. **59,** 579 (1937).
[21] J. Research NBS **14,** 217 (1935) RP765.

WASHINGTON, September 24, 1937.

U. S. Department of Commerce National Bureau of Standards

RESEARCH PAPER RP1044

*Part of Journal of Research of the National Bureau of Standards, Volume 19, November 1937*

# ENTROPY OF ISOPRENE FROM HEAT-CAPACITY MEASUREMENTS

By Norman Bekkedahl and Lawrence A. Wood

ABSTRACT

Measurements of heat capacity were made on a sample of isoprene of high purity from 20 to 300°K with an adiabatic vacuum-type calorimeter. At 20°K the heat capacity of the crystalline material was found to be 11.8 j/(mole·degree), and with increase in temperature the heat capacity increases, following the usual type of curve for crystalline substances. At 100°K the heat capacity of the solid is 64.7 j/(mole·degree), and at the melting point, 126.4°K, the heat of fusion is determined to be 4,830 ±15 j/mole. The heat capacity of the substance increases about 60 percent during the change from solid to liquid. Above the fusion temperature the curve is characteristic of liquids, and the heat capacity attains a value of 152.6 j/(mole·degree) at 298.2°K (25°C). Utilization of the data, according to the third law of thermodynamics, yields 229.3 ±1.0 j/(mole·degree) for the entropy of isoprene at this temperature.

CONTENTS

| | | Page |
|---|---|---|
| I. | Introduction | 551 |
| II. | Sample investigated | 552 |
| III. | Calorimeter and its operation | 552 |
| IV. | Heat capacity | 552 |
| V. | Heat of fusion | 556 |
| VI. | Entropy | 557 |
| VII. | References | 558 |

## I. INTRODUCTION

In a previous investigation [3][1] the heat capacity, entropy, and free energy of the rubber hydrocarbon $(C_5H_8)_x$ were determined. Similar work has also been undertaken for substances related to rubber in order that thermodynamic relationships may be established among them. Isoprene, 2-methyl-1,3-butadiene, having the same empirical formula as rubber hydrocarbon, is produced in the destructive distillation of rubber as one of the two major constituents of the distillate [8]. It can be polymerized to form a product similar in many respects to natural rubber and is thought not only to be the substance from which rubber is formed in plants but also to play an important role in the growth of plant cells [1, 6, 16, 17]. Because of the chemical similarity and relationship between isoprene and the rubber hydrocarbon, a knowledge of the free energy of formation of isoprene from its elements would be useful in the study of the thermodynamics of reactions involving the two substances. A convenient method for obtaining this free energy or thermodynamic potential for isoprene involves determinations of the heat of combustion and of

[1] The numbers in the brackets here and elsewhere in the text refer to references at the end of this paper.

the entropy, the latter by means of the application of the third law of thermodynamics to data on low-temperature heat capacities and latent heats. From these are calculated the heat $\Delta H$ and the entropy $\Delta S$ of formation, which are combined according to the relation $\Delta F = \Delta H - T\Delta S$ to obtain the free energy of formation $\Delta F$.

The present report gives, for the range 20 to 300°K, the results of measurements made in the Cryogenic Laboratory of this Bureau, of the heat capacities for both the liquid and crystalline solid and of the heat of fusion. From these a value of the entropy is calculated by means of the third law. The free energy in turn is calculated from the entropy and heat of combustion. Work on the heat of combustion is now in progress.

## II. SAMPLE INVESTIGATED

The sample of isoprene used was prepared by the cracking of dipentene vapors by means of the improved "isoprene lamp" [7, 18]. The details of its preparation and purification and many of its physical properties are described in a previous paper [4]. Immediately after purification the difference between the boiling and condensation temperatures of the sample was determined according to the method of Świętosławski [15] and found to be $\Delta t = 0.002°$ C, which in conjunction with the small freezing range [4] is indicative of high purity. Since isoprene is known to oxidize and polymerize on standing it was purified by distillation just previous to its introduction into the sample-container of the calorimeter. All the measurements on heat capacity were made within 2 weeks after the last distillation of the sample, and during most of this time it was kept at liquid-air temperatures in order to prevent polymerization. Also the sample practically filled the container and was hermetically sealed so that there was very little opportunity for oxidation. Repeated measurements of the heat capacity at various given temperatures showed no changes in the values with time. The weight of the isoprene sample was 34.175 g. This is equivalent to 0.5018 mole, the gram-molecular weight of isoprene being taken as 68.11.

## III. CALORIMETER AND ITS OPERATION

The calorimeter used for the measurements of the heat capacity and also the heat of fusion of the crystalline material was the same as that used for similar measurements on rubber [3, 14], the only change of any importance being the replacement of the old copper sample-container by one made of a platinum-iridium alloy. The resistance thermometer was rechecked at the ice point and was found to have the same value, within 0.001 ohm, as that obtained about 3 years previously. This change in resistance would be equivalent to less than 0.004° C, and the check was considered to be close enough so that a recalibration was not necessary. The method of operation of the calorimeter and accessory apparatus was the same as that previously described [3].

## IV. HEAT CAPACITY

The results obtained in the measurements of heat capacity are represented by graphs in figures 1 and 2, which give the relation

between heat capacity and temperature. Table 1 gives the heat capacity values for all observed points. The temperature ranges of heating varied from 3 to 10° C, except in the region of the melting point. Table 2 gives the heat-capacity values at 5° intervals taken from a large-scale drawing of the curve. All quantities of heat in this paper are expressed in international joules. The factor for conversion into calories is 4.1833 j/cal [12]. The method of calculation of the results from the data will not be shown here since it is the same as that previously described in detail [3].

TABLE 1.—*Heat capacity of isoprene*

| Temperature | Heat capacity | Temperature | Heat capacity | Temperature | Heat capacity |
|---|---|---|---|---|---|
| °K | *j/(mole·degree)* | °K | *j/(mole·degree)* | °K | *j/(mole·degree)* |
| 23.41 | 15.87 | 120.71 | 123.82 | 203.32 | 127.74 |
| 28.66 | 21.85 | 123.29 | 251.76 | 206.77 | 128.02 |
| 34.17 | 27.22 | 123.52 | 308.00 | 211.61 | 129.29 |
| 39.29 | 31.61 | 125.31 | 706.8 | 216.11 | 129.97 |
| 45.40 | 35.67 | 126.10 | 2,062 | 222.98 | 131.82 |
| 52.57 | 40.45 | 126.41 | 4,441 | 225.46 | 131.84 |
| 59.83 | 44.85 | 126.59 | 5,312 | 234.35 | 134.31 |
| 67.36 | 48.99 | 127.15 | 856.0 | 234.81 | 134.21 |
| 74.36 | 52.66 | 130.17 | 122.96 | 244.14 | 136.54 |
| 81.82 | 56.60 | 133.05 | 123.54 | 245.71 | 137.12 |
| 85.80 | 57.94 | 140.15 | 122.88 | 253.46 | 138.83 |
| 89.78 | 60.52 | 140.37 | 123.12 | 257.05 | 139.79 |
| 92.07 | 61.42 | 146.12 | 123.14 | 262.79 | 141.62 |
| 92.62 | 61.44 | 152.05 | 123.04 | 268.46 | 143.27 |
| 97.40 | 64.33 | 160.22 | 123.10 | 272.04 | 144.41 |
| 99.97 | 65.40 | 161.97 | 123.68 | 278.55 | 146.48 |
| 100.24 | 64.53 | 169.61 | 123.90 | 281.22 | 147.34 |
| 105.50 | 71.20 | 178.79 | 124.53 | 287.61 | 149.31 |
| 107.56 | 70.26 | 188.02 | 125.69 | 290.40 | 149.91 |
| 109.99 | 72.89 | 196.20 | 126.72 | 296.65 | 152.14 |
| 114.43 | 81.10 | 198.53 | 126.29 | 298.46 | 153.29 |
| 115.76 | 86.12 | 200.23 | 127.28 | | |

TABLE 2.—*Heat capacity of isoprene*

| Temperature | Heat capacity | Temperature | Heat capacity | Temperature | Heat capacity |
|---|---|---|---|---|---|
| ° K | j/(mole·degree) | ° K | j/(mole·degree) | ° K | j/(mole·degree) |
| 20 | 11.8 | 120 | [a] 73.2 | 215 | 129.7 |
| 25 | 17.9 | 125 | [a] 75.3 | 220 | 130.7 |
| 30 | 23.2 | 126.4 | (b) | 225 | 131.8 |
| 35 | 27.9 | 130 | 123.0 | 230 | 133.0 |
| 40 | 32.0 | 135 | 123.0 | 235 | 134.3 |
| 45 | 35.6 | 140 | 123.0 | 240 | 135.5 |
| 50 | 38.9 | 145 | 123.0 | 245 | 136.7 |
| 55 | 42.0 | 150 | 123.0 | 250 | 137.9 |
| 60 | 44.9 | 155 | 123.1 | 255 | 139.3 |
| 65 | 47.7 | 160 | 123.3 | 260 | 140.7 |
| 70 | 50.3 | 165 | 123.6 | 265 | 142.2 |
| 75 | 52.9 | 170 | 123.9 | 270 | 143.7 |
| 80 | 55.3 | 175 | 124.2 | 275 | 145.2 |
| 85 | 57.7 | 180 | 124.6 | 280 | 146.8 |
| 90 | 60.1 | 185 | 125.2 | 285 | 148.3 |
| 95 | 62.5 | 190 | 125.8 | 290 | 149.9 |
| 100 | 64.7 | 195 | 126.4 | 295 | 151.6 |
| 105 | [a] 66.9 | 200 | 127.0 | 298.2 | 152.6 |
| 110 | [a] 69.0 | 205 | 127.7 | 300 | 153.3 |
| 115 | [a] 71.1 | 210 | 128.7 | | |

[a] Extrapolated values, taken from dotted curve in figure 1.
[b] Fusion.

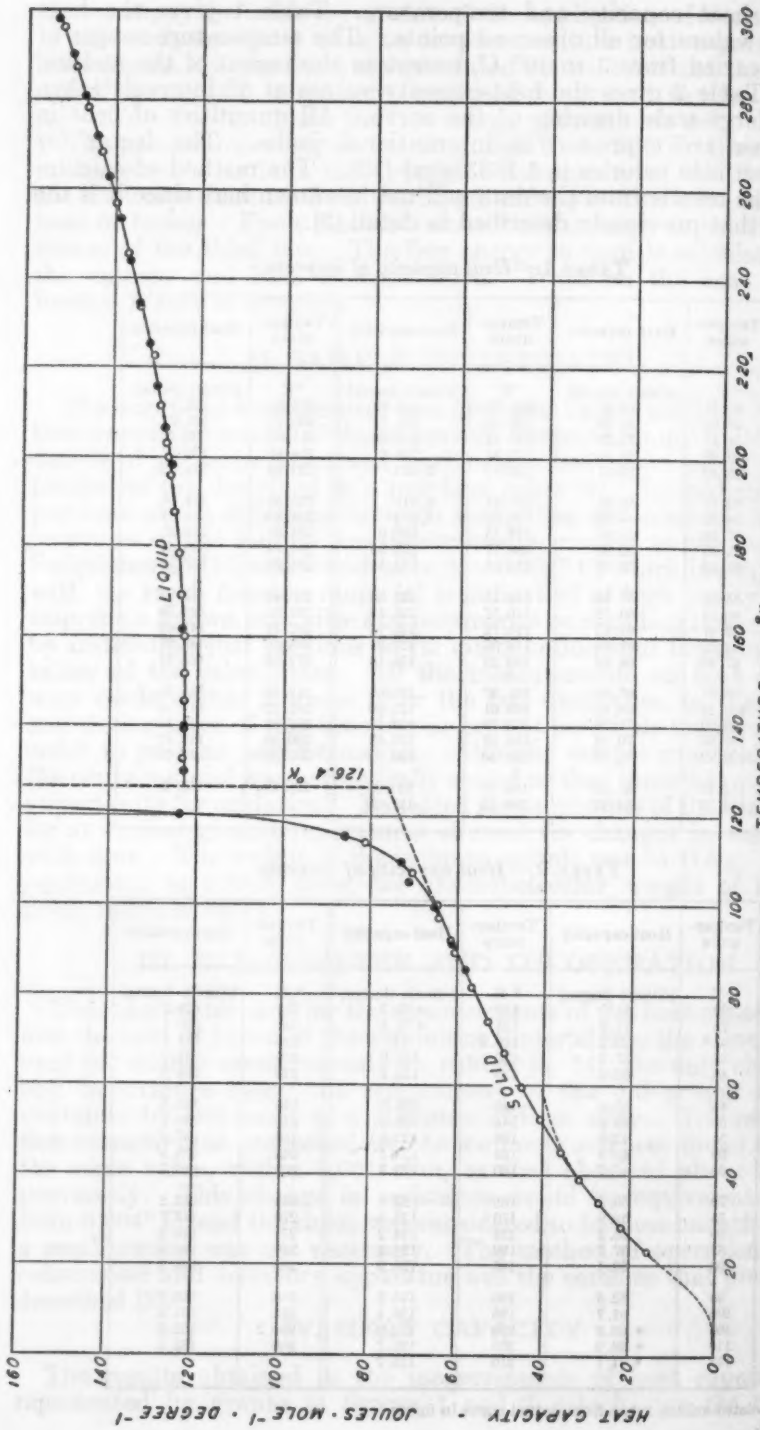


FIGURE 1.—*Relation between heat capacity of isoprene and temperature.*

The dotted curve at the extreme low temperatures represents values of the heat capacity taken from tables of Debye for a $\frac{\theta}{T}$ value of 127. The dotted curve just below the melting temperature indicates a heat-capacity curve for the solid isoprene extrapolated to its melting point at 126.4° K. The points represented by the open and by the solid circles are for two distinct sets of observations.

When the sample of isoprene was cooled rapidly through its freezing point to liquid-air temperatures it did not become completely crystallized. This was evident from the fact that there was an evolution of heat when the sample was heated to 115° K while measurements of heat capacity were being made. Without the further addition of external heat the temperature of the sample continued to rise until conversion to the crystalline state was complete, or until the melting point was reached. This phenomenon occurs with many other organic substances including the rubber hydrocarbon [2, 3], in which the freezing is slower and has been studied in more detail. Complete crystallization of the isoprene, like that of many other substances, can be obtained by a very slow cooling through the freezing point, or by holding the temperature not more than a few degrees below the freezing point for several hours. However, if the temperatures are too low, the same supercooling occurs as in the case of rubber. All the observations reported here were taken after the sample had been cooled so slowly that on warming no evolution of heat caused by crystallization could be observed.

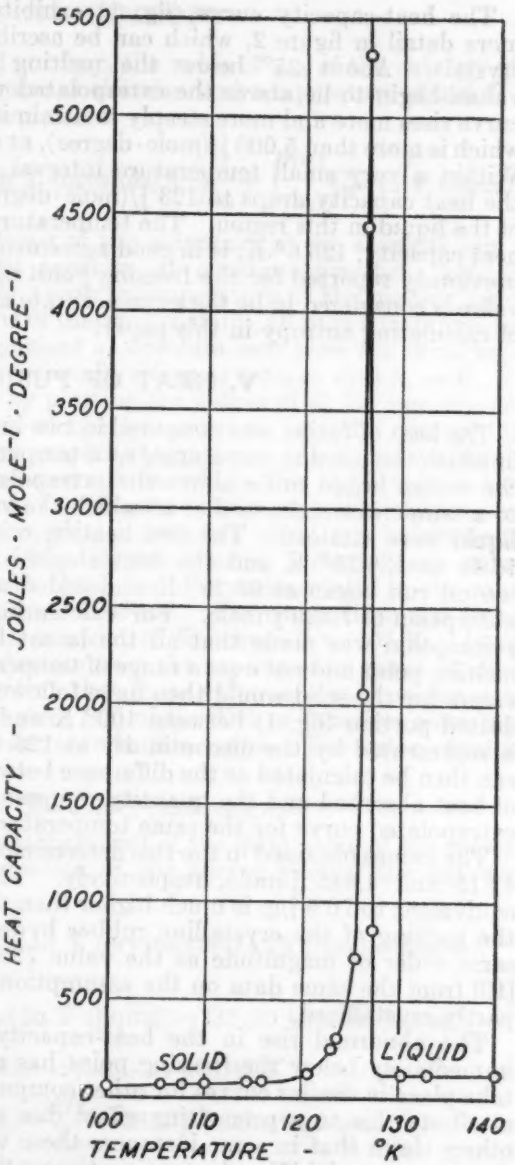


FIGURE 2.—*Relation between heat capacity of isoprene and temperature in the region of the transition from the solid to the liquid state.*

The heat-capacity curve (fig. 1) exhibits an anomaly, shown in more detail in figure 2, which can be ascribed to the melting of the crystals. About 25° below the melting point the heat-capacity values begin to lie above the extrapolated values for the solid. The curve rises more and more steeply to attain its highest observed value, which is more than 5,000 j/(mole·degree), at a temperature of 126.6° K. Within a very small temperature interval above this highest value the heat capacity drops to 123 j/(mole·degree), a value characteristic of the liquid in this region. The temperature at this highest observed heat capacity, 126.6° K, is in good agreement with the value 126.4° K previously reported for the freezing point of isoprene [4]. The latter value is considered to be the more accurate and is used for the purpose of calculating entropy in this paper.

## V. HEAT OF FUSION

The heat of fusion was measured in two independent determinations in which the heating was started at a temperature below that at which the values began to lie above the extrapolated curve, and continued to a temperature above that at which the values characteristic of the liquid were attained. The first heating raised the temperature from 96.49 to 136.75° K and the heat absorbed was 8,183 j/mole. The second run began at 96.29° K and ended at 131.15° K, with a heat absorption of 7,539 j/mole. For calculating the heat of fusion the assumption was made that all the latent heat was absorbed at the melting point and not over a range of temperature. The heat-capacity values for the solid would then have followed the curve shown by the dotted portion (fig. 1) between 100° K and the melting point, which is represented by the discontinuity at 126.4° K. The heat of fusion can then be calculated as the difference between the observed quantity of heat absorbed and the quantity represented by the area below the extrapolated curve for the same temperature range.

The values obtained in the two determinations of this difference were 4,815 and 4,845 j/mole, respectively. The average, 4,830 j/mole, equivalent to 70.9 j/g, is much higher than the value 16.7 j/g found for the melting of the crystalline rubber hydrocarbon [3], and is of the same order of magnitude as the value 72.8 j/g calculated by Parks [10] from the same data on the assumption that the rubber was only partly crystallized.

The abnormal rise in the heat-capacity curve at a temperature immediately below the freezing point has previously been noticed to take place in similar curves for other compounds. Some investigators attribute this to a premelting effect due to impurities [9, 19] while others claim that in some instances these values are characteristic of the pure material [5]. As previously mentioned, the isoprene for this investigation was purified to a very high degree, but other tests indicate that isoprene may absorb moisture from the atmosphere. Since there was some possibility of this occurrence during the introduction of the sample into the calorimeter, it is not known whether this abnormal rise in the curve immediately below the melting point is due to the presence of water or whether it is characteristic of the pure material.

## VI. ENTROPY

From the definition of entropy, the value $S°_{298.2}$ of the entropy of a substance in the liquid state at the standard temperature of 298.2° K (25° C) is given by the equation:

$$S°_{298.2}=S_0+\int_0^{T_{mp}} C_p d \ln T \text{ (crystals)}+\frac{\Delta H_f}{T_{mp}}+\int_{T_{mp}}^{298.2} C_p d \ln T \text{ (liquid)}$$

Here $S_0$ denotes the entropy of the substance at the absolute zero of temperature, $C_p$ the heat capacity at constant pressure, $\Delta H_f$ the heat of fusion, and $T_{mp}$ the absolute temperature of the melting point. According to the third law of thermodynamics, all pure substances in a perfect crystalline arrangement at absolute zero have the same value of entropy, which is conventionally taken as zero, so that $S_0 = 0$.

Curves were prepared by plotting the values of $C_p$ for isoprene as a function of the logarithm of the temperature, and the entropy differences were obtained by graphic integration. As a check a similar integration was made on a graph in which the $C_p/T$ values were plotted as a function of $T$. Since no heat-capacity values were obtained below 20° K, graphical integration could not be continued below this point. The Debye approximation formula gave values which agree very well with those found experimentally in the range from 20 to 40° K for a $\beta\nu$ value of 127. For comparison the Debye curve is shown in figure 1 as a dotted line from 0 to 60° K. It can be seen that it begins to deviate from the experimental curve at about 40° K. With the assumption that these values are valid in the range from 0 to 20° K, entropy tables [13] of the Debye function were used to calculate the entropy increase in this range. The value obtained in this manner was

$$S_{20}-S_0=4.55 \text{ j/(mole·degree)}$$

This amounts to only about 2 percent of the total value of the entropy at 25° C. Graphic integration of the curves yielded the following values:

$$S_{126.4}-S_{20}=\int_{20}^{126.4} C_p d \ln T \text{ (crystals)}=74.73 \text{ j/(mole·degree)}.$$

$$S_{298.2}-S_{126.4}=\int_{126.4}^{298.2} C_p d \ln T \text{ (liquid)}=111.80 \text{ j/(mole·degree)}.$$

The entropy of fusion of the crystals at 126.4° K is

$$S_{126.4} \text{ (fusion)}=\frac{\Delta H_f}{T_{mp}}=38.2 \text{ j/(mole·degree)}.$$

The entropy of isoprene at 298.2° K, assuming $S_0$ to be zero, is then equal to the sum of these four terms, or 229.3 j/(mole·degree) (54.8 cal/(mole·degree)).[2] This value is believed to be correct within 1.0 j/(mole·degree) (0.2 cal/(mole·degree)).

---

The authors express their appreciation to the staff of the Cryogenic Laboratory for their generous assistance.

[2] It is interesting to note that equations of Parks and Huffman [11], who have developed a method for the calculation of entropies of organic compounds on the basis of their structural formulas, predict an estimated value of 53.6 cal/(mole·degree) for the entropy of liquid isoprene at 25° C.

## VII. REFERENCES

[1] Aschan. Ber. deut. chem. Ges. **55**B, 2944 (1922); Chem.-Ztg. **49,** 689 (1925).
[2] Bekkedahl. J. Research NBS **13,** 441 (1934) RP717. Reprinted in Rubber Chem. Tech. **8,** 5 (1935).
[3] Bekkedahl and Matheson. J. Research NBS **15,** 503 (1935) RP844. Reprinted in Rubber Chem. Tech. **9,** 264 (1936).
[4] Bekkedahl, Wood, and Wojciechowski. J. Research NBS **17,** 883 (1936) RP951. Reprinted in India-Rubber J. **93,** 648 (1937); and also in Rubber Chem. Tech. **10,** 451 (1937).
[5] Egan and Kemp. J. Am. Chem. Soc. **59,** 1264 (1937).
[6] Emde. Helv. chim. acta **14,** 888 (1931).
[7] Harries and Gottlob. Liebigs Ann. Chem. **383,** 228 (1911).
[8] Midgley and Henne. J. Am. Chem. Soc. **51,** 1216. (1929). Reprinted in Rubber Chem. Tech. **2,** 441 (1929).
[9] Overstreet and Giauque. J. Am. Chem. Soc. **59,** 254 (1937).
[10] Parks. J. Chem. Phys. **4,** 459 (1936). Reprinted in Rubber Chem. Tech. **10,** 135 (1937).
[11] Parks and Huffman. Free Energies of Some Organic Compounds, Am. Chem. Soc. Monograph no. 60, p. 210 (Chemical Publishing Co., New York, N. Y. 1932.)
[12] Rossini. BS J. Research **9,** 679 (1932) RP 499. Also Chem. Rev. **18,** 233 (1936).
[13] Simon. Handbuch der Physik **10,** 367 (1926).
[14] Southard and Brickwedde. J. Am. Chem. Soc. **55,** 4378 (1933).
[15] Świętosławski. J. Phys. Chem. **38,** 1169 (1934).
[16] Wallach. Ber. deut. chem. Ges. **24,** 1525 (1891).
[17] Weber. Ber. deut. chem. Ges. **33,** 779 (1900).
[18] Whitby and Crozier. Can. J. Research **6,** 203 (1932). Reprinted in Rubber Chem. Tech. **5,** 546 (1932).
[19] Witt and Kemp. J. Am. Chem. Soc. **59,** 273 (1937).

WASHINGTON, September 15, 1937.

U. S. Department of Commerce National Bureau of Standards

RESEARCH PAPER RP1045

*Part of Journal of Research of the National Bureau of Standards, Volume 19, November 1937*

# RECOMBINATION IN THE AFTERGLOW OF A MERCURY DISCHARGE

By Fred L. Mohler

ABSTRACT

A mercury-arc discharge through a 500-cm³ bulb is extinguished by short-circuiting two anodes on each side of the bulb by a commutator, and probe measurements are made at varying time intervals after the cutoff. Most of the measurements are limited to discharges of 6 and 4 amperes at a vapor pressure of 270 $\mu$. Probe measurements of the number of ions per cubic centimeter in the bulb and of the ion current to the bulb wall give the number of ions recombining in the space and the recombination coefficient $2.3\times10^{-10}$. The electron temperature decreases with time from 3,000° K at $10^{-3}$ sec to 1,600 at $6\times10^{-3}$ sec. Theoretical considerations indicate that this is probably not a spontaneous two-body recombination.

CONTENTS

| | Page |
|---|---|
| I. Introduction | 559 |
| II. Method | 560 |
| III. Experimental results | 561 |
| IV. Discussion | 564 |

## I. INTRODUCTION

Another paper[1] reports experiments on the rate of recombination of ions and electrons in the afterglow of a cesium discharge. The method was to measure the number of ions per cubic centimeter at different time intervals after cutting off the discharge and also to measure the flow of ions to the walls. From these data one can derive the number of ions which recombine in the space and the recombination coefficient, $\alpha$ defined by the equation

$$dn/dt=-\alpha n^2, \qquad (1)$$

where $n$ is the number of ions or electrons per cubic centimeter. A value of $\alpha=3.4\times10^{-10}$ was found at pressures ranging from 10 to 33 $\mu$ and an electron temperature of about 1,200° K.

It is of interest to obtain comparable measurements in other elements. The only other published value for this coefficient under low-pressure discharge conditions is an estimate obtained by Kenty [2] of $2\times10^{-10}$ for ions in the afterglow of an argon discharge. He estimates an uncertainty of fivefold in this result and, in view of this, it remains of interest to see whether different elements have comparable values of $\alpha$ at low pressure. Experiments by Webb and Sinclair on the

[1] Fred L. Mohler. J. Research NBS 19, 447 (1937) RP1036.
[2] Kenty. Phys. Rev. 32, 624 (1928).

radiation emitted by a jet of vapor from a mercury discharge [3] add interest to the project for they reach conclusions that seem quite incompatible with some of the cesium results. Using the intensity of the visible spectrum as a measure of recombination, they conclude that the rate of recombination increases as the first power of the electron concentration and decreases very rapidly and exponentially with increasing electron temperature.

## II. METHOD

A mercury-cathode arc was used for the discharge, and as this cannot be interrupted and restarted by a simple circuit, the device was used of having two anodes on each side of a 500-cm³ bulb, which

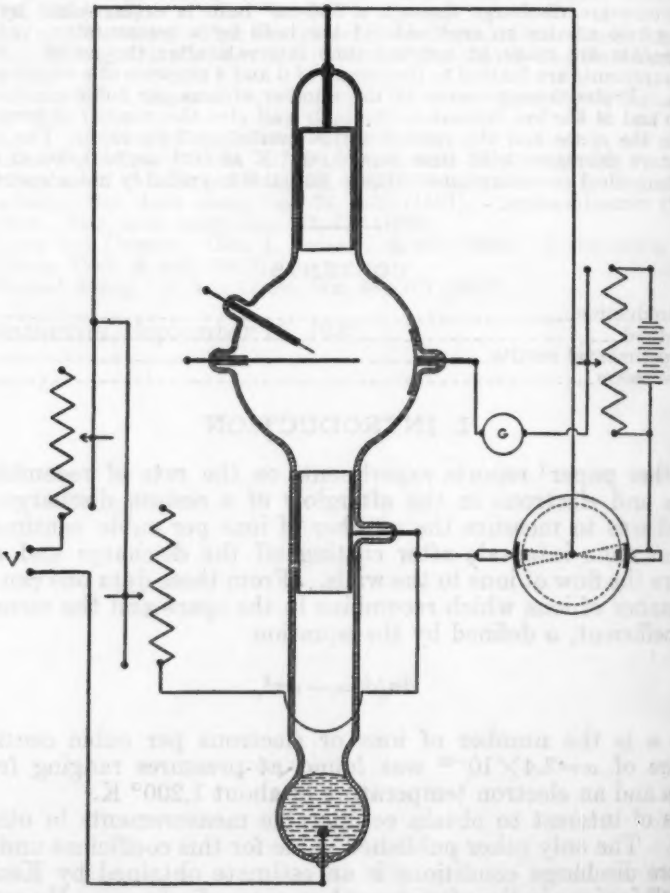


FIGURE 1.—*Discharge bulb with external connections indicated diagrammatically.*

were short-circuited by a commutator to extinguish the discharge in the bulb. Figure 1 shows the discharge tube and external circuits diagrammatically. The lower tube, up to the first anode, was in a stirred water bath and the vapor pressures quoted correspond to the

[3] *Recombination in mercury vapor.* Phys. Rev. **37**, 182 (1931).

temperatures of the bath. Actually, a somewhat higher vapor pressure was probably maintained by the arc. At a pressure of a few microns of mercury the glow extends well above the lower anode when the two anodes are short-circuited. At higher pressures this is not noticeable and check measurements show that the fast electrons diffusing into the space are quite negligible in comparison with the currents obtained when the commutator is running. There is a potential drop of 1 or 2 volts across the commutator brush when the commutator is closed. This has been compensated by a low-resistance potential divider (not shown in the diagram). If it is not compensated, and the potential of the upper anode is slightly positive, then the probe currents in the afterglow period are larger and the recombination coefficient somewhat smaller. This effect has been discussed by Hayner[4] and Kenty.[5]

The motor-driven commutator short-circuits the discharge for about 0.004 sec twice in a revolution at full speed. A second commutator throws one of the three probes into the circuit for 0.001 or 0.002 sec at an adjustable interval after the discharge is cut off. The motor was run at about 1,200 and 600 rpm.

The flow of ions to the wall was measured by a disk electrode 3 cm in diameter. A small positive probe of 4-mil wire 0.5 cm long measured electron concentration by the conventional method. As the precision of this measurement was rather low, a second method was also used. The positive current to a large negative probe was measured and by comparison with the small positive probe the proportionality factor between ion current and ion concentration was found. The time change in ion concentration was obtained with better precision from the change in positive current.

## III. EXPERIMENTAL RESULTS

In the interpretation of the probe measurements it is assumed that the ion current density measured by the disk is characteristic of the entire bulb wall and that the ion concentration as measured by the probes is typical of the entire volume. In the case of the cesium afterglow, stroboscopic observations indicated that this was a fair approximation, but such observations have not yet been made with the mercury afterglow.

Figure 2 gives three groups of current-voltage curves for the three probes at different time intervals after cutting off a 6-ampere discharge in mercury vapor at 270 $\mu$ pressure. The group at the lower right gives the positive-ion current to the disk. The slope at negative voltages comes from a capacity effect which approaches zero at the wall potential, so that a linear extrapolation to the wall potential gives the flow of ions to an insulated surface. The group of curves at the left shows the positive current to the large probe. The slope at negative voltages is here largely accounted for by the area of the space-charge sheath. This area is equal to the area of the wire at the space potential and this potential has been obtained from the current-voltage curve of the small probe. The ion current at the space potential has been computed from the measured current at various negative potentials by means of the space-charge equations for cylindrical

[4] Hayner. Z. Phys. **35**, 365 (1925).
[5] Kenty. Phys. Rev. **32**, 624 (1928).

collectors.[6] The upper curves show the electron current to the small probe on a semilogarithmic scale. The applied potentials have been corrected for the voltage drop across the microammeter. Since the instantaneous voltage drop is 25 times that for an equal steady current this correction becomes very important. The curves show the two

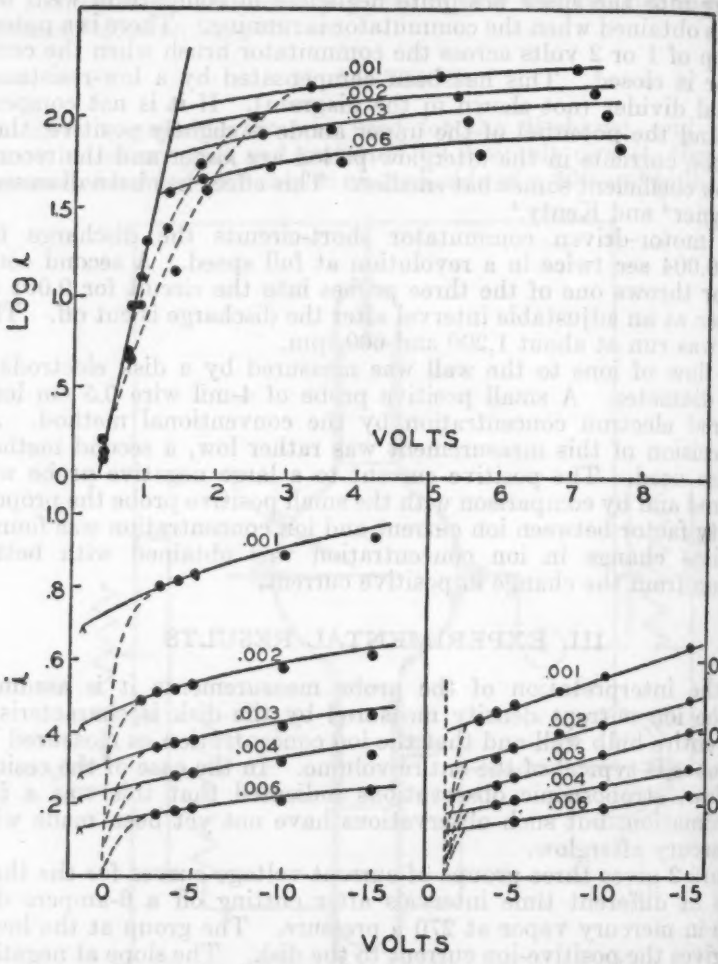


FIGURE 2.—*Current-voltage curves for the three probes.*

Numbers on the curves indicate time in seconds after the cutoff. Above, semilog plot of electron current to small positive probe; lower left, positive current to large probe; lower right, positive current to disk.

characteristic branches at potentials negative and positive with respect to the space potential, while close to the space potential there is a rounding off of the observed points, which, for small time intervals, extends over several volts. At longer intervals there is very little rounding off, and the results compare favorably with the best probe measurements under static conditions.

The slope of the branch on the left gives the electron temperature but with low precision, because the curve is very steep. This tem-

[6] Langmuir and Blodgett. Phys. Rev. 22, 347 (1923).

perature drops with increasing time (the separate curves could not be shown on the scale of fig. 2). A representative series of measurements of electron temperature is shown in table 1, and for comparison, figures read from a published curve of Randall and Webb for a jet of mercury streaming from an arc at 390 $\mu$. The two methods are entirely concordant. The temperature in the discharge is about 8,000° K.

TABLE 1.—*Electron temperatures in an afterglow at a pressure of 270 $\mu$ and in a jet at 390 $\mu$*

| Time | Afterglow (4-amperes discharge) | Jet[1] |
|---|---|---|
| *Seconds* | °K | °K |
| 0.001 | 2,960 | 3,000 |
| .002 | 2,270 | 2,500 |
| .003 | 2,020 | 2,000 |
| .004 | 1,900 | 1,900 |
| .006 | 1,600 | 1,600 |

[1] Randall and Webb. Phys. Rev. 48, 544 (1935).

The right branches of the upper curves can be accounted for, as in the case of the negative probe, by the area of the space-charge sheath, and the same method was used to find the current density.

Electron concentration was derived from the current density by the relation,

$$n_e = 4.03 \times 10^{13} i_e^{\cdot} / T_e^{\frac{1}{2}}, \tag{2}$$

where $T_e$ is the electron temperature. The ratio of $n_e$ to the current density of positive ions, as measured by the large probe, was found for each set of measurements and the mean value, excluding measurements at 0.001 sec, was

$$n_e = 1.18 \times 10^{15} i_+^{\cdot} \tag{3}$$

There is an uncertainty of about 10 percent in individual measurements, while at 0.001 sec the ratio is less and the error greater. The evidence is that this error is largely in the electron-current measurements. It is of interest that this constant is nearly equal to the rate at which ions would diffuse to the probe by thermal agitation at a temperature equal to the gas temperature. Taking this temperature as 400° K, the equation for positive ions analogous to eq 2 gives,

$$n_e = 1.22 \times 10^{15} i_+^{\cdot}$$

This is not a relation that could be assumed a priori, for at lower pressures pure diffusion does not account for the currents.[7] It seems probable that the ion temperature, unlike the electron temperature, will drop almost instantly to the gas temperature and that the coefficient in eq 3 will remain nearly constant over the range of time intervals used.

The rate of change of the total number of ions in the bulb is assumed to be equal to the rate at which they flow to the walls, plus the rate at which they recombine in free space.

$$\Delta N/\Delta t = A i_+/e + V \alpha n_e^2, \tag{4}$$

[7] Tonks and Langmuir. Phys. Rev. 34, 876 (1929).

where $A$ is the area of the walls, $i_+/e$ the number of ions flowing to the walls per square centimeter per second, $V$ is the volume of the bulb, and $n_e$ the number of electrons or ions per cubic centimeter. In practice $\Delta t$ is far from infinitesimal and mean values of $i$ and $n_e$ over the interval $\Delta t$ are used.

Figure 3 includes all measurements at 270 $\mu$ made with currents of 6 and 4 amperes. Curve $I$ gives the rate of change of the total number

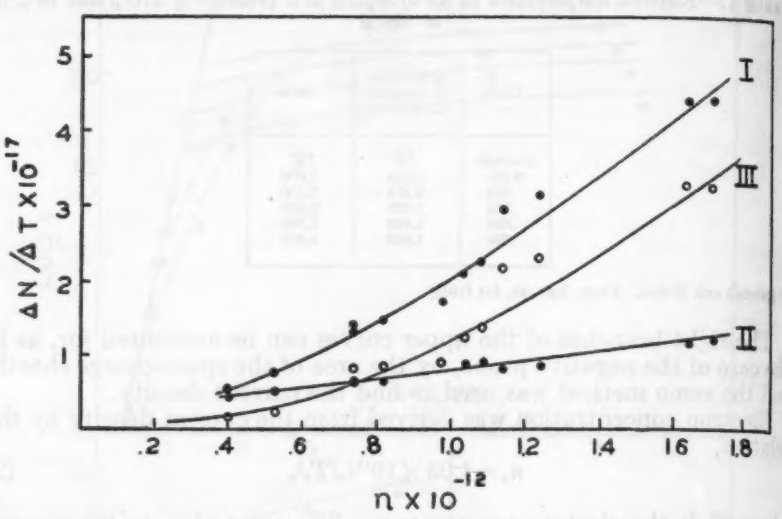


FIGURE 3.—*$\Delta N/\Delta t$ as a function of the mean electron concentration over the time $\Delta t$.*

Curve *I* shows the decrease in total number of electrons in the bulb; *II*, the flow of ions to the wall; and *III*, the volume recombination.

of ions as a function of the mean value of $n_e$, curve *II* is the rate of flow of ions to the walls, and curve *III*, the difference between *I* and *II*, is the number recombining in the space per second. Curve *III* has been drawn proportional to $n_e^2$ and, with two exceptions, it fits the observations within the range of experimental uncertainty. This curve gives the value $\alpha=2.3\times10^{-10}$, and the mean error of the 10 measurements is $0.4\times10^{-10}$. Measurements at lower pressures give comparable values but with much greater uncertainty, and it is doubtful whether they have any significance. The procedure of maintaining a discharge in the side tube during the afterglow may vitiate the low-pressure results.

## IV. DISCUSSION

The value of the recombination coefficient of mercury ions, $2.3\times10^{-10}$, pertains to an electron temperature of about 2,000° K and a pressure of 270 $\mu$. This is to be compared with the experimental result for cesium of $3.4\times10^{-10}$ at an electron temperature of about 1,200° K and pressures between 10 and 30 $\mu$. The value reported by Kenty for argon ions at a pressure of 800 $\mu$ is not significantly different from either of these. It is of interest that the values for common gases as measured near atmospheric pressure would give a similar magnitude of about $5\times10^{-10}$ at 300 $\mu$, on the assumption that $\alpha$ is proportional to the pressure. This may be entirely accidental as quite different

processes seem to be involved. In the afterglow free electrons recombine, while at higher pressures electron attachment to form negative ions probably precedes recombination.

The question as to whether the low-pressure recombination coefficients pertain to spontaneous two-body recombination involves theoretical uncertainties indicated by the following considerations.

The recombination of hydrogen ions into various quantum levels has been evaluated for two approximations. For the case in which the kinetic energy of the electron is small compared to the energy of the quantized level, the recombination coefficient $\alpha_n$ for levels of total quantum number $n$ can be expressed [8]

$$\alpha_n = 5.94 \times 10^{-13} A_n V^{-1/2} \tag{5}$$

$$A_n = 0.326/n \text{ for } n=3 \text{ or more,}$$

where $V$ is the energy of the electron in electron volts. For the case in which the kinetic energy of the electron is much greater than the energy of the quantized level, Oppenheimer [9] gives a relation which can be expressed

$$\alpha_n = 6.3 \times 10^{-11}/V^2 n^3 \tag{6}$$

The recombination coefficient for electrons of kinetic energy $V$ is the sum of $\alpha_n$ for all values of $n$. Equation 5 can be used for values of $n$ less than $n_0$, where

$$n_0 = (13.54/V)^{1/2}, \tag{7}$$

while eq 6 is valid for values of $n$ much greater than $n_0$. As a rough approximation, one can apply eq 5 and 6 to all values of $n$ which are respectively less or greater than $n_0$. For $V=0.1$ volt $n_0$ falls between 11 and 12. From eq 5 and published values of $A_n$

$$\sum_{1}^{11} \alpha_n = 1.7 \times 10^{-12} \tag{8}$$

From eq 6 and 7 and the approximation $\sum_{n_0}^{\infty} n^{-3} = \frac{n_0^2}{2}$

$$\sum_{n_0}^{\infty} \alpha_n = \frac{6.3 \times 10^{-11}}{V^2} \sum_{n_0}^{\infty} \frac{1}{n^3} = \frac{2.3 \times 10^{-12}}{V} \tag{9}$$

For 0.1-volt electrons eq 6 gives $2.3 \times 10^{-11}$ for the contribution of all levels with $n$ greater than 12. Large errors are introduced by assuming that eq 6 is valid from $n_0$ to $2n_0$, but the summation is certainly greater than one-fourth of the above value. The contribution of all levels with $n$ less than $n_0$ is negligible, and eq 6 alone can be used to compute the recombination coefficient. As levels of large $n$ and $l$ values are

[8] Stueckelberg and Morse. Phys. Rev. **36**, 16 (1930), give values for all $n$ and $l$ states to $n=5$, and the author has evaluated their equations for $n=5$ and $n=6$.
[9] Oppenheimer. Phys. Rev. **31**, 349 (1928).

predominant all singly charged ions will be very similar to hydrogen and it is probably permissible to apply the hydrogen equations to mercury and cesium ions. However, serious physical limitations in testing the theory arise from the fact that energy levels of high $n$ values are important. Under laboratory conditions of pressure and ion concentrations, such levels are greatly perturbed.

In spite of the theoretical uncertainties, it seems fairly certain that the experimental values of 2 or $3\times10^{-10}$ cannot be considered as coefficients of spontaneous recombination and that at pressures as low as 10 $\mu$ in cesium the effect of pressure is to enhance the probability of recombination. It is evident that atomic and electronic collisions will also have an opposite effect of ionizing excited states, so that what is here called recombination is more accurately the difference between the rate of recombination and the rate at which ions are created in the afterglow. This ionization of highly excited states is exactly the type of process postulated by Webb and Sinclair to explain the rapid decrease in recombination radiation with increasing electron temperature.[10] This work gives no evidence of any large change in the recombination coefficient as the mean electron temperature changes from 2,800 to 1,800° K for curve *III* of figure 3 would not change as $n_e^2$ if this were the case. The conditions of measurement and the quantities measured are entirely different in the two experiments, so that the results are not necessarily contradictory. It is important to measure the recombination coefficient over a wide range of conditions, but the type of discharge tube used here is not well adapted to the purpose.

WASHINGTON, August 10, 1937.

[10] Webb and Sinclair. Phys. Rev. 37, 182 (1931).

U. S. DEPARTMENT OF COMMERCE NATIONAL BUREAU OF STANDARDS

RESEARCH PAPER RP1046

*Part of Journal of Research of the National Bureau of Standards, Volume 19, November 1937*

# TEST OF FLOOR COVERINGS FOR POST-OFFICE WORKROOMS

By Warren E. Emley and Carl E. Hofer

ABSTRACT

Twenty kinds of floor coverings were tested to learn their relative suitabilities in the workrooms of post offices. The 20 samples included 8 of wood, 5 of concrete, 2 each of asphalt, magnesite, and rubber, and 1 of linoleum. The test consisted in the continuous operation of two post-office platform trucks around a track. The trucks have steel wheels and were loaded to 1,000 and 1,500 pounds, respectively. The results are shown by photographs taken after 60,000 passages of the truck. The results show that maple, linoleum, or perhaps rubber should give satisfactory durability in this service.

CONTENTS

| | | Page |
|---|---|---|
| I. | Introduction | 567 |
| II. | Description of testing equipment | 567 |
| III. | Description of test | 568 |
| IV. | Results | 569 |
| V. | Summary | 570 |
| VI. | Interpretation of results | 570 |

## I. INTRODUCTION

What type of floor covering is best suited to meet the exacting and difficult conditions found in the workroom and on the loading platform of a post office? This question has been before the U. S. Treasury Department, which installs the floors, and the U. S. Post Office Department, which uses them, for a number of years. While experience has been an excellent guide with conventional materials, the lack of service experience naturally prevents the use of any of the newly developed or improved materials now being offered. The service in a post-office workroom is so different from other kinds of service that experience gained from ordinary installations is of dubious value.

In an attempt to answer this question, accelerated wear tests were made during the winter of 1936–37. The floor coverings were selected by the Treasury Department and installed according to their specifications. The test method was designed to duplicate the service conditions found in post-office workrooms. The work was done by the National Bureau of Standards.

## II. DESCRIPTION OF TESTING EQUIPMENT

A concrete slab about 45 feet square by 8½ inches thick was laid on a cinder fill. This fill permitted surface water to drain out from under

the concrete and thereby prevented the slab from becoming unduly wet. On this slab was erected a circular track, about 4 feet wide by 40 feet in diameter, with a metal-sheathed concrete curb on each side. The track was partitioned off by I-beams into 20 sections, each about 6 feet long, the lower ends of which were set in the concrete and the upper faces brought to the level of the finished floor. The exposed face of each I-beam was scored to produce the same conditions as exist at a steel threshold set flush in an opening between a workroom and a loading platform. In each section, a concrete subfloor was laid, the thickness of which was determined by the thickness of the floor covering to be used in that section, so that when the floor covering was applied over the subfloor, the final surface of the entire track was level and flush with the tops of the I-beams.

To protect it from the weather, the structure was surmounted by a frame housing. An attempt was made to heat the building with salamanders, but was soon abandoned as being ineffective and somewhat dangerous.

The testing equipment consisted of two post-office trucks arranged in tandem with a specially designed separate driving wheel, as shown in figure 1. Each truck had two steel wheels 11½ inches in diameter by 2½-inch face. Each truck also had two swivel castors which carried no loads when the truck was properly balanced. One truck was loaded to 1,500 pounds with sand; the other carried the driving motor and trolleys and enough additional load to make 1,000 pounds. The separate driving wheel was 4 feet in diameter and shod with eight wooden blocks, each of which carried a wearing surface of leather, the arrangement being such as to produce a bumping and slipping action between the wheel and the track.

The assembly was guided around the track by rollers attached to the front and rear ends of each truck. These took up the side thrust by bearing against the metal sheathing of the curbs.

## III. DESCRIPTION OF TEST

The concrete slab was poured on June 25, 1936. The concrete subfloors were placed on September 4 to 9. The floor coverings were placed on September 15 to 18. The test was started on October 23. It will be noted that ample time was allowed for the setting and drying of the concrete.

The trucks were driven at a speed of 2 miles per hour. The direction of travel was reversed twice: once on November 19, after 13,015 circuits, and again on December 4, after 30,080 circuits. The track was swept at least once a day to remove loose dust and fragments. The test was stopped on January 15, 1937, after 60,000 circuits. The condition of the floors at that time is shown in the accompanying photographs.

In making each photograph, a fine wire was stretched tautly across the depression in the floor caused by the wear of the truck wheels, the ends of the wire resting upon the unworn surfaces. This wire was made to cast a shadow by placing a source of light over the track with the rays at an angle of 45° with the surface. The distance from the wire to the shadow is therefore equal to the amount of wear which the floor has undergone. The smallest division on the scale shown on each photograph is ½ inch.

FIGURE 1.—*Floor-testing equipment.*

Two post-office trucks, the forward one loaded to 1,500 pounds with sand, the rear one carrying the motor and trolleys. Leather-shod driving wheel in foreground.

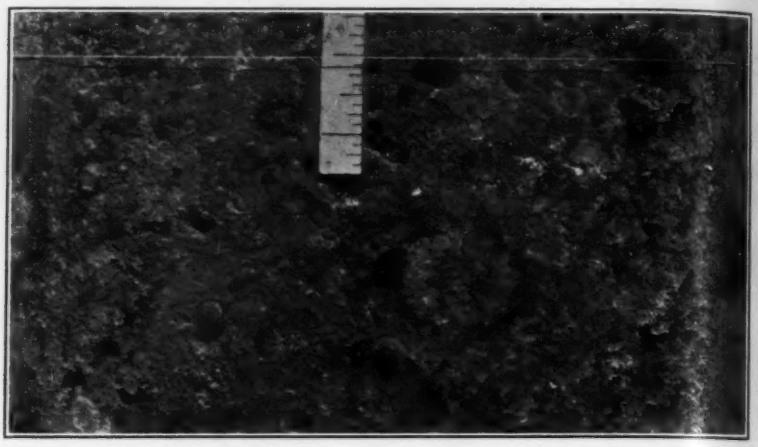

FIGURE 2.—*Plain concrete—no surface treatment.*

FIGURE 3.—*Concrete with abrasive aggregate in wearing surface.*

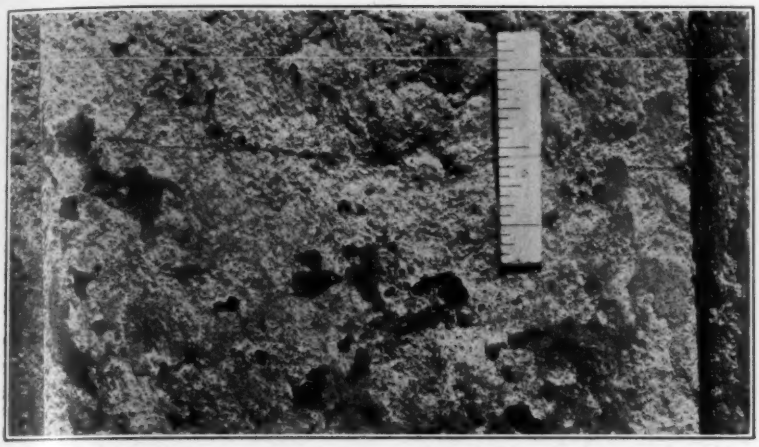

FIGURE 4.—*Concrete surfaced with 1:3 cement mortar.*

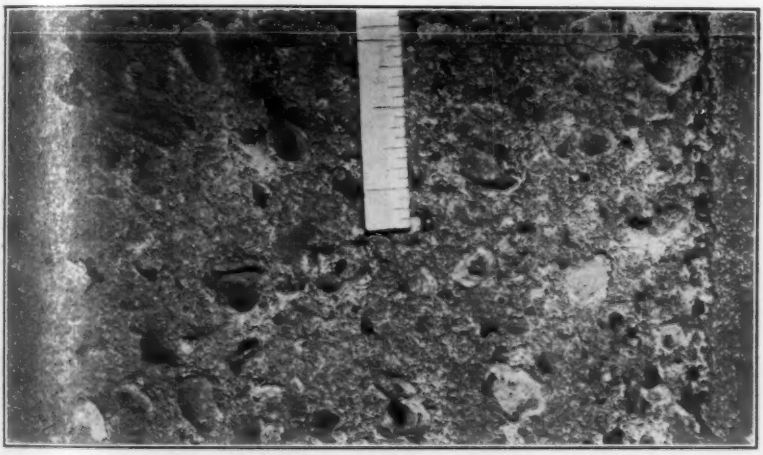

FIGURE 5.—*Concrete treated with three coats of liquid hardener after the concrete had set.*

FIGURE 6.—*Concrete with fine metallic hardener in wearing surface.*

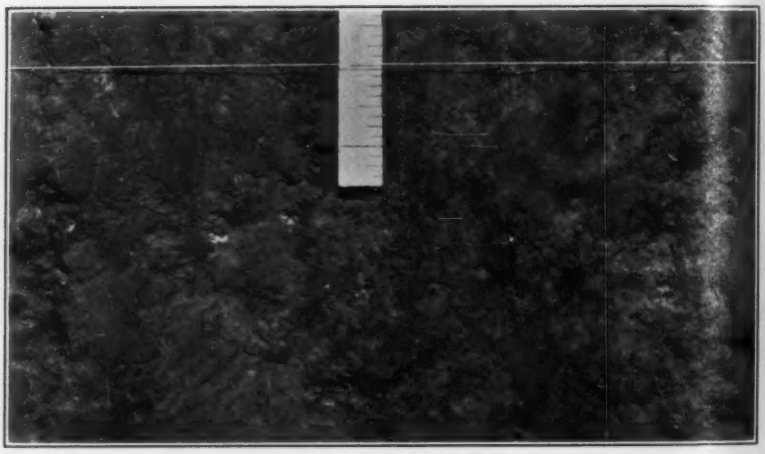

FIGURE 7.—*Asphalt blocks 5 by 12 by 2 inches.*

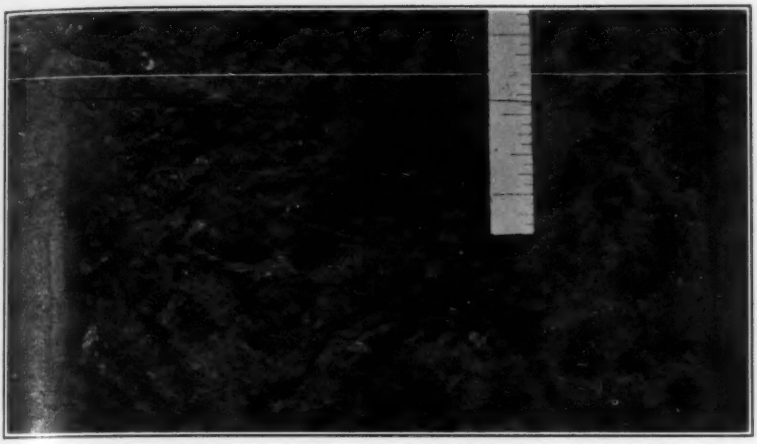

FIGURE 8.—*Asphalt plank ½ inch thick.*

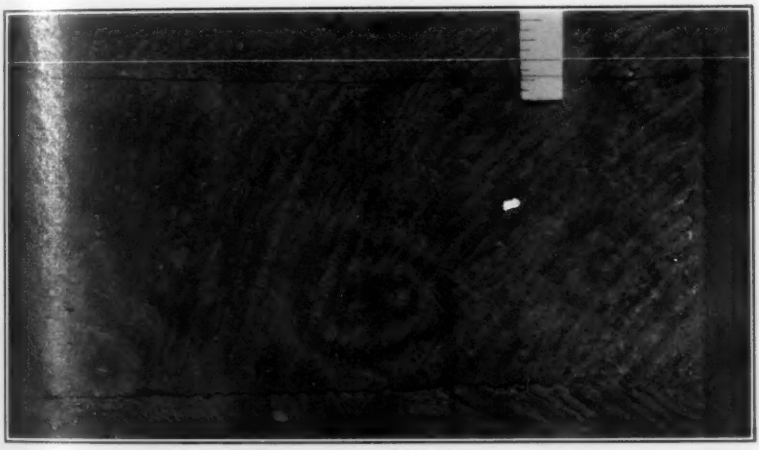

FIGURE 9.—*Southern yellow pine end-grain blocks 2½ inches thick, set in mastic.*

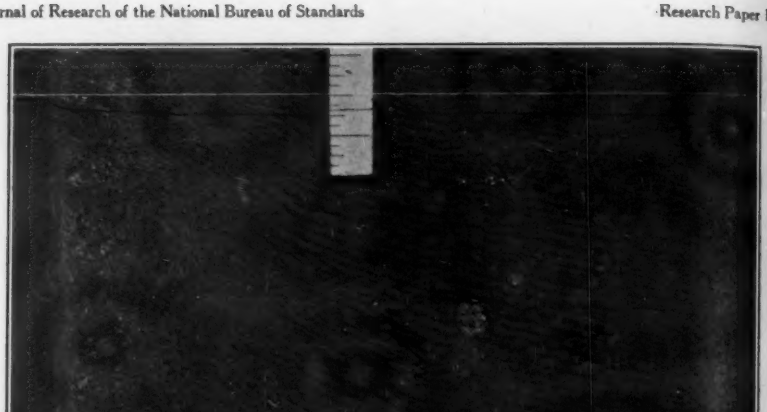

FIGURE 10.—*Douglas fir end-grain blocks 2½ inches thick, set in mastic.*

FIGURE 11.—*Quarter-sawed red oak 25/32 inch thick, set in mastic.*

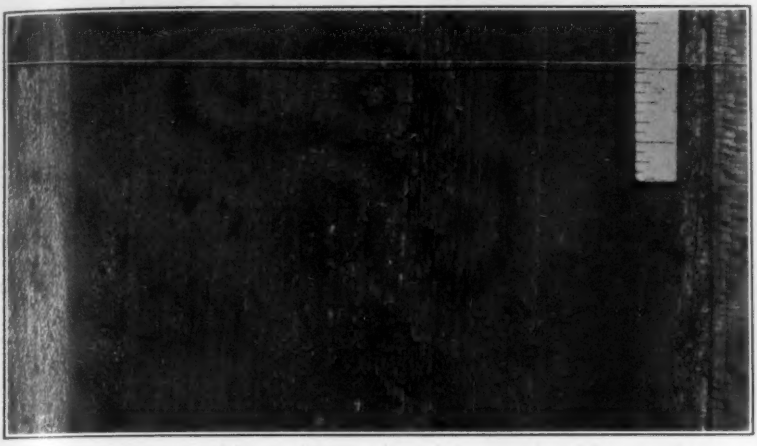

FIGURE 12.—*Maple, edge grain 2⅛ inches thick set in mastic.*

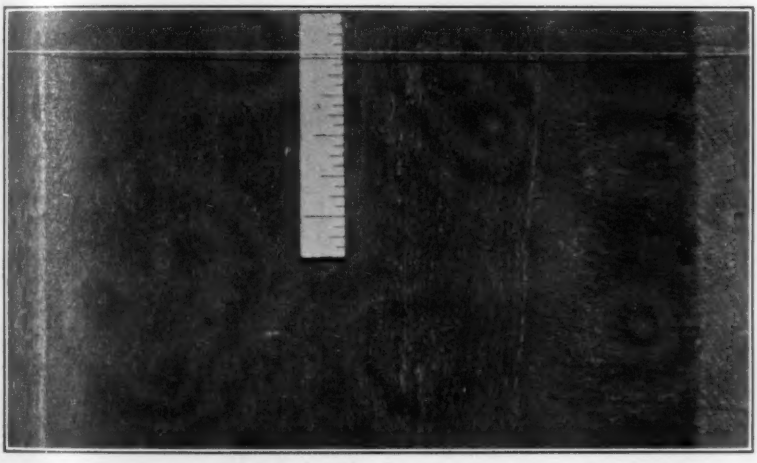

FIGURE 13.—*Maple unit blocks 31/32 inch thick, set in mastic.*

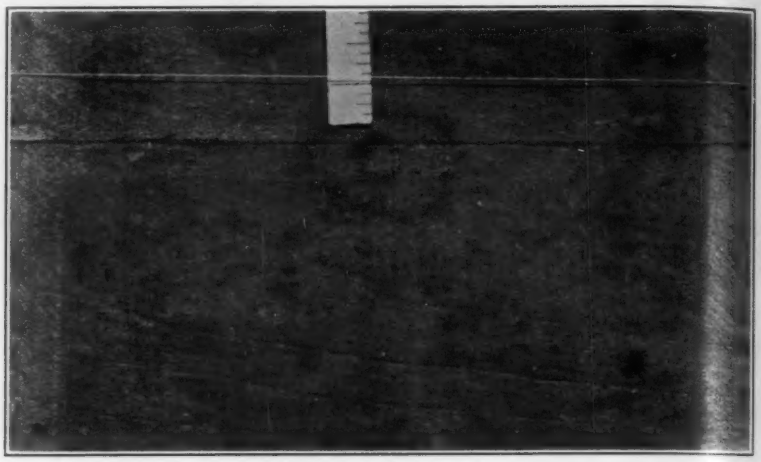

FIGURE 14.—*Maple plain strips $^{33}/_{32}$ inch thick, set on sleepers.*
Finished with one coat sealer, two undercoats, one finish coat.

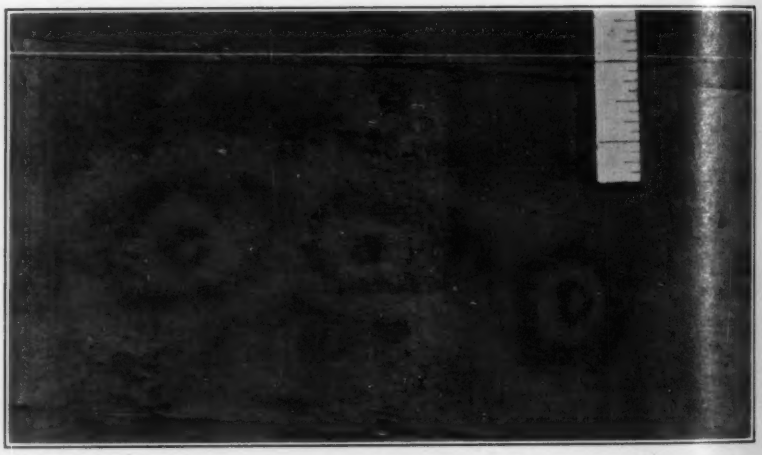

FIGURE 15.—*Maple plain strips $^{33}/_{32}$ inch thick, set on sleepers.*
Finished with one coat sealer and one finish coat.

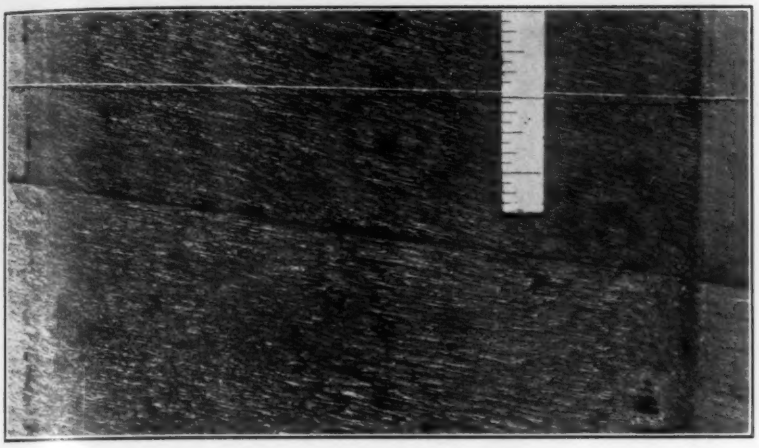

FIGURE 16.—*Maple plain strips $^{33}/_{32}$ inch thick, set on sleepers.*
Finished with two coats linseed oil and turpentine.

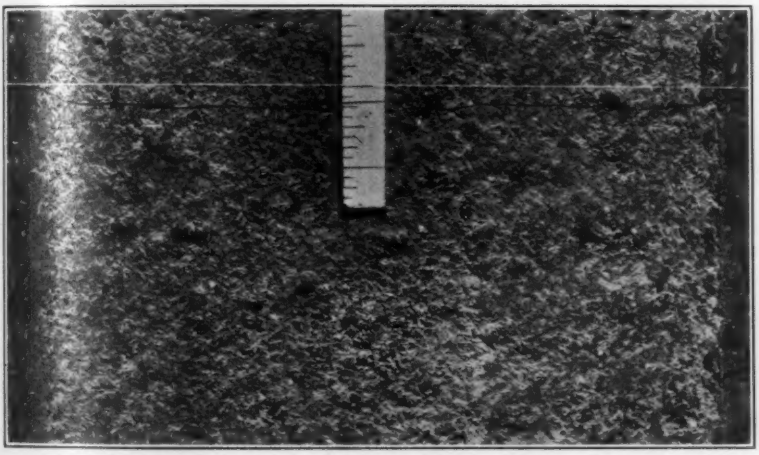

FIGURE 17.—*Magnesite with hardwood fiber aggregate 1 inch thick.*

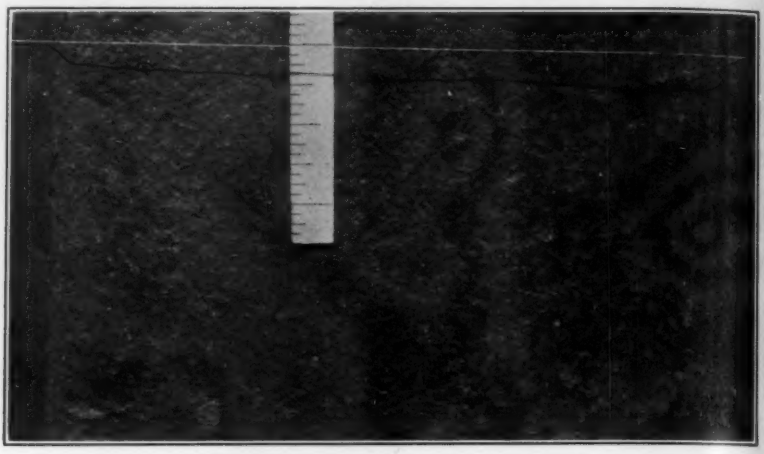

FIGURE 18.—*Plain magnesite ½ inch thick.*

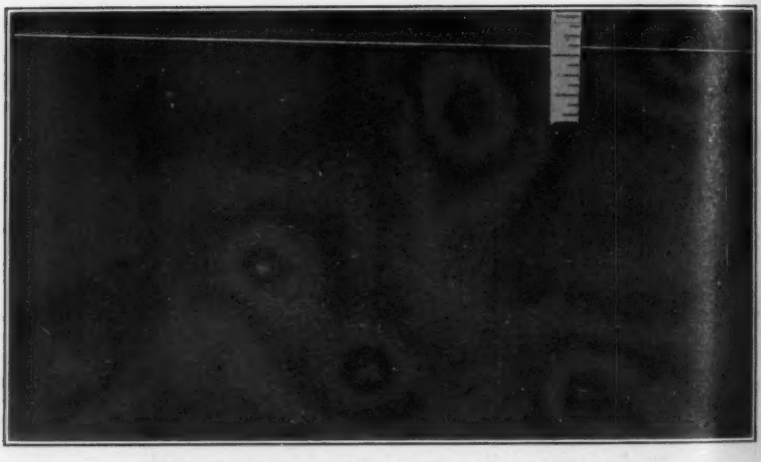

FIGURE 19.—*Battleship linoleum ¼ inch thick.*

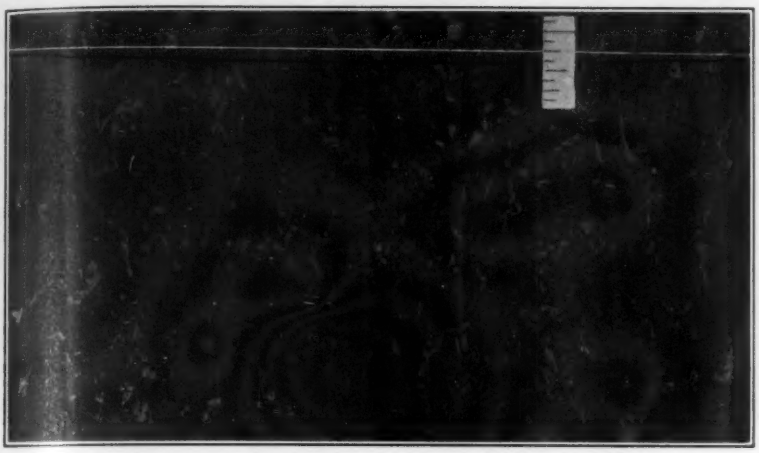

FIGURE 20.—*Rubber sheet ¼ inch thick.*

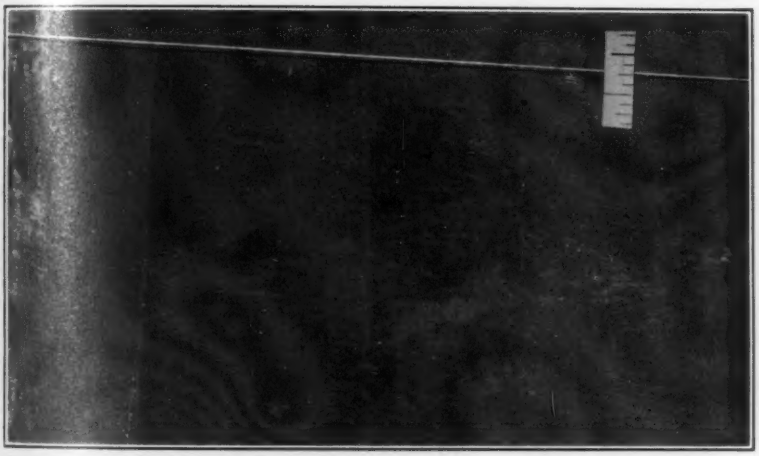

FIGURE 21.—*Rubber tile ¼ inch thick.*

UNIV. OF MICH.

## IV. RESULTS

The 20 specimens tested included 5 of concrete, 8 of wood, 2 of magnesite, 2 of asphalt, 2 of rubber, and 1 of linoleum.

For those interested in the details of construction, complete specifications used in laying these floors may be had free upon request addressed to the National Bureau of Standards, Washington, D. C.

Concrete specimens 2, 3, 5, and 6 were made of 1:1:1½ concrete 1½ inches thick. Number 2 was given no surface treatment; number 3 had an abrasive aggregate in the wearing surface; number 5 was treated with three coats of liquid hardener after the concrete had set; and number 6 had a fine metallic aggregate or hardener in the wearing surface. Number 4 was made of 1:3 cement mortar, ¾ inch thick. The photographs show that the cement-mortar finish (no. 4) did not stand up well under this test. The plain concrete (no. 2) was not particularly durable, nor was it much improved by any of the three treatments tried.

Asphalt specimen 7 was made of blocks 5 by 12 by 2 inches set in ½ inch of mortar. Specimen 8 was asphalt plank, ½ inch thick. The surfaces of both block and plank roughened quite readily under this treatment, and for this reason they could not be kept clean by sweeping. The plank showed considerably more wear than the block.

Wood specimen 9 was made of end-grain blocks of Southern yellow pine, 2½ inches thick, set in mastic. Number 10 was the same as no. 9, except that the wood was Douglas fir. Number 11 was quartersawed red oak, $^{25}/_{32}$ inch thick, set in mastic. The remaining specimens were all maple: No. 12, edge grain, $^{17}/_{8}$ inch thick, set in mastic; no. 13, unit blocks $^{31}/_{32}$ inch thick. set in mastic; no. 14, plain strips $^{33}/_{32}$ inch thick, set on sleepers and treated with one coat of sealer, two undercoats, and one finish coat; no. 15, same as no. 14, except that the two undercoats were omitted; no. 16, same as no. 15, except that the treatment consisted of two coats of linseed oil and turpentine.

The photographs show that the end grain (nos. 9 and 10) and the quartersawed grain (no. 11) wore appreciably under this test. Of the maple floors, there is little choice between the edge grain (no. 12) and the flat grain (no. 13); both stood up very well. Of the three methods of finishing examined, the four-coat job (no. 14) is better than the two-coat job (no. 15), and both are better than the linseed-oil finish. The differences, however, are in the appearance and the ability to keep the floor clean; there is not much difference in the wear.

Magnesite specimen 17 contained an aggregate of hardwood fiber and was 1 inch thick; no. 18 was ½-inch plain magnesite. Both of these specimens showed wear to such an extent as to indicate their unsuitability for this kind of service.

Specimen 19 was ¼-inch battleship linoleum. This showed very little wear. There was a tendency to creep in the direction of the traffic, but the movement was not sufficient to break the bond between the linoleum and the concrete subfloor.

The first sample of rubber tile (no. 20) could not be made to stick to the concrete. It was finally taken up on November 14 and replaced by sheet-rubber flooring ¼ inch thick. The second sample of rubber tile (no. 21) adhered somewhat better, but it caused a great deal of trouble, tiles having to be replaced every few days. The results indicate that rubber will withstand the service fairly well, if some adhesive can be found to hold it to the concrete.

## V. SUMMARY

The results show that, for this particular service, maple, either flat or edge grain, linoleum, and, perhaps, rubber should give satisfactory durability. The different types of finishes used for maple flooring may improve its cleanability but have little effect on its durability. A better adhesive to hold linoleum and rubber flooring to concrete is needed. If this can be found, perhaps the rubber flooring will be as good as the linoleum. The amount each floor was worn is shown in table 1.

TABLE 1.—*Wear of various flooring materials after 60,000 truck cycles*

| Figure | Material | Wear (thirty-seconds of an inch) |
|---|---|---|
| 2 | Plain concrete | 3 |
| 3 | Concrete with abrasive aggregate | 3 |
| 4 | Concrete surfaced with 1:3 mortar | 21 |
| 5 | Concrete with liquid hardener | 3 |
| 6 | Concrete with metallic hardener | 4 |
| 7 | Asphalt blocks | 2 |
| 8 | Asphalt plank | 7 |
| 9 | End-grain southern yellow pine | 4 |
| 10 | End-grain Douglas fir | 4 |
| 11 | Quartersawed red oak | 4 |
| 12 | Edge-grain maple | 2 |
| 13 | Maple unit blocks | 2 |
| 14 | Maple strips, 4-coat finish | 2 |
| 15 | Maple strips, 2-coat finish | 2 |
| 16 | Maple strips, linseed-oil finish | 2 |
| 17 | Magnesite with hardwood fiber | 6 |
| 18 | Plain magnesite | 7 |
| 19 | Linoleum | 1 |
| *20 | Rubber sheet | 3 |
| 21 | Rubber tile | 1 |

* The sheet-rubber flooring was subjected to only 46,985 truck cycles.

## VI. INTERPRETATION OF RESULTS

This test was designed to compare the relative merits of floor coverings for use in post-office workrooms and on loading platforms. The test simulated the ordinary trucking found therein, but not the gouging which might be caused by the dropping of heavy parcels with sharp corners. This service is quite out of the ordinary. The results of the test, therefore, should not be interpreted as indicating the relative merits of various floor coverings when used under other conditions.

WASHINGTON, August 17, 1937.

U. S. DEPARTMENT OF COMMERCE NATIONAL BUREAU OF STANDARDS

RESEARCH PAPER RP1047

*Part of Journal of Research of the National Bureau of Standards, Volume 19, November 1937*

# EVALUATION OF CRUSH-RESISTANT FINISHING TREATMENTS FOR FABRICS

By Herbert F. Schiefer

ABSTRACT

The results of measurements by the compressometer method of certain compressional characteristics of representative transparent velvet fabrics before and after the application of commercial crush-resistant finishes are reported and discussed. These finishing treatments markedly change the compression and recovery characteristics of the untreated fabrics and, in general, increase the "compressional resilience" of the pile. These changes appear to correlate with the changes in the appearance produced in the fabrics when small areas of the various specimens are compressed with the compressometer.

CONTENTS

| | Page |
|---|---|
| I. Introduction | 571 |
| II. Procedure | 571 |
| III. Discussion of results | 572 |

## I. INTRODUCTION

The utility of pile fabrics depends, among other things, upon the resistance to crushing or deformation and matting of the yarns and fibers forming the pile. Pile dress fabrics, notably transparent velvets with rayon pile, have been particularly troublesome in this respect. The application to such fabrics of synthetic resins by what are called crush-resistant finishing treatments has resulted in much more serviceable products. The work reported in this paper was undertaken to determine the applicability of the compressometer to the evaluation of crush-resistant treatments on pile dress fabrics.

## II. PROCEDURE

Representative transparent velvet fabrics, before and after the application of crush-resistant finishing treatments, were furnished for the work by several manufacturers. Samples of these fabrics were conditioned by exposure for several days in an atmosphere of 65-percent relative humidity and a temperature of 70° F, and were tested in this condition.

The compressometer illustrated in figure 1 is described in detail in a previous publication.[1] By turning the knurled knobs, shown in the center of the figure, the circular presser foot, which is 1 inch in

[1] Herbert F. Schiefer. *The compressometer, an instrument for evaluating the thickness, compressibility, and compressional resilience of textiles and similar materials.* BS J. Research **10**, 705 (1933) RP561.

diameter, is lowered and a fabric placed on the anvil below it is compressed. The load applied to the fabric by the foot for any position of the knurled knobs is indicated on the upper dial of the instrument. The thickness of the fabric at that load, that is, the distance from the presser foot to the anvil, is indicated on the lower dial.

The fabric to be tested was subjected to a series of increasing pressures from 0.25 to 5.0 lb/in.$^2$ in increments of 0.25 lb/in.$^2$ for pressures up to 1.0 lb/in.$^2$ and of 0.5 lb/in.$^2$ thereafter, and the thickness at each pressure was observed and recorded. Similar observations were then made for decreasing pressures. The time between observations was about 10 seconds. Each fabric was measured in at least five different places and the averages of the values for each pressure were used. It was found necessary to adjust the presser foot parallel to the anvil before starting to measure each new place on pile fabrics.

The results were plotted in the form of curves, showing the compression and recovery of the fabrics. In addition, the energy expended in compressing the fabric as the pressure was increased from 0.25 to 5.0 lb/in.$^2$ and the energy recovered when the pressure was decreased over this range were calculated.[2] The ratio of the energy of recovery to the energy of compression was taken as a measure of the "compressional resilience" of the fabircs.

## III. DISCUSSION OF RESULTS

In a transparent velvet the cut tufts of the pile yarns, which are exposed on one side of the fabric, are bound in with the warp and filling yarns comprising the woven back. The pile yarns are composed of numerous rayon fibers which project a given distance beyond the surface of the back fabric and are oriented substantially perpendicular to it. The load exerted by the compressometer is applied to the ends of the pile fibers, substantially parallel to their longitudinal axes, and tends to bend them over. The amount of bending of the fibers of a given fabric depends upon the number of fibers per unit area, their stiffness, and the applied load. The fibers deflect in all directions, and thereby reinforce each other to some degree. However, as the load is increased a value is eventually reached which is greater than can be supported by the pile fibers and a sudden bending over of the fibers at their base results. This collapse of the pile, equivalent to a sudden decrease in the thickness of the fabric, is indicated by an abrupt change in the compression curve. A fabric in which this condition has been produced is here described as having been "crushed."

Typical curves representing the compression and recovery of two transparent velvet fabrics, measured before and after the application of crush-resistant treatments, are plotted in figure 2. They show clearly that the pile of both fabrics before treatment is crushed by pressures less than 5 lb/in.$^2$ and that the fabrics do not recover to their original thickness when the load is removed. The treatment applied to fabric *A*, no. 4 in table 1, has greatly improved it both with respect to the extent of the compression, which is very small for a

[2] The energy of compression is equal to the area between the compression curve and the thickness axis, that is, the vertical axis. The energy of recovery is the corresponding area for the recovery curve. Unless a planimeter is available, the simplest method of calculating these areas is to divide each area by horizontal lines into a series of trapezoids. The area of each trapezoid is calculated by using the formula "area equals base times average altitude", where the base is the distance between the two horizontal lines forming the trapezoid and the average altitude is the average of these two horizontal lines, that is, distance from the thickness axis to their intersection with the curve.

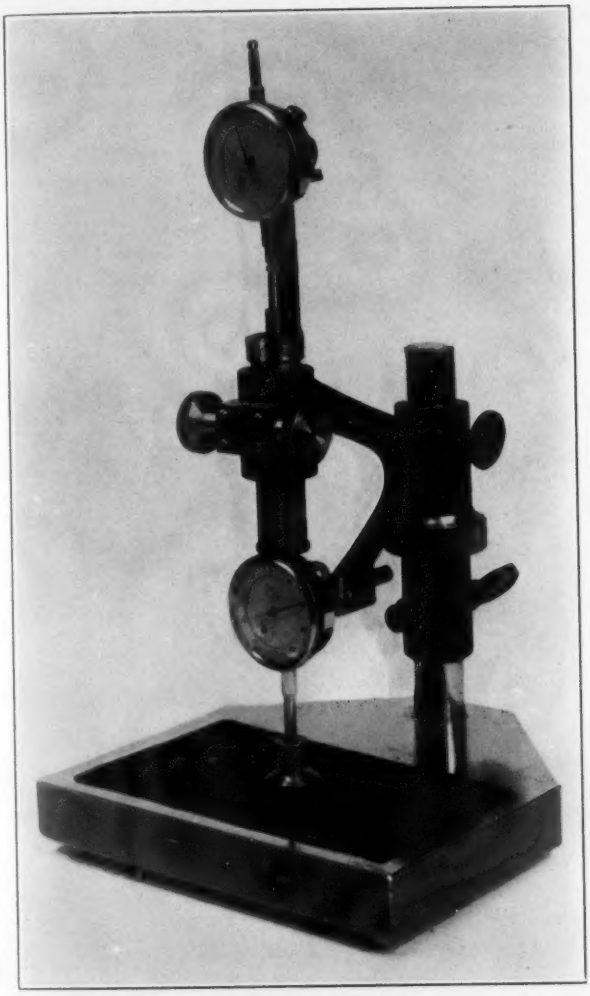

FIGURE 1.—*Compressometer.*

UNIV. OF MICH.

pressure of 5 lb/in.$^2$ and with respect to the recovery. The pile of this fabric is not crushed. The improvement in fabric *B*, no. 5 in table 1, resulting from the treatment is much less with respect to the compression and recovery and the pile of the treated fabric is crushed.

Two of the six velvet fabrics tested were compressed but little under a pressure of 5 lb/in.$^2$, either before or after the application of the crush-resistant treatment. The compression and recovery curves of these fabrics are similar to the treated curves of velvet *A*, figure 2. In two cases the pile was crushed before but not after the treatment (fig. 2, velvet *A*), while for the remaining two fabrics the pile was crushed both before and after the treatment (fig. 2, velvet *B*). The compression and recovery curves obtainable with the compressometer

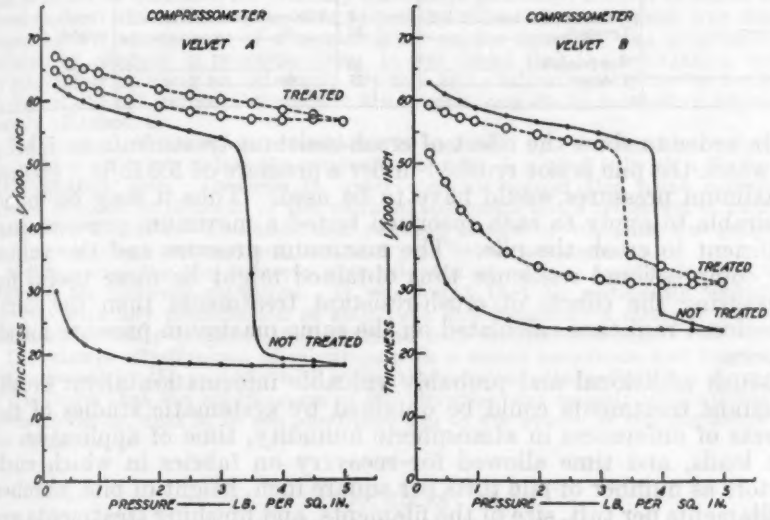


FIGURE 2.—*Effect of crush-resistant finishing treatments on compression and recovery curves of two transparent velvet fabrics as measured by the compressometer.*

show clearly the difference in these fabrics. It is concluded that the instrument should be useful in evaluating the effectiveness of crush-resistant treatments and in studying variations in them.

In general there was observed a more marked change in appearance between the compressed and uncompressed areas of an untreated velvet fabric than in the treated specimen of the same fabric. This difference in appearance was more permanent in the untreated fabrics. Also, in comparing the six velvet fabrics with each other with respect to appearance, the two untreated velvets in which the pile was not crushed changed less in appearance than the four untreated velvets in which the pile was crushed. Similarly, the four treated velvets in which the pile was not crushed changed less in appearance than the two treated velvets in which the pile was crushed.

The compressional resilience for each of the six velvet fabrics tested is given in table 1. This quantity is increased by the crush-resistant finishing treatments. It can be correlated with the change in appearance produced when the compressed areas are compared with areas that have not been compressed. These changes in appearance are also noted in the table.

TABLE 1.—*Effect of crush-resistant finishing treatments on transparent-velvet fabrics*

| Specimen | Designation | Compressional resilience | Remarks | Change in appearance |
|---|---|---|---|---|
| | | *Percent* | | |
| 1 | Not treated | 38 | Pile not crushed | Slight. |
| | Treated | 50 | do | Very slight. |
| 2 | Not treated | 41 | do | Do. |
| | Treated | 43 | do | Do. |
| 3 | Not treated | 6 | Pile crushed | Great. |
| | Treated | 46 | Pile not crushed | Very slight. |
| 4 | Not treated | 7 | Pile crushed | Very great. |
| | Treated | 55 | Pile not crushed | Very slight. |
| 5 | Not treated | 9 | Pile crushed | Great. |
| | Treated | 27 | do | Slight. |
| 6 | Not treated | 10 | do | Great. |
| | Treated | 17 | do | Slight. |

In order to show the effect of crush-resistant treatments on fabrics in which the pile is not crushed under a pressure of 5.0 lb/in.$^2$, greater maximum pressures would have to be used. Thus it may be found desirable to apply to each specimen tested a maximum pressure just sufficient to crush the pile. The maximum pressure and the values for compressional resilience thus obtained might be more useful for measuring the effects of crush-resistant treatments than the compressional resilience calculated on the same maximum pressure for all fabrics.

Much additional and probably valuable information about crush-resistant treatments could be obtained by systematic studies of the effects of differences in atmospheric humidity, time of application of the loads, and time allowed for recovery on fabrics in which such factors as number of pile tufts per square inch, height of pile, number of filaments per tuft, size of the filaments, and finishing treatments are varied systematically. The present work indicates that the compressometer would be useful for such an investigation and the results should be valuable to both manufacturers and users of pile fabrics.

---

The author acknowledges his indebtedness to Kenneth Barnard of the Pacific Mills and chairman of the Committee on Test Methods for Crease Resistance and Permanent Finishes of the American Association of Textile Chemists and Colorists, and to Dr. D. H. Powers, who is also a member of the committee, for suggestions and interest in this work. Grateful acknowledgment is also made to Röhm and Haas Co., Cheney Brothers, and the Rossie Velvet Co. for furnishing material for testing.

WASHINGTON, September 3, 1937.

U. S. DEPARTMENT OF COMMERCE NATIONAL BUREAU OF STANDARDS

RESEARCH PAPER RP1048

*Part of Journal of Research of the National Bureau of Standards, Volume 19, November 1937*

# STUDY OF VIBRATED CONCRETE

By John Tucker, Jr., G. L. Pigman, E. A. Pisapia, and J. S. Rogers

ABSTRACT

Starting with a basic 1:2.2:3.8 mix (the ratio of cement to sand to gravel which was selected as desirable for ordinary placement methods), a series of mixes was developed in which the segregation caused by vibration, and which was manifested by the appearance of a mortar layer on the concrete, was progressively reduced by changes in proportioning. It was found that the segregation could be minimized by using an extremely dry mix or by adjusting the mortar content so that it did not exceed the voids in the large aggregate by more than approximately 15 percent.

The strength of the concrete could not be increased by vibration above that of the rodded cylinders unless the concrete was very dry, that is, with a slump of approximately zero. Decrease in water content beyond this point caused a further increase in strength of the vibrated specimens but a reduction in that of the rodded concrete. The additional strength caused by vibration was greatest at 7 days (earliest test age) and least at 1 year (latest test age).

Molds containing the concrete were vibrated at various amplitudes and frequencies for different durations. It was found that by sufficiently vibrating concrete with any combination of amplitude and frequency a strength was obtained which was not appreciably increased with further vibration.

The relative effectiveness of vibration with a stated amplitude and frequency was measured by the rapidity with which the concrete attained a given strength. It was found that the effectiveness of the vibration was roughly proportional to the acceleration, that is, to the amplitude and to the square of the frequency of the vibration.

CONTENTS

| | Page |
|---|---|
| I. Introduction | 575 |
| II. Apparatus, materials, and tests | 576 |
| 1. Vibrator | 576 |
| 2. Materials | 577 |
| 3. Tests: scope and methods | 577 |
| III. Development and design of mixes | 579 |
| IV. Test results | 580 |
| 1. Influence of amplitude, frequency, and duration upon effectiveness of vibration | 580 |
| 2. Influence of vibration on properties of concrete with varying water contents | 584 |
| (a) Strength | 584 |
| (b) Solidity | 587 |
| (c) Surface condition | 587 |
| (d) Segregation | 589 |
| 3. Energy required for compaction | 590 |
| V. Summary and conclusions | 590 |

## I. INTRODUCTION

The use of vibration to compact concrete is not new, vibrating tables having been used as early as 1890.[1] In 1906 the concrete in the test beams made by the U. S. Geological Survey and reported in

[1] Sci. et Ind. No. 14, p. 46 (February 1934).

Bureau of Standards Technologic Paper T2 was placed by the aid of pneumatic vibrators. A short study of the problem was made by the National Bureau of Standards in 1915, but the strengths obtained with the concrete which had been vibrated into the molds were not greater than those obtained by the then common laboratory method of placing the concrete by ramming it with a heavy tamper. The potential increase in the strength of concrete due to vibration was not then apparent, and the studies were discontinued.

The method was first used to an appreciable extent during the World War. Independently, in 1917, M. Freyssinet, in France, and the U. S. Shipping Board applied the method to the construction of concrete ships. It was not, however, until about 1925 that the vibration of concrete came into extensive use.

Studies on the effect of vibration have already been made by others.[1] Although the effectiveness of the vibration depends upon the amplitude and frequency, test data have been for the most part qualitative.[2] It was the purpose of this investigation to determine the properties of concrete compacted into molds which were vibrated with known frequencies and amplitudes.

## II. APPARATUS, MATERIALS, AND TEST METHODS

### 1. VIBRATOR

The vibrator is spring-suspended, as schematically shown in figure 1. The amplitude of vibration is a function of the eccentricity and

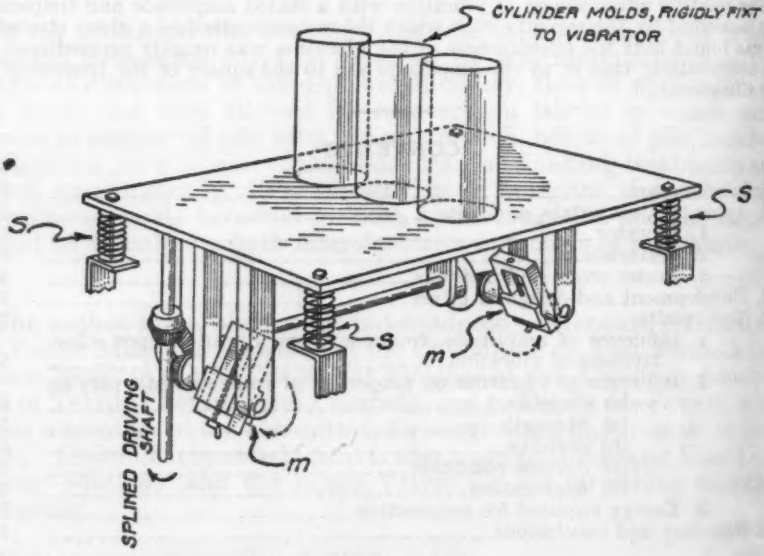


FIGURE 1.—*Vibrator.*

angular velocity of the rotating masses ($m$), of the constants of the four springs ($S$), and of the ratio of the magnitude of the two rotating

[1] For example, see bibliography, Proc. Am. Concrete Inst., p. 454 (1936).

[2] At the time this investigation was begun there were no quantitative data. Articles have since appeared in Proc. Am. Concrete Inst., p. 528 (1935); Prof. Withey, Proc. Highway Research Board (1935); Inst. Civil Engrs., London (March 1937), which present quantitative data.

masses ($m$) to the total mass of the machine (including that of the rotating masses, $m$).

The masses $m$ were adjusted closely to have the same eccentricity. The resultant horizontal component of the dynamic forces they exerted on the vibrator should have been zero, if the adjustment were perfect, but there was some horizontal vibration of the table, especially at the highest frequency. The machine vibrated the cylinder mold vertically, with a close approximation to simple harmonic motion.

The vibrator was designed so that the natural frequency, 4.4 vps (vibrations per second), of the vibrator was well below the frequencies used in the tests. The forced-amplitude type was selected in order to eliminate the uncertainty of the amplitude at resonance.

## 2. MATERIALS

The aggregate was Potomac River sand and gravel. The sand had a fineness modulus of 2.8. The sand and the gravel each had a specific gravity of 2.65. The gravel was recombined from four sizes: no. 4 to ⅜ in.; ⅜ to ¾ in.; ¾ to 1 in.; and 1 to 1½ in. The cement was of one lot of one brand of portland cement. It was stored in sealed metal drums.

## 3. TESTS: SCOPE AND METHODS

The proportions of the mixes are given in table 1. The initial tests were made on mix $A$, a nominal 1:2:4 mix. Mixes $B$ to $G$ were developed through study of the segregation caused by vibration. Mix $G$ (1:1.1:4.9) of the same richness in cement to aggregate by weight as $A$, was of most unusual proportions, in which the mortar was just in excess of the voids in the coarse aggregate, and in which the segregation had thus been reduced. Mixes $B$ to $F$ were used in segregation and development studies only. The characteristics of mixes $A$ and $G$, both normally rodded into place and compacted by varying degrees of vibration, were determined over a wide range of water contents, as shown in figures 8 and 9. The vibration characteristics (amplitude, frequency, and durations) used for compacting the concretes are shown in figure 3.

TABLE 1.—*Proportions by weight of mixes of dry materials*

| Mix | Concrete | | | Coarse aggregate | | | |
|---|---|---|---|---|---|---|---|
| | Cement | Aggregate | | No. 4 to ⅜ in. | ⅜ to ¾ in. | ¾ to 1 in. | 1 to 1½ in. |
| | | Fine | Coarse | | | | |
| | | | | % | % | % | % |
| *A* | 1.00 | 2.22 | 3.80 | 20.0 | 30.0 | 20.0 | 30.0 |
| *B* | 1.00 | 2.00 | 6.50 | 15.4 | 23.1 | 23.1 | 38.4 |
| *C* | 1.00 | 1.40 | 4.60 | 15.6 | 23.0 | 23.0 | 38.4 |
| *D* | 1.00 | 1.56 | 7.85 | 15.4 | 24.7 | 20.7 | 39.2 |
| *E* | 1.00 | 1.70 | 7.37 | 16.8 | 26.1 | 20.5 | 36.6 |
| *F* | 1.00 | 1.66 | 6.45 | 16.7 | 26.1 | 20.5 | 36.7 |
| *G* | 1.00 | 1.10 | 4.90 | 15.3 | 23.1 | 23.1 | 38.5 |

The batches for mixes $A$ to $F$, inclusive, were hand-mixed for 2 minutes, one batch for each cylinder. The batches for mix $G$, enough

for 3 cylinders, were machine-mixed for 2 minutes. The slump test [4] was made in the usual manner. The flow was determined on concrete stirred into the mold, and recorded as the increase in diameter after 15 ½-in. drops in 10 sec on the 30-in. flow table.[5] It is to be noted that the concretes studied were all of very dry consistency, the wettest being drier than is normally used in construction (except, perhaps, for highways, or very special work). Because of the dryness of the concretes, the flow-table readings were less than those ordinarily encountered, reaching a minimum and then *increasing* with decreasing water content (figs. 8 and 9). The driest concretes (e. g. mix *A*, $C/W=2.50$), with water content less than that corresponding to minimum flow, may be said to have largely lost their plastic properties and to have a consistency similar to that of foundry moulding sand.

All concrete cylinders, 6 by 12 in., were made in watertight sheet-metal molds, the tops of which were sealed on with asphalt immediately after filling. The cylinders that were compacted by vibration were made by loosely filling the sheet-metal molds and superimposed hopper with a quantity of concrete which was almost enough, when compacted, to fill the molds.

The following combinations of frequencies and amplitudes were used: 21 vps at 0.043, 0.095, and 0.145 in.; 30 vps at 0.018, 0.045, and 0.095 in.; 42 vps at 0.01, 0.026, and 0.053 in.; 60 vps at 0.013, 0.021, and 0.04 in.[6] The nominal duration of vibration was the elapsed time from the instant the vibrator attained the designated frequency, as indicated by a tachometer, to the time of shutting off the power. The rodded cylinders were molded by American Society for Testing Materials Standard Method C–39–33 (1933) test procedure. All specimens were made and stored in a laboratory maintained at $70\pm2°$ F.

All strength-test specimens for each age and method of vibration were made in triplicate. On the date of test the sheet-metal molds were removed from the cylinders and the top and bottom surfaces of the cylinders ground to a plane surface. The dimensions and weights of the cylinders were determined immediately after making, and from these the weight of the concrete per unit volume and the solidity [7] were calculated.

The segregation was usually manifested by an accumulation of mortar on top of the cylinder (see fig. 2). For convenience, the

[4] Proc. Am. Soc. Testing Materials. Tentative Test Method 32, part 1, D–138–32T (1932).

[5] Proc. Am. Soc. Testing Materials. Tentative Test Method 35, part 1, C–124–36T (1936).

[6] These were the observed values obtained by microscopic measurement from lines made on horizontally moving cards by the sharp points of pencils rigidly attached to the vibrator. The greatest absolute variation of the observed values from the computed was about 0.007 in., and the greatest percentage variation was 18 percent, excluding, in both cases, the frequency of 60 vps. The rigidity of the machine was not adequate to eliminate flexure at 60 vps, and consequently secondary vibrations were set up. This emphasizes the necessity of special precautions in vibrator design and construction and also the necessity of experimentally checking the computed amplitudes and frequencies.

[7] The solidity is the ratio of the sum of the bulk volumes of the particles of the dry materials to the volume of the concrete. It is computed from the equation:

$$\text{Solidity}=\frac{W_c}{D_c}+\frac{W_s}{D_s}+\frac{W_g}{D_g}$$

in which $W_c$, $W_s$, and $W_g$ are the weights of cement, sand, and gravel in a unit volume of concrete, and $D_c$, $D_s$, and $D_g$ are the bulk densities of the cement, sand, and gravel particles, respectively, as computed from the equation:

$$D=\frac{W_d\times W}{W_w-W_i}$$

where $W_d$ is the weight of the dry material, $W_w$ is the weight of the water-saturated material in air, $W_i$ is its weight submerged in water, and $W$ is the weight of a unit volume of water.

segregation was taken as the difference in cement content of the upper and lower halves expressed as a percentage of the content in the lower half. The determination of the proportions of the concrete in the segregation studies was made by the proposed American Society for Testing Materials method.[8]

The surface condition of all cylinders was recorded as the estimated total area of pitting, pockets, or honeycombing on the surface.

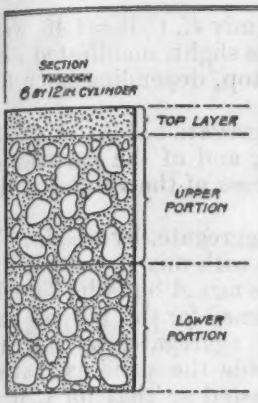


| | PROPORTIONS, BY WEIGHT | | | | PER CENT WATER | RATIO: CEMENT TO AGGREGATE | |
|---|---|---|---|---|---|---|---|
| | WATER | CEMENT | AGGREGATE | | | | |
| | | | FINE | COARSE | | | |
| | 0.55 | 1.00 | 2.2 | 3.8 | 7.8 | 1:6 | ORIGINAL MIX |
| TOP LAYER | 0.51 | 1.00 | 1.9 | 0.1 | 17.0 | 1:2 | AFTER VIBRATION |
| UPPER PORTION | 0.59 | 1.00 | 2.43 | 5.98 | 6.3 | 1:8.4 | |
| LOWER PORTION | 0.54 | 1.00 | 2.43 | 6.03 | 5.7 | 1:8.4 | |

FIGURE 2.—*Segregation, mix A, C/W=1.82, after vibration.*

## III. DEVELOPMENT AND DESIGN OF MIXES

Table 1 gives the proportions of all mixes. Mix *A*, when made with the sand and gravel at hand, was well suited for laboratory use without vibration. The proportion of the several sizes of gravel was an arbitrary one which had been found satisfactory in previous Bureau studies.

Mix *A*, when vibrated, showed a distinct tendency to segregate in the wetter consistencies. A cylinder mold full of concrete from a batch of mix *A*, $C/W=1.82$, by weight, was vibrated, and as the mortar rose to the top of the cylinder more and more of the batch was added. The displaced mortar flowed over the top of the mold until the cylinder was apparently a uniform compact mass with no mortar excess on top. This mass was analyzed and the same proportions of dry materials were used in mix *B*. In this and subsequent proportionings, the amounts of the four gravel sizes were chosen to the nearest whole percentage of the total mix.

Mix *C* was selected to have the same cement-aggregate ratio as mix *A*, and the same sand-gravel ratio and the same grading of coarse aggregate as mix *B*.

There was still pronounced segregation in vibrated specimens of mix *C*, for $C/W=1.82$. Mix *D* had the same cement-sand ratio and the same grading of coarse aggregate as the bottom half of the vibrated cylinders of mix *C*, but the ratio of mortar to coarse aggregate was reduced so that the mortar would exactly fill the voids in the rodded coarse aggregate.

It was found that mix *D*, $C/W=1.43$, also segregated but in the reverse manner from the previous mixes. The bottom half of the

[8] Proc. Am. Soc. Testing Materials 31, Part 1, 383 (1931).

cylinder contained a larger portion of mortar than the top, thus indicating a mortar deficiency in mix *D*.

The proportions in the lower half of mix *D* were used in mix *E*. The segregation of mix *E*, $C/W=1.46$, was in the same direction as in mix *D*, $C/W=1.43$, i. e., the lower half of the cylinder contained more mortar than the upper half. The difference in the proportions in the upper and lower halves was, however, very small, and about a fourth that of mix *D*.

The proportions found in the lower half of mix *E*, $C/W=1.46$, were used in mix *F*. The segregation in mix *F* was slight, manifested with more mortar either in the bottom or in the top, depending upon the wetness of the mix.

Mix *F*, $C/W=1.92$, gave practically no segregation. At this $C/W$ ratio the sum of the bulk volumes of water, and of the particles of cement, sand, and gravel was 7 percent in excess of the volume of the rodded gravel.

Mix *F* was proportioned 1:8.1, cement to aggregate, by weight. It was, however, desired to have for comparison with mix *A* another mix which had the same cement-aggregate ratio as mix *A* but which would have minimum segregation. Mix *G* was designed for this purpose and was therefore proportioned 1:6, cement to aggregate, by weight. The grading of the coarse aggregate was made the same as that of mix *F*; the ratio of sand to gravel was adjusted so that for $C/W=2.50$, the bulk volume of water, cement, sand, and gravel was made, as in mix *F*, $C/W=1.92$, 7 percent more than the bulk volume of the rodded coarse aggregate. It was found that the segregation in mix *G*, $C/W=2.1$, (the same water content as mix *D*, $C/W=1.43$) was approximately the same as the segregation of this latter batch but in the opposite direction. Mix *G* appeared to be the mix with a cement-aggregate ratio of 1:6 in which the segregation was a minimum, for even the most severe vibration.

## IV. TEST RESULTS

Complete test data were obtained only on mix *A*. Data on mix *G* were obtained for vibration periods of 30 and 90 sec only. Data were obtained for mix *C* for only one $C/W$ ratio (2.50). Mixes *B*, *D*, *E*, and *F* were used as steps in the determination of the mix with minimum segregation.

### 1. INFLUENCE OF AMPLITUDE, FREQUENCY, AND DURATION UPON EFFECTIVENESS OF VIBRATION

Figure 3 summarizes the strength-test results. It is apparent that with the exception of mix *A*, $C/W=2.50$, and mix *G*, $C/W=3.20$, vibration for the shortest duration was as effective as vibration for the longest duration in developing strength in the concrete. It can also be seen that the application of the vibration for the longest test periods (up to 90 sec) did not cause a reduction in strength.

Data on mix *A*, $C/W=2.50$, are given in detail in figure 4. It is apparent from this figure that the various combinations of amplitudes and frequencies differed in their efficacy, as indicated by the strength of the concrete. From the results it is seen that vibration at 42 vps and 0.01-in. amplitude was the least effective, and that in most cases

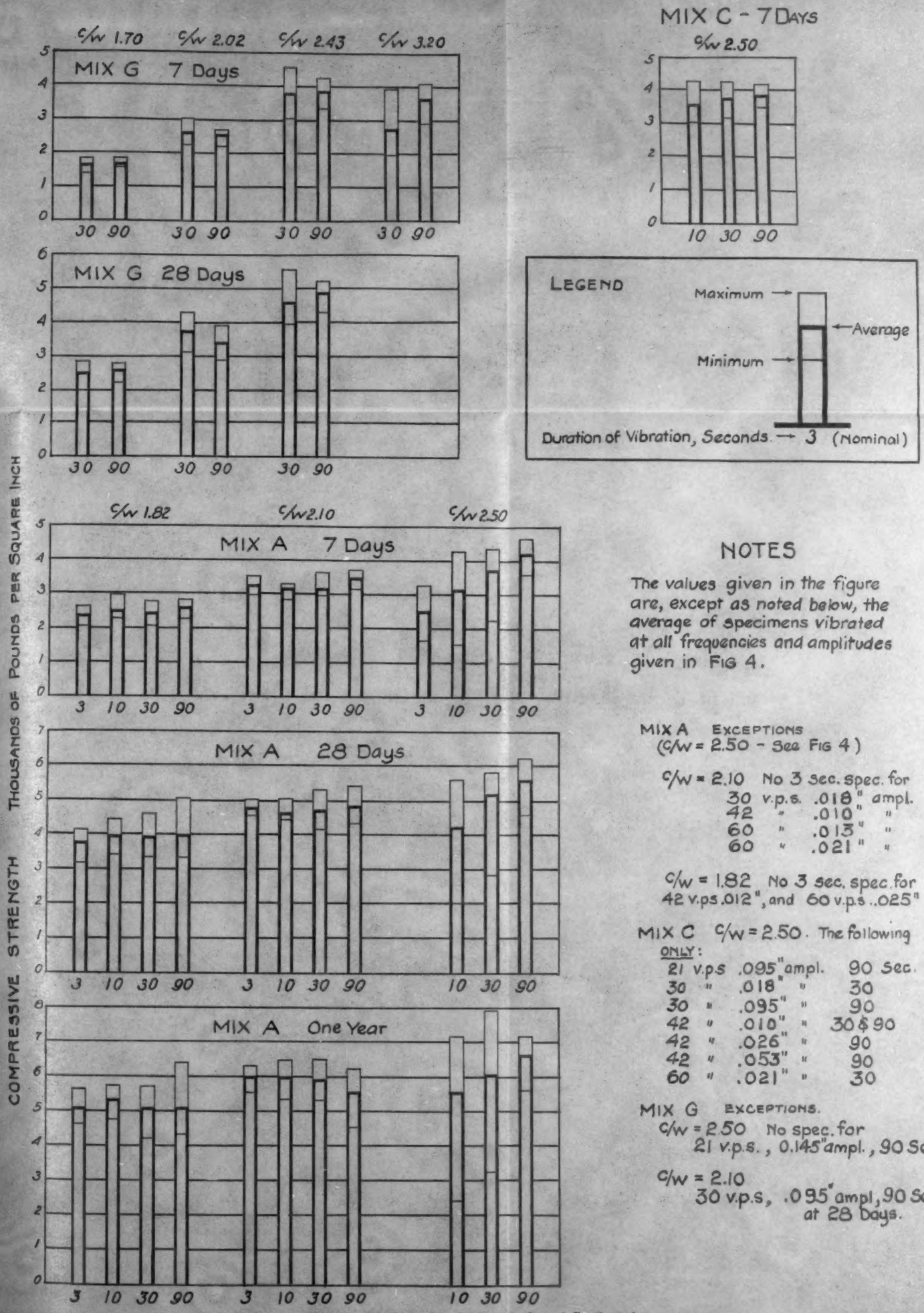
MIX C - 7 DAYS
c/w 2.50
10 30 90
c/w 1.70
c/w 2.02
c/w 2.43
c/w 3.20
MIX G 7 Days
30 90 30 90 30 90 30 90
MIX G 28 Days
30 90 30 90 30 90
LEGEND
Maximum
Average
Minimum
Duration of Vibration, Seconds → 3 (Nominal)
c/w 1.82
c/w 2.10
c/w 2.50
MIX A 7 Days
3 10 30 90 3 10 30 90 3 10 30 90
MIX A 28 Days
3 10 30 90 3 10 30 90 10 30 90
MIX A One Year
3 10 30 90 3 10 30 90 10 30 90
COMPRESSIVE STRENGTH THOUSANDS OF POUNDS PER SQUARE INCH

## NOTES

The values given in the figure are, except as noted below, the average of specimens vibrated at all frequencies and amplitudes given in FIG 4.

MIX A EXCEPTIONS
(c/w = 2.50 - See FIG 4)

c/w = 2.10 No 3 sec. spec. for
30 v.p.s. .018" ampl.
42 " .010" "
60 " .013" "
60 " .021" "

c/w = 1.82 No 3 sec. spec. for 42 v.p.s .012", and 60 v.p.s ..025"

MIX C c/w = 2.50. The following ONLY:

| | | |
|---|---|---|
| 21 v.p.s | .095" ampl. | 90 Sec. |
| 30 " | .018" " | 30 |
| 30 " | .095" " | 90 |
| 42 " | .010" " | 30 & 90 |
| 42 " | .026" " | 90 |
| 42 " | .053" " | 90 |
| 60 " | .021" " | 30 |

MIX G EXCEPTIONS.
c/w = 2.50 No spec. for 21 v.p.s., 0.145" ampl., 90 Sec.

c/w = 2.10
30 v.p.s, .095" ampl, 90 Sec at 28 Days.

FIGURE 3.—*Strengths of mixes A, C, and G, vibrated.*

19521—37 (Face p. 580) No. 1

UNIV OF MICH

# MIX A

C/W = 2.50

EACH VALUE IS THE AVERAGE OF THREE TEST CYLINDERS.

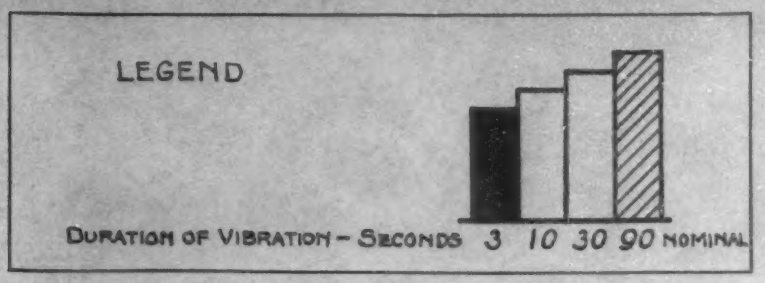


| | | | | | | | | | | | | |
|---|---|---|---|---|---|---|---|---|---|---|---|---|
| FREQUENCY VIB. PER SEC. | 21 | 21 | 21 | 30 | 30 | 30 | 42 | 42 | 42 | 60 | 60 | 60 |
| AMPLITUDE INCHES | .043 | .095 | 0.145 | .018 | .045 | .095 | .010 | .026 | .053 | .013 | .021 | .04 |

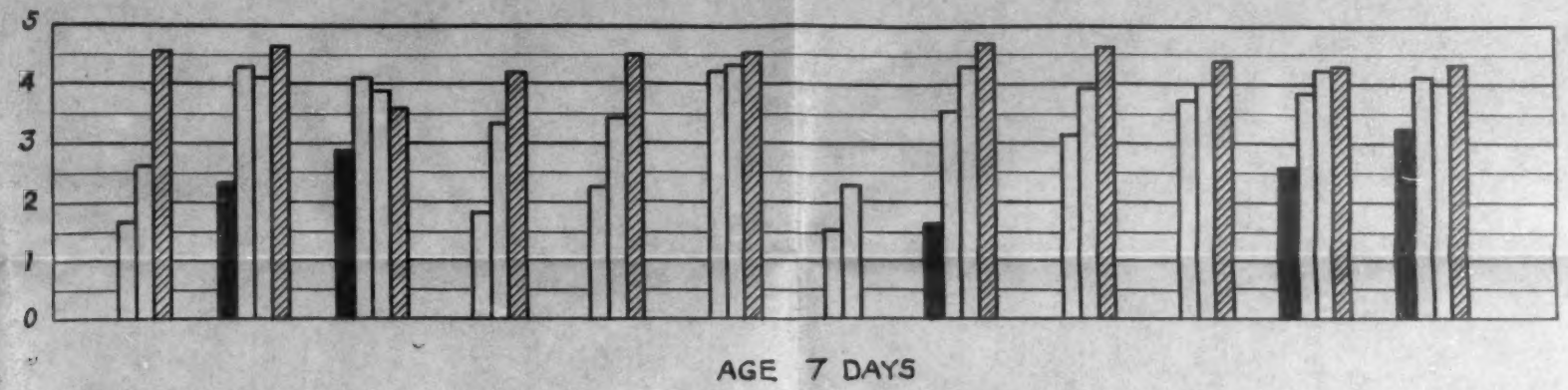


AGE 7 DAYS

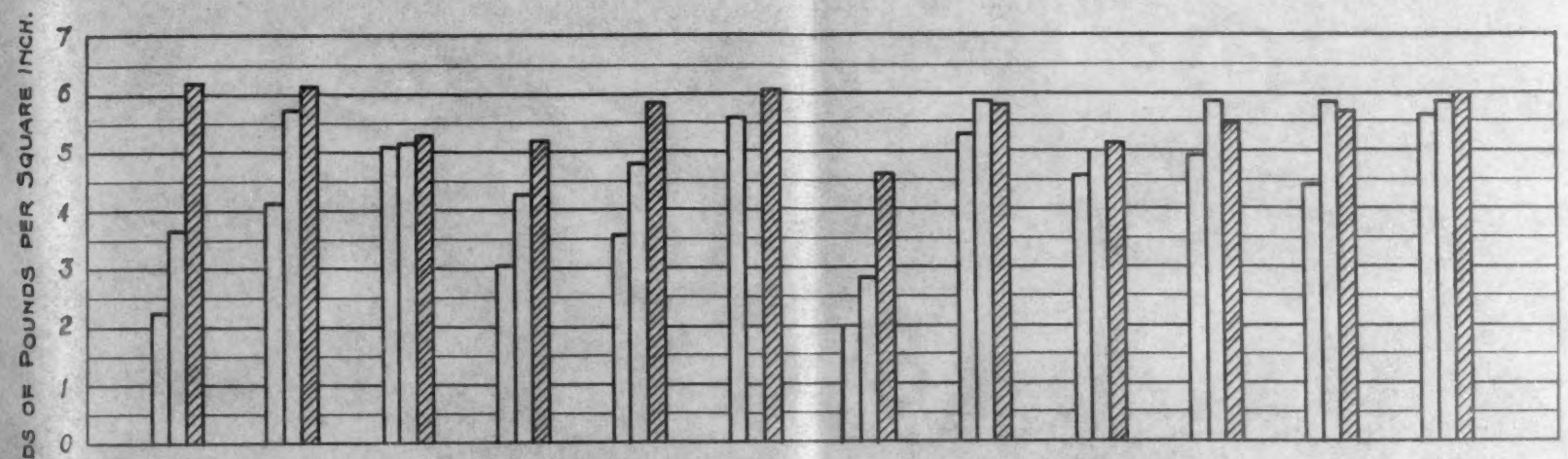


AGE 28 DAYS

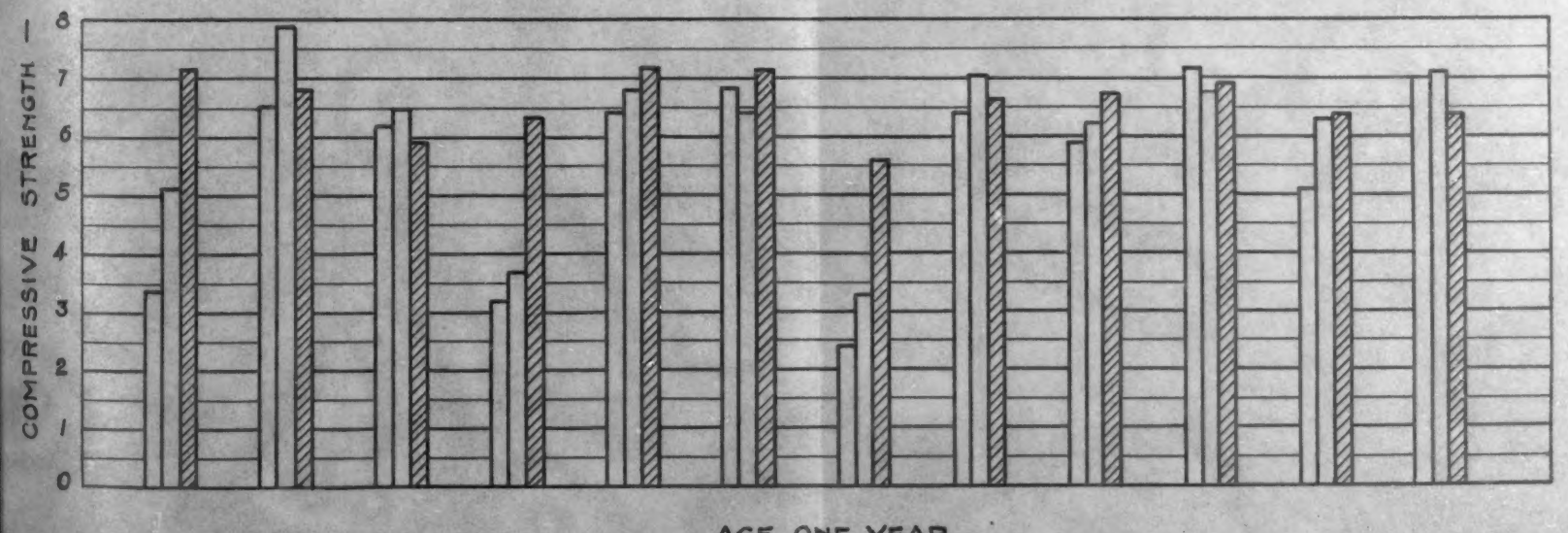


AGE ONE YEAR

FIGURE 4.—*Strength of mix A, C/W=2.50 when vibrated for several durations with various combinations of frequencies and amplitudes.*

19521—37 (Face p. 580) No. 2

UNIV OF MICH

the concrete was still increasing in strength even at the end of 90 sec of vibration. On the other hand, it appears that for some combinations of amplitude and frequency (such as 60 vps, 0.04-in. amplitude) the increase in strength due to vibration was practically completed in 10 sec or less.

In order to study further the effect of amplitude and frequency, figures 5 and 6 were drawn.[9] The curves showing increase in strength

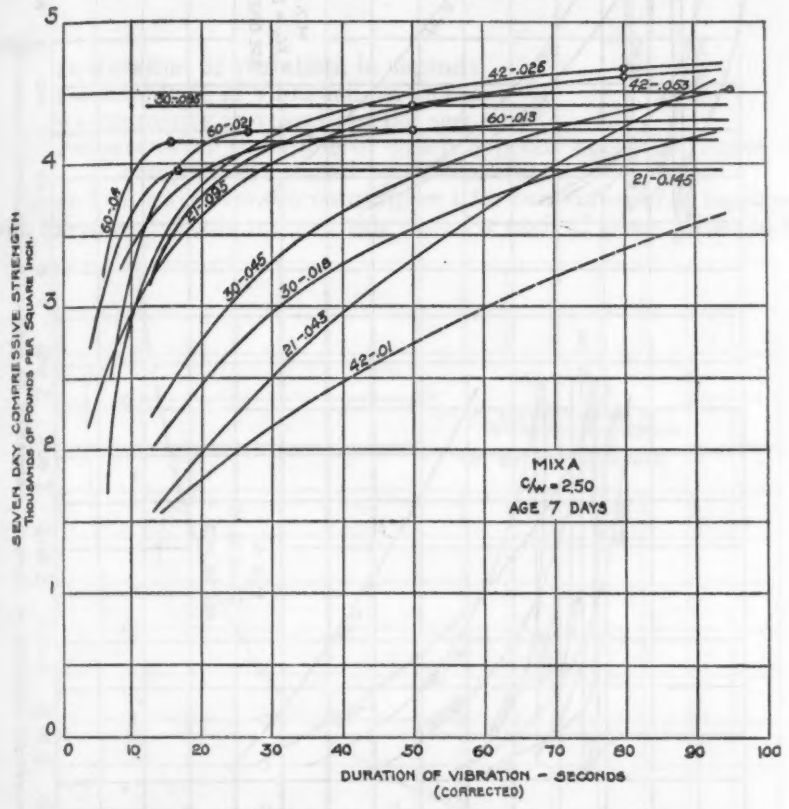


FIGURE 5.—*Relation of strength and duration of vibration.*

7 day strength mix *A*, *C*/*W*=2.50.
Vibration characteristics shown in the form 42-0.01 indicate a frequency of 42 vps with an amplitude of 0.01 in.

with duration of vibration indicate the tendency for strength to increase rapidly at first, then less and less rapidly as the strength approaches a limiting value for the particular concrete with a fixed water content. The optimum strength was defined as that strength beyond which the increase, with continued vibration, was negligible.

The relative efficacy of different combinations of frequency and amplitude may be expressed by the reciprocal of the time required to attain a given strength, such as the strength of the rodded cylinders of

[9] The time-frequency curves of starting and stopping the vibrator were determined. Corrections computed from these curves were added to the nominal durations of vibration, such revised durations being designated as the "corrected duration of vibration", and plotted in figures 5, 6, and 7. The data points were omitted in figures 5 and 6 to avoid confusion. In a few instances inconsistent points were given smaller weight in obtaining the curves.

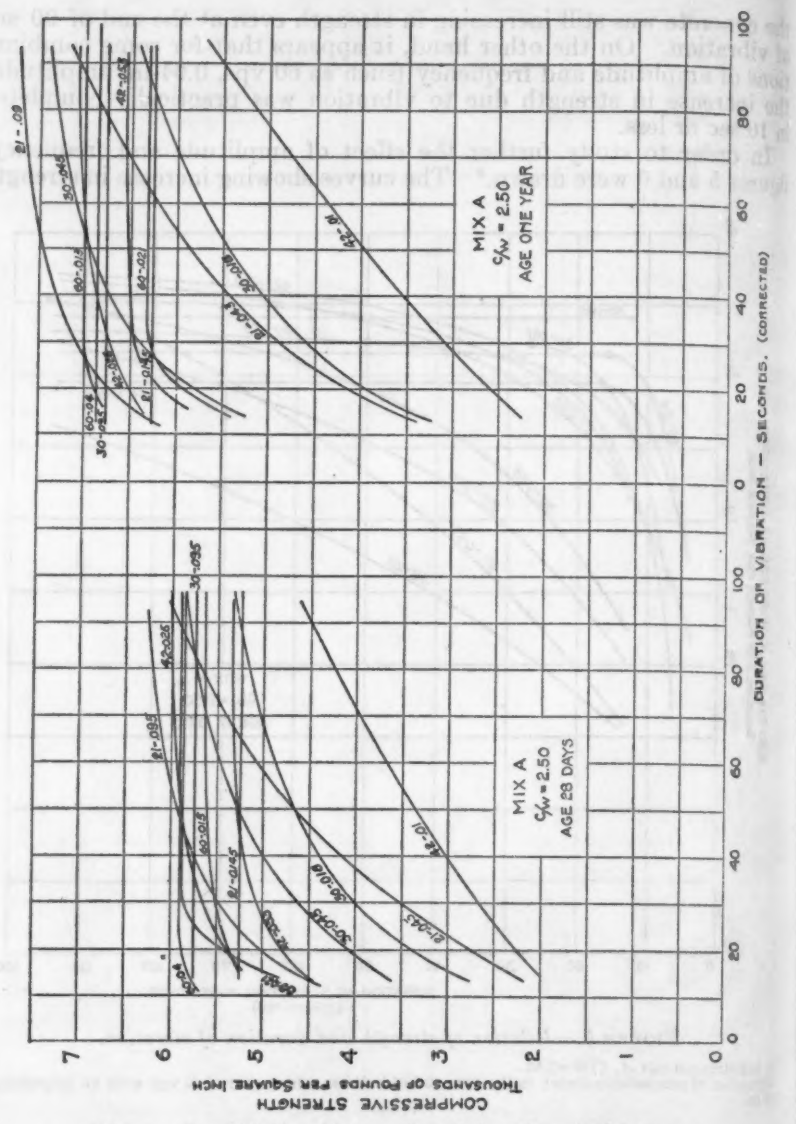


FIGURE 6.—*Relation of strength and duration of vibration.*

28-day and 1-year strengths, mix *A*, *C*/*W*=2.50.
Vibration characteristics shown in the form 42-0.01 indicate a frequency of 42 vps with an amplitude of 0.01 inch.

equal age and *C*/*W* ratio. Before tests were started it was assumed that the vibrational efficacy would be a function of the vibrational acceleration. This is proportional to the amplitude and to the square of the frequency.

In the preparation of the vibrated concrete specimens used in this study there were apparently present some variables not present in the rodded concrete specimens, which variables account for the greater spread in the results obtained in the vibrated-cylinder tests beyond

that ordinarily encountered in studies of concrete. Consequently, the correlation of results was not as good as might be desired. However, from a careful examination of the data it appeared that, in accord with the original assumption, the effectiveness of the vibration was, to a first approximation, in integral powers of the variables, given by the relation

$$t=\frac{k}{rn^2}, \text{ or } trn^2=k \ldots . \quad (1)$$

where

$t$=duration of vibration, in seconds.
$r$=amplitude of vibration, in inches.
$n$=frequency in vibrations per second.
$k$=parameter the value of which depends upon the degree of compaction reached by the concrete.

Figure 7 shows curves representing eq 1 for two values of $k$, together with the sets of points representing data for each of these values of $k$.

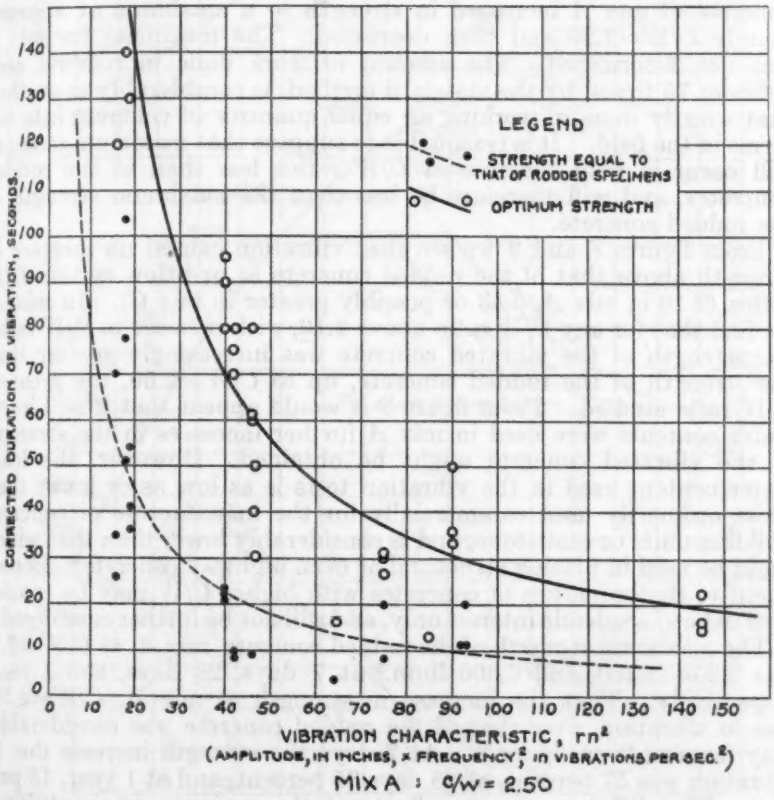
LEGEND
STRENGTH EQUAL TO THAT OF RODDED SPECIMENS
OPTIMUM STRENGTH
CORRECTED DURATION OF VIBRATION, SECONDS.
VIBRATION CHARACTERISTIC, rn²
(AMPLITUDE, IN INCHES, x FREQUENCY², IN VIBRATIONS PER SEC.²)
MIX A : C/W = 2.50

FIGURE 7.—*Graph of equation 1.*

Data for all three test ages are assembled in this figure. The set of dots represents the durations of vibration required to develop strengths equal to those of rodded specimens of equal age and equal $C/W$ ratio. The dotted line gives the curve representing eq 1 best fitting

these points. The set of circles represents the durations required to attain optimum strength, the solid line giving the curve representing eq 1 best fitting these points. Since there were only a few cases in which the specimens definitely attained a condition such that continued vibration could be interpreted as producing absolutely no increase in strength, the durations of vibration required for attaining optimum strength were taken as those durations beyond which the increase in strength with continued vibration was slight. The points indicated by circles in figure 5 were selected for computing the circles which represent the optimum strengths in figure 7. Only about two-thirds of the curves in figures 5 and 6 lent themselves to the selection of such points.

## 2. INFLUENCE OF VIBRATION UPON PROPERTIES OF CONCRETES WITH VARYING WATER CONTENTS

### (a) STRENGTH

Figure 8 indicates that with decrease in water content the rodded concrete of mix $A$ increased in strength to a maximum at approximately $C/W=2.20$ and then decreased. The maximum for mix $G$ was not determined. The amount of work done in rodding each cylinder 75 times, by the standard method, is considerably more than that usually done in working an equal quantity of concrete into the forms in the field. It is reasonable to suppose that maximum strength will occur in field concrete at $C/W$ ratios less than in the rodded concretes, and will therefore be less than the maximum strength of the rodded concrete.

From figures 8 and 9 we see that vibration caused no increase in strength above that of the rodded concrete at or below certain $C/W$ ratios (2.10 in mix $A$, 2.43 or possibly greater in mix $G$). In mix $A$, we find that for any $C/W$ ratio above 2.10, with increase in $C/W$ ratio, the strength of the vibrated concrete was increasingly greater than the strength of the rodded concrete, up to $C/W=2.50$, the greatest $C/W$ ratio studied. From figure 8 it would appear that if still lower water contents were used in mix $A$ further increases in the strength of the vibrated concrete might be obtained. However, the least water content used in the vibration tests is as low as or lower than those ordinarily used commercially for the manufacture of concrete building units or cast stone, and is considerably lower than that which could be used in placing structural or even highway concrete. Consequently, the properties of concretes with higher $C/W$ may be considered to be of academic interest only, and will not be further considered.

The maximum strength of the rodded concrete, mix $A$, at $C/W=2.2$, was 3,250, 4,700, and 6,300 lb/in.$^2$ at 7 days, 28 days, and 1 year, respectively. That the increase in strength of mix $A$, $C/W=2.50$, due to vibration, over that of the rodded concrete was considerable, may be seen from figure 8. At 7 days the strength increase due to vibration was 57 percent, at 28 days 35 percent, and at 1 year, 15 percent. The difference in the effects at the various ages is striking. Not alone was the percentage increase much larger at 7 days, but the absolute increase in strength was greater at the earlier ages—1,600 lb/in.$^2$ at 7 days and 950 lb/in.$^2$ at 1 year.

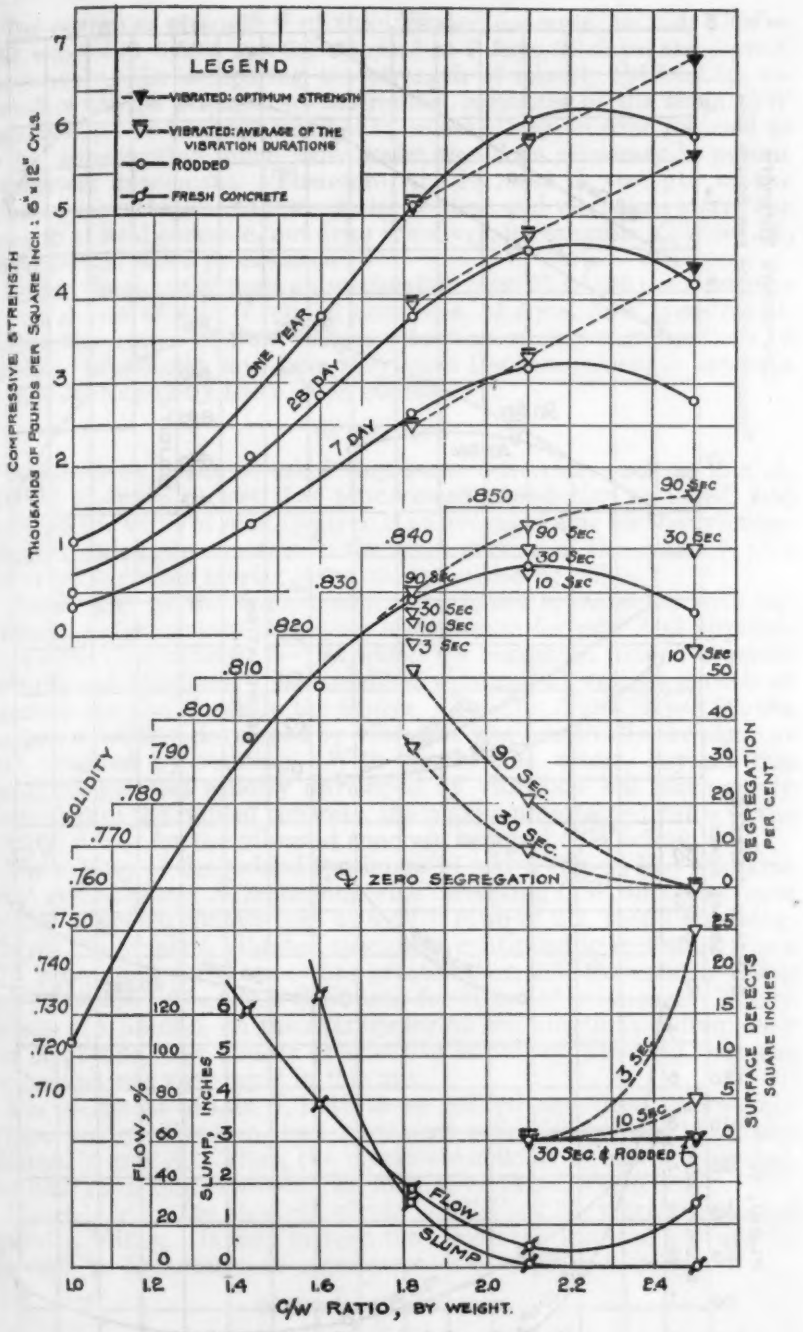


FIGURE 8.—*Characteristics of mix A.*

The values for the vibrated concretes are averages from figure 4.

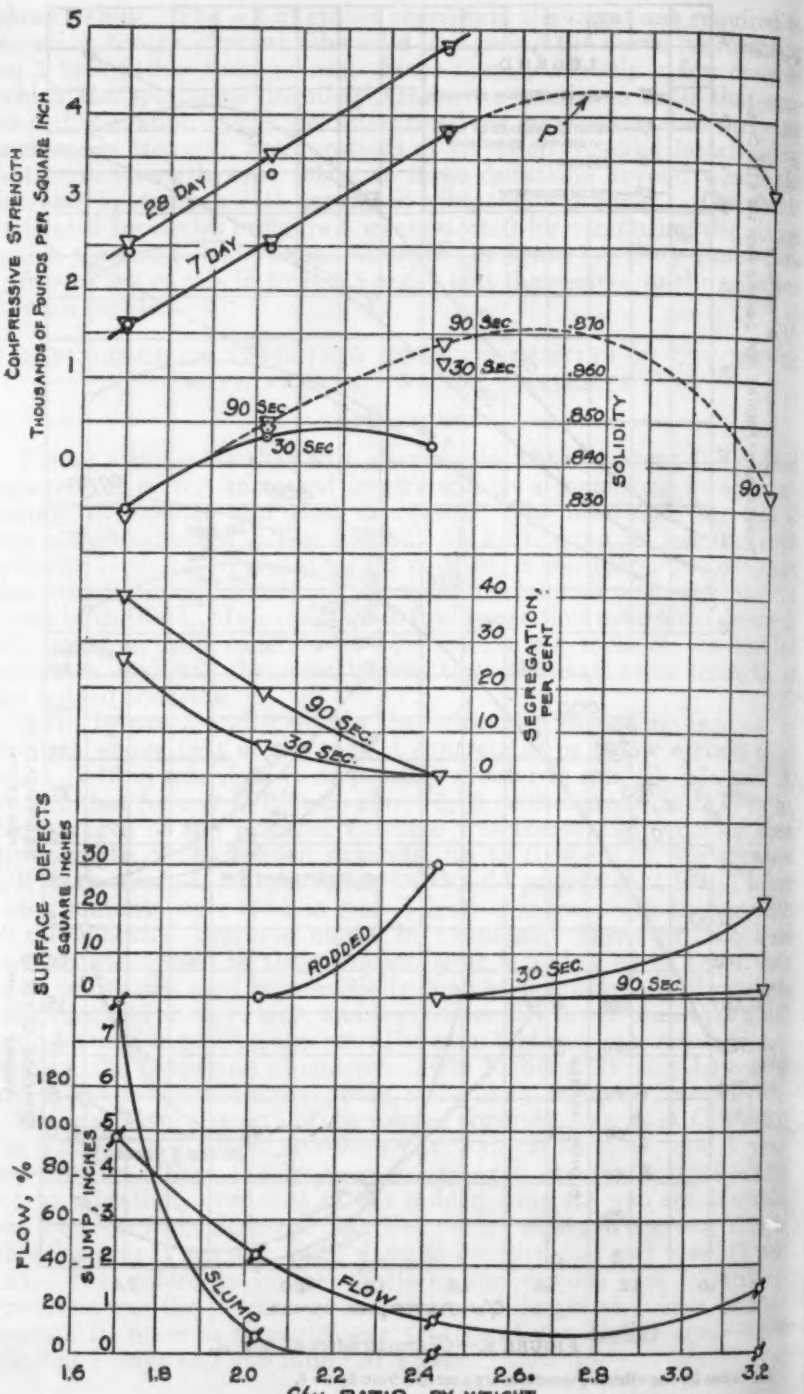


FIGURE 9.—*Characteristics of mix G.*

The values for the vibrated concretes are from figure 3. See legend of figure 8.

The optimum strength [10] of the vibrated concrete, mix $A$, $C/W=2.50$, was 4,400, 5,800, and 6,900 lb/in.$^2$ at 7 days, 28 days, and 1 year, respectively. In comparing the strength of mix $A$, $C/W=2.50$, vibrated, with the strength of the rodded concretes of the same $C/W$ ratio, it must be borne in mind that unless vibration were resorted to in field construction much more water would be necessary to permit satisfactory placement. Therefore, the increase in strength of the vibrated concrete, due to lower water content and vibration, above the strength of field concrete, not drier than, say, for example, $C/W=1.82$, would be still more pronounced.

Within the range of flows approximately from 35 to 100 the strengths of mix $A$ and of mix $G$ rodded concretes, of equal flow, were equal. Within this range of flow values, vibration at any combinations of duration, amplitude, and frequency gave the same strength concrete as that developed by the rodded concrete.

### (b) SOLIDITY

It should be borne in mind that some concretes, such as mix $A$, $C/W=1.82$, were so wet that pronounced segregation occurred, and therefore the value of solidity given is an average value for the cylinder, which included the concrete in the main portion of the cylinder, plus the very dissimilar mortar layer on top. (See fig. 2.)

The solidity of the rodded concretes, figure 8, increased with decrease in water content, attaining a maximum for mix $A$ at approximately the $C/W$ ratio (2.2—) at which the maximum rodded concrete strength was obtained. The solidities obtained at various periods of vibration are also shown in the figures. For mix $A$ at $C/W=1.82$, the maximum solidity developed by vibration was practically the same as that obtained by rodding. With decrease in water, beyond this point, the greatest solidity developed by vibration was increasingly above that of the rodded concrete, the maximum attained value of the solidity, 0.853, for the vibrated concrete being at $C/W=2.50$.

The solidity of the rodded specimens of mix $G$ (fig. 9) had the same trend as that of mix $A$, increasing with increasing $C/W$, to a maximum solidity of approximately 0.85 at a $C/W$ ratio of 2.2, then decreasing. The solidity of mix $G$ vibrated specimens continued to increase up to a $C/W$ ratio apparently somewhat greater than 2.5, the solidity being approximately 0.87 at this $C/W$ ratio for 90 sec of vibration. Thirty seconds of vibration, on the average for all combinations of frequency and amplitude, was almost as effective as 90 sec, showing that the compaction was very rapid in this mix.

The specimens of mix $G$, both those rodded and those thoroughly compacted by vibration, had maximum solidities greater than any obtained in mix $A$. Thus, the maximum solidity of mix $G$, vibrated, was 0.871, and that estimated for mix $A$, vibrated, was 0.853.

Figure 10 gives the strength of mix $A$, $C/W=2.50$, vibrated, plotted against solidities. It may be seen that there is a trend at any age for the strength to increase at a greater rate as solidity increases.

### (c) SURFACE CONDITION

The surface condition was measured by the estimated area of surface defects, expressed as a percentage of the cylindrical surface. A surface with less than 2 or 3 percent of defects was considered satis-

[10] The mean optimum strengths shown in figure 8 for $C/W=2.50$ are the averages of the strengths of mix $A$ concrete subjected to 90 sec. of vibration for all frequencies and amplitudes (except 420-0.012).

factory. The appearance of all rodded cylinders of mix *A* was quite satisfactory, principally because each cylinder was carefully rodded around the periphery.

There was no significant difference in the surface condition of mix *A* cylinders vibrated with any combination of frequency and amplitude for any one period of time, except for the cylinders, *C*/*W* greater

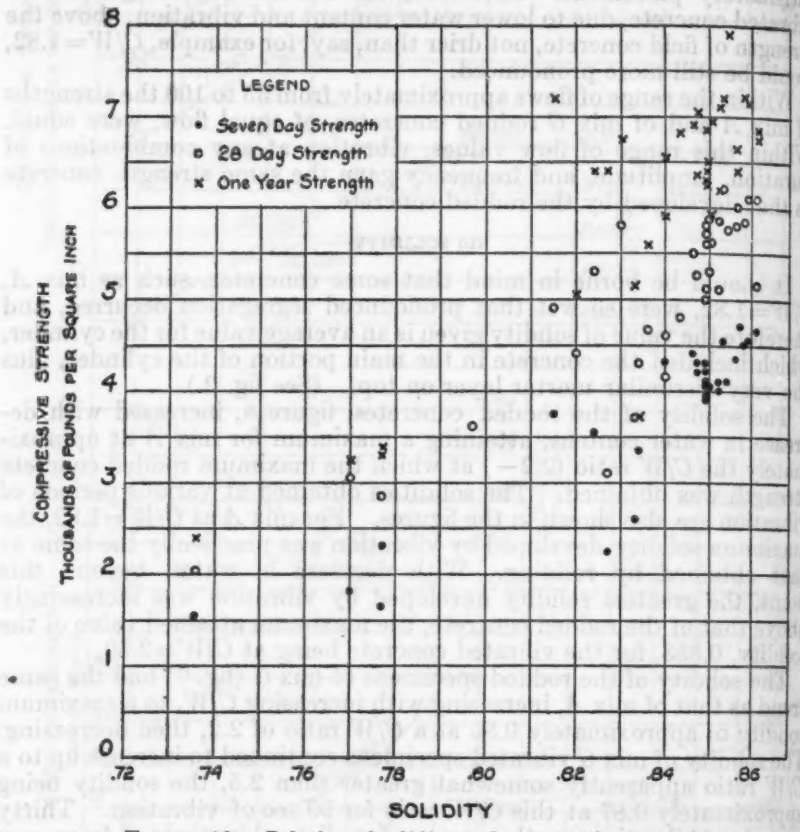


FIGURE 10.—*Relation of solidity and compressive strength.*

Mix *A*, *C*/*W*=2.50, vibrated.

than 2.10, vibrated at the least effective combination of frequency and amplitude for 10 sec or less (see fig. 8). With increase in *C*/*W* beyond 2.10, the amount of vibration necessary to produce a satisfactory surface rapidly increased, and for *C*/*W*=2.50 at least 30 sec of vibration was necessary, for the least effective vibration.

The condition of the rodded specimens of mix *G* rapidly approached an undesirable condition with decrease in water beyond *C*/*W* ratio= 2.10, the cylinders at *C*/*W*=2.43 being badly honeycombed, with about 15 percent of the area so affected. Only 30 sec of vibration was necessary to reduce the surface defect to zero for *C*/*W*=2.43.

The surfaces of mixes *A* and *G* specimens were practically perfect for all vibrational treatments, for *C/W* ratios of 2.10 or less in mix *A* or 2.43 or less in mix *G*.

### (d) SEGREGATION

When in mix *A* the *C/W* was 1.82 or 2.10, there was apparently a slight tendency for the segregation to be greater for the more efficient combinations of amplitude and frequency. (Data not given.) The tendency appeared to be very secondary to the duration of vibration or to the water content, and the average values for all vibration combinations of *n* and *r* have been plotted in figures 8 and 9.

There was no appreciable segregation in the vibrated specimens of mix *A*, at *C/W*=2.50. With an increased water content, however, segregation occurred, as shown in figure 8. The increase in segregation became more and more pronounced with increase in water content; thus at *C/W*=2.10, the average segregation at 90 sec was 21 percent, whereas at *C/W*=1.82, the 90 sec segregation was 52 percent. The rapidity with which segregation occurred was also much greater with higher water contents; thus for *C/W*=2.10, the 30 sec segregation was 9 percent, or only 43 percent of that of the 90 sec segregation, whereas for *C/W*=1.82, the 30 sec segregation was 33 percent, or 63 percent of that of the 90 sec segregation. Thus the desirability of holding the water content to the very minimum was demonstrated, if segregation is to be avoided. In practice, if a mix equivalent to mix *A*, *C/W*=1.82 were used, before the concrete at a distance from the vibrator were compacted, greatly excessive segregation would occur in the zone immediately surrounding the vibrator.

It was observed that a wet mortar appeared on the surface of the vibrating concrete cylinder, mix *A*, *C/W*=1.82 and 2.10, within a few seconds after the start of vibration; optimum strength was found to be developed within the same time. Consequently, the instant of appearance of such wet mortar appears to be an indication of the completion of compaction, vibration beyond this time merely causing more segregation.

Table 2 gives the original proportions of mixes *A*, *F*, and *G*, together with the extreme range in proportions of the lower halves of cylinders of those concretes vibrated in their wetter consistencies to the point where no appreciable further segregation occurred.

It appears that unless a very dry mix, which will not segregate under the most severe vibration, be used, the proportions must be carefully selected. Thus, the *F* mix, 1:8.1, was the richest mix in which segregation was negligible in the moderately wet[11] mixes (flow=35). In both mixes *A* and *G* the cement and sand were not radically separated by vibration but the mortar in excess of that required to fill the voids in the coarse aggregate moved upward. The mortar of mix *F* was present in 17 percent excess of the amount required to fill the coarse aggregate voids. (See table 2).

[11] For vibration.

TABLE 2.—*Comparative segregation of mixes A, G, and F with approximately equal C/W ratios*

| Mix | Proportions of cement, sand, gravel, and water, by weight, in lower half of cylinder | | Volume of mortar expressed as percentage of voids in dry rodded aggregate [1] |
|---|---|---|---|
| | Original | Limits after vibration | |
| *A* | 1:2.2:3.8:0.55 | 1:2.4:5.3:0.49 | 200 |
| | 1:2.2:3.8:0.55 | to | 146 |
| | 1:2.2:3.8:0.55 | 1:2.4:6.0:0.52 | 151.0 |
| *G* | 1:1.1:4.9:0.55 | 1:1.2:6.9:0.56 | 134 |
| | 1:1.1:4.9:0.55 | to | 90.8 |
| | 1.1.1:4.9:0.55 | 1:1.5:6.1:0.51 | 110 |
| *F* | 1:1.66:6.45:0.52 | change negligible | 117 |

[1] Assuming no air voids in mortar.

### 3. ENERGY REQUIRED FOR COMPACTION

With even the least effective vibrational treatment used for specimens of mix *A*, $C/W=2.10$ ($n=21$, $r=.045$ in.), optimum strength was attained at 3 sec or less, as shown by the minimum values in figure 3. It required more than 90 sec of vibration to compact specimens of mix *A*, $C/W=2.50$, (fig. 5), vibrated with this same frequency and amplitude, sufficiently to obtain optimum strength. Since the former duration was only 3 percent of the latter it is obvious that in the first case only approximately 3 percent as much electrical energy was expended in operating the vibrator as in the latter.

The energy which the vibrator would have required to obtain optimum strength in specimens with $C/W=1.82$ cannot be estimated from the test data, but it was apparent, from observation, that less time was required than for the compaction of specimens with $C/W=2.10$. All of the cylinders of both $C/W$ ratios attained optimum strength at even the shortest vibration duration. Mix *A*, $C/W=2.50$, specimens required much more time to obtain optimum strength than the specimens of mix *G*, $C/W=2.43$, the latter with but little more water. Hence it may be concluded that, for equal cement-water ratios, specimens of mix *G* required less time for compaction, and therefore less energy was consumed in operating the vibrator.

## V. SUMMARY AND CONCLUSIONS

This paper describes the results of tests on concrete specimens of which the mold was subjected approximately to simple harmonic vertical vibrations of known frequencies and amplitudes. This vibration differed from that effected with portable commercial vibrators, because in the case of the latter, the amplitude of vibration rapidly decreases as the distance from the vibrator increases. The amplitude, even in close proximity to vibrators of the portable type, is much less than the amplitude of the freely suspended vibrator, since attaching the vibrator to the form or immersing it in the concrete greatly reduces the amplitude. It is to be carefully noted that the amplitude of vibration quoted in the following conclusions refers to the amplitude of the mold. Moreover, it appears impractical by vibration to obtain

strengths in structural concrete as high as those obtained with the driest mixes studied in this investigation. Such dry mixes can be vibrated commercially only in the manufacture of cast stone and prefabricated concrete building units. As the mixes are made wetter not only do they lose strength but the tendency to segregate increases at an increasing rate with the water content.

The tests warrant the following conclusions:

1. A vibrated concrete proportioned 1:2.2:3.8 by weight (mix *A*), in which Potomac River sand and 1½-in. gravel were used (an ideal mix for ordinary use without vibration) underwent pronounced segregation, even at a consistency extremely dry for ordinary use (flow of 35), and at the least effective vibration treatment. This segregation was exhibited as an accumulation of a layer of mortar on the surface of the concrete.

2. For the concretes with 1½-in. maximum size aggregate the segregation was reduced by decreasing the sand-gravel ratio to about 0.22 (mix *G*—1:1.1:4.9) and was eliminated, with any sand-gravel ratio, when the mix was made excessively dry ($C/W=2.50$, zero slump, and water content less than that required for minimum flow—see fig. 8). Segregation was also minimized by proportioning the mix 1:1.7:6.5 (mix *F*), which latter alternative permitted the use of sufficient water to give the concrete a flow of 35. In this case the volume of cement, sand, and water exceeded that of the voids in the dry rodded aggregate by 17 percent, and the sand-gravel ratio was 0.26.

3. For the normal 1:2.2:3.8 mix, no increase in strength over that of rodded specimens was developed by vibration until the water content had been reduced to $C/W=2.1$, which gave approximately minimum flow. With further decrease in the water content to that of $C/W=2.5$, (an abnormally dry mix) the strength of the vibrated concrete continued to increase, although the strength of rodded concrete of the same $C/W$ ratio decreased. The greatest strengths obtained by vibration, which occurred with mix *A* at $C/W=2.50$, were 4,400, 5,800, and 6,900 lb/in.$^2$ at 7 days, 28 days, and 1 year, respectively. These strengths were considerably greater than the maximum strength obtained with the rodded specimens. It is to be noted that the percentage increase was greatest at 7 days, the increase being less at 28 days and still less at 1 year. For flows between 35 and 100 the strengths of the vibrated and rodded specimens of mix *A* were equal (fig. 8). The same is true for mix *G* (fig. 9). Within this flow range the strengths of mixes *A* and *G* were equal.

4. The solidities of the rodded and vibrated specimens of mix *A* for equal $C/W$ ratios were the same for water contents as low as approximately $C/W=1.8$, and the same was true for mix *G* to a water content as low as that in $C/W=2.0$. With lower water contents the solidity of the specimens vibrated to compaction was greater than that of the rodded specimens.

5. The surface appearance of the concretes was excellent for water contents down to those corresponding to $C/W=2.1$ for mix *A*, and $C/W=2.4$ for mix *G*. With decrease in water content, the amount of surface defects of the concrete, unless thoroughly compacted, rapidly increased. Those specimens that were vibrated to optimum strength, even for the driest consistencies used, had a satisfactory appearance.

6. The effectiveness of the vibration was defined as the reciprocal of the time required to obtain a concrete of given strength and was roughly proportional to the maximum vibrational acceleration. This acceleration is proportional to the amplitude and to the square of the frequency. The increase in strength with vibration continued with the duration of the vibration, the increase being slower and slower, until a strength was attained which did not materially change with further vibration. This value is referred to herein as the optimum strength.

7. If the vibrational acceleration is a measure of the efficacy in developing strength, then for a fixed acceleration, the energy required varies inversely as the frequency of the vibration, or directly as the square root of the amplitude.

8. The time required to vibrate mix *A*, $C/W=2.50$ to optimum strength with any assigned frequency and amplitude was approximately 30 times as great as that required to vibrate the same mix with $C/W=2.10$ to optimum strength. For equal $C/W$ ratios, considerably less time was required to compact mix *G*.

9. Those mixes with a low ratio of fine to coarse aggregate required a much shorter duration of vibration to obtain optimum strength than mixes with a normal sand-gravel ratio. A mix which required a relatively short duration of vibration, and which had low segregation, was proportioned so that the total of the bulk volumes of water, cement, and fine aggregate was 17 percent greater than the volume of voids in the rodded coarse aggregate. (Mix *F:* 1:1.7:6.5.)

---

G. L. Pigman assisted in the design of the vibrator, and with E. A. Pisapia and J. S. Rogers made all tests. John Tucker, Jr., designed the vibrator, supervised the investigation, and wrote the paper. The authors gratefully acknowledge the advice of P. H. Bates, in general charge of the investigation, especially for his recognition of the importance of quantitative studies of segregation.

WASHINGTON, July 1, 1937.

U. S. Department of Commerce National Bureau of Standards

RESEARCH PAPER RP1049

*Part of Journal of Research of the National Bureau of Standards, Volume 19, November 1937*

# STUDY OF BALL PACKINGS FOR LABORATORY RECTIFYING COLUMNS [1] [2]

By Augustus R. Glasgow, Jr.,[3] and Sylvester T. Schicktanz [4]

ABSTRACT

The efficiency, liquid hold-up, and surface area of packings composed of glass balls 2.95 and 3.80 mm in diameter, lead balls 2.05 and 4.05 mm in diameter, and copper balls 4.00 mm in diameter, have been determined. The description and operation of the glass experimental column are given. For a column 2.6 cm in diameter packed with balls 0.2 to 0.4 cm in diameter, it is found that: (1) the heat conductivity and the nature of the material of the packing have no effect on the efficiency of separation, liquid hold-up, or through-put of the still; (2) the efficiency is substantially directly proportional to the total surface area exposed in the packed column, and approximately linear with the reciprocal of the diameter of the balls; and (3) the hold-up is approximately linear with the total surface area.

CONTENTS

| | Page |
|---|---|
| I. Introduction | 593 |
| II. Description of distillation assembly | 594 |
| III. Packings investigated | 594 |
| IV. "Test" mixture used | 595 |
| V. Experimental procedure and data | 595 |
| 1. Determination of optimum back pressure | 595 |
| 2. Determination of efficiency of separation | 596 |
| 3. Determination of hold-up | 598 |
| 4. Determination of vapor velocity | 599 |
| 5. Determination of surface area of packing | 600 |
| VI. Discussion of results | 601 |
| VII. References | 603 |

## I. INTRODUCTION

The purpose of the present investigation was to obtain information concerning the effect of the following factors on the efficiency, hold-up, and related properties of laboratory distilling columns: (1) the nature of the material of the packing; (2) the surface area of the packing; and (3) the size of the packing. The nature of the material was varied by using balls of approximately the same diameter (4 mm) made of materials of quite different heat conductivities. The total surface and the size of the packing were varied by using balls of different diameters (2 to 4 mm).

[1] Financial assistance for this work has been received from the research fund of the American Petroleum Institute. This work is part of Project 6, The Separation, Identification, and Determination of the Constituents of Petroleum.

[2] The work described in this paper has been submitted by A. R. Glasgow, Jr., to the Graduate School of the University of Maryland in partial fulfillment of the requirements for the degree of Master of Science.

[3] Research Associate at the National Bureau of Standards, representing the American Petroleum Institute.

[4] Formerly associated with API Research Project 6, now with Alcohol Tax Unit, Bureau of Internal Revenue, U. S. Treasury Department.

## II. DESCRIPTION OF DISTILLATION ASSEMBLY

In figure 1 is shown, to scale, the complete distillation unit used to determine the various characteristics of the different packings investigated. The apparatus is made of Pyrex glass throughout and sealed together to insure against leaks during operation.

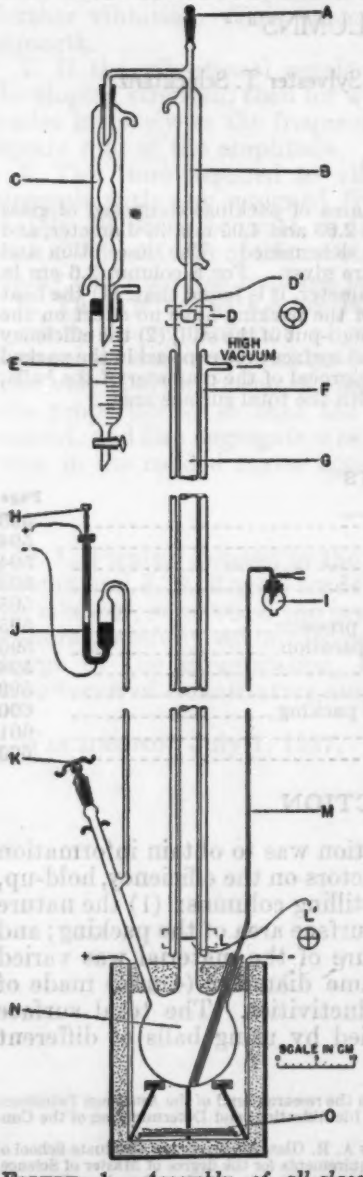


FIGURE 1.—*Assembly of all-glass rectifying still in which the various packings were investigated.*

The assembly consists of a 1-liter still pot $N$, equipped with a tube $K$ for convenience in introducing and removing the test mixture, and a capillary tube $M$, whose upper end empties into the vial $I$ for removing small test samples during operation. The column proper, $G$, is 25.8 mm in internal diameter and 140 cm long, and contains a sealed-in cross bar, $L$,$L'$, to support the packing. In the upper part is sealed a small cup, $D$,$D'$, of 2-ml capacity, which collects the condensate returning from the condenser $B$. $A$ is a ground-glass stopper, through which samples are removed from the cup $D'$ by means of a long capillary pipette. $C$ is an auxiliary condenser used during actual distillation, and $E$ is a receiver unit for collecting the distillate.

To maintain a constant back pressure, and consequently a constant rate of boiling, the still pot is connected to the manometer $J$, which automatically controls the energy input to the heating unit $O$, by means of a set of electrical relays and resistances not shown in the figure. Variations in the rate of distillation are obtained by adjustment of the screw $H$ attached to the contact point in the manometer.

To maintain adiabatic conditions during the tests, the column is surrounded by a vacuum-jacketed sleeve $F$, which is completely silvered except for narrow, clear vertical windows 1 cm wide in both front and back, which permit visual inspection of the column during operation. To obtain and maintain a constant low pressure ($10^{-5}$ mm Hg), the jacket is connected to a mercury diffusion pump, which is operated continuously.

## III. PACKINGS INVESTIGATED

The ball type of packing was selected for investigation for the following reasons: the surface area can be readily determined; the

area of contact between units is small; the distribution is fairly uniform; and the volume of free space does not change markedly with the size of the balls.

Two sizes of soft-glass balls were used, the average diameters being 3.80 and 2.95 mm, respectively, with an average deviation of approximately 10 percent. The copper packing consisted of machined balls having an average diameter of 4.00 mm, with a variation of about 1 percent. The lead balls were of two sizes, having average diameters of 4.05 and 2.05 mm, respectively, with a variation of about 10 percent in each case. The lead balls were not perfect spheres and, because of the softness of the material, tended to be flattened at the points of contact.

The locket-chain packing was made of brass and had single links. The wire from which the links were made had an average diameter of 0.33 mm and each link had a circumference of 6.2 mm.

## IV. "TEST" MIXTURE USED

In order to calculate the number of theoretical plates in a distillation column, it is necessary to use, as a "test" mixture, a binary system whose vapor-liquid phase diagram is known. The binary system of benzene and ethylene chloride [1][5] was chosen for the following reasons: the mixture is nearly an ideal one; the difference in boiling point (3.5° C) of the two constitutents is small; the vapor-liquid phase diagram is known [2]; and the determination of the composition can be made readily by means of measurements of refractive index. The constants for the two components used in the mixture are: benzene, bp (760 mm) 80.2° C, $n_D^{25.2}$ 1.4976; ethylene chloride, bp (760 mm) 83.7° C, $n_D^{25.2}$ 1.4418. The number of theoretical plates was determined with this binary mixture by means of the graphical method of McCabe and Thiele [3].

## V. EXPERIMENTAL PROCEDURE AND DATA

### 1. DETERMINATION OF OPTIMUM BACK PRESSURE

The resistance to the flow of vapor ascending from the still pot to the still head produces a back pressure. The optimum back pressure is that which yields the greatest separation of the two components when the column is operating with a high vapor velocity. A discussion of the variation of the number of theoretical plates with vapor-velocity is given in an article by Arthur Rose [4].

An 800-ml sample of the test mixture of known composition (approximately 40 mole percent of benzene and 60 mole percent of ethylene chloride) was charged into the still and sufficient material (about 50 ml) was distilled to remove a small amount of water that adhered to the packing and to the walls of the column. The back pressure was then set at some arbitrary value and the still run under total reflux. Samples of the liquid distillate and of the liquid in the pot were withdrawn and their composition determined. Consecutive check determinations, taken 10 minutes apart, served to indicate when the column was in equilibrium. The pressure was then varied several millimeters by changing the energy input at the pot, and the measure-

[5] The figures given in brackets here and elsewhere in the text correspond to the numbered references at the end of the paper.

ments were repeated. In this manner it was possible to determine the back pressure that produced the greatest separation. Table 1 shows the variation of back pressure with the various packings.

TABLE 1.—*Data obtained on measurements of back pressure*

| Type of packing | Observation | Back pressure | Mole percent of benzene | |
|---|---|---|---|---|
| | | | Vapor | Pot |
| | | mm | | |
| Glass balls (3.80 mm diam) | 1 | 5 | 74.8 | 37.2 |
| | 2 | 10 | 75.2 | *37.2 |
| | 3 | 15 | 74.0 | 37.0 |
| Copper balls (4.00 mm diam) | 1 | 8 | 58.3 | 20.0 |
| | 2 | 10 | 59.0 | *20.0 |
| | 3 | 12 | 58.0 | 20.0 |
| Glass balls (2.95 mm diam) | 1 | 14 | 78.0 | 37.0 |
| | 2 | 12 | 80.7 | *37.0 |
| | 3 | 10 | 79.8 | 37.0 |
| Lead balls (2.05 mm diam) | 1 | 17 | 80.3 | 26.2 |
| | 2 | 15 | 81.0 | *20.6 |
| | 3 | 13 | 80.7 | 21.4 |
| Locket chain (0.33 mm diam of rod and 6.2 mm circumference of link) | 1 | 15 | 79.2 | 34.6 |
| | 2 | 12 | 84.5 | 34.3 |
| | 3 | 10 | 85.0 | *34.0 |
| | 4 | 8 | 85.0 | 34.0 |

* Value used for the determination of the number of theoretical plates.

The optimum back pressure for the locket chain and for the balls of approximately 4 mm diameter was found to be about 10 mm of mercury. With the smaller balls of 3 and 2 mm diameter, the optimum back pressures were, respectively, 12 and 15 mm. This increase in pressure drop for the smaller balls was caused by the greater resistance offered to the flow of vapor by the smaller interstices formed in packing, since the free space remained substantially constant.

## 2. DETERMINATION OF EFFICIENCY OF SEPARATION

The number of theoretical plates was evaluated by the graphical method [3], the composition of vapor and liquid being obtained with the still operating at the optimum back pressure. The composition of the binary mixture of benzene and ethylene chloride was varied to correspond with different regions of the phase diagram by distilling some of the material and then changing again to total reflux. The value of $(n-1)$ theoretical plates,[6] divided by the height of the packing in the column gives the height equivalent to one theoretical plate (hetp).

TABLE 2.—*Data on the efficiency of separation obtained with various packings*

| Determination | Refractive index $n_D^{25.3}$ | | Mole percent of benzene | | Number of theoretical plates less one * $n-1$ |
|---|---|---|---|---|---|
| | Vapor | Pot | Vapor | Pot | |
| GLASS BALLS (3.8 mm diameter) | | | | | |
| 1 | 1.4832 | 1.4614 | 75.3 | 36.6 | 22 |
| 2 | 1.4807 | 1.4575 | 71.2 | 29.4 | 21 |
| 3 | 1.4784 | 1.4555 | 67.0 | 25.8 | 21 |
| 4 | 1.4753 | 1.4522 | 61.6 | 19.5 | 22 |
| | | | | | Average...21.5 |

* The number of theoretical plates was determined to the nearest one-half plate.

[6] $n$ is the total number of theoretical plates that the entire still produces. $(n-1)$ is the number attributed to the column proper. One plate is subtracted for the change from the pot to the column.

TABLE 2.—*Data on the efficiency of separation obtained with various packings*—Con.

| Determination | Refractive index $n_D^{23.3}$ | | Mole percent of benzene | | Number of theoretical plates less one [a] n−1 |
|---|---|---|---|---|---|
| | Vapor | Pot | Vapor | Pot | |
| **GLASS BALLS, PLUS COPPER BALLS** (50:50 mixture; glass, 3.8 mm diameter; copper, 4.0 mm diameter) | | | | | |
| 1 | 1.4811 | 1.4507 | 71.9 | 33.5 | 20.5 |
| 2 | 1.4784 | 1.4572 | 67.0 | 28.8 | 20 |
| 3 | 1.4745 | 1.4530 | 60.1 | 21.0 | 20 |
| 4 | 1.4709 | 1.4503 | 53.9 | 16.0 | 20 |
| | | | | | Average...20 |
| **COPPER BALLS** (4.0 mm diameter; length of packing 5 cm[illegible] less) | | | | | |
| 1 | 1.4812 | 1.4610 | 72.0 | 36.0 | 19 |
| 2 | 1.4797 | 1.4587 | 69.4 | 31.6 | 19.5 |
| 3 | 1.4772 | 1.4556 | 65.0 | 26.0 | 19 |
| 4 | 1.4738 | 1.4526 | 59.0 | 20.2 | 20 |
| | | | | | Average...19.5 |
| **LEAD BALLS** (4.05 mm diameter) | | | | | |
| 1 | 1.4808 | 1.4595 | 71.3 | 33.7 | 20 |
| 2 | 1.4780 | 1.4554 | 66.3 | 25.6 | 20 |
| 3 | 1.4753 | 1.4528 | 61.6 | 20.6 | 20 |
| 4 | 1.4714 | 1.4518 | 54.8 | 18.8 | 19 |
| | | | | | Average...20 |
| **GLASS BALLS** (2.95 mm diameter) | | | | | |
| 1 | 1.4862 | 1.4599 | 80.5 | 33.8 | 28 |
| 2 | 1.4829 | 1.4548 | 74.8 | 24.3 | 28 |
| 3 | 1.4784 | 1.4500 | 67.0 | 15.2 | 28 |
| 4 | 1.4709 | 1.4456 | 53.8 | 7.2 | 28 |
| | | | | | Average...28 |
| **LEAD BALLS** (2.05 mm diameter) | | | | | |
| 1 | 1.4893 | 1.4572 | 85.8 | 28.8 | 36 |
| 2 | 1.4883 | 1.4549 | 84.1 | 24.6 | 37 |
| 3 | 1.4865 | 1.4523 | 81.0 | 19.6 | 37 |
| | | | | | Average...36.5 |
| **LOCKET CHAIN** (0.33 mm diameter of rod; link 6.2 mm in circumference) | | | | | |
| 1 | 1.4888 | 1.4062 | 85.0 | 34.4 | 32 |
| 2 | 1.4876 | 1.4581 | 83.0 | 30.4 | 33 |
| 3 | 1.4872 | 1.4556 | 82.3 | 26.0 | 34 |
| 4 | 1.4858 | 1.4537 | 79.8 | 22.5 | 34 |
| 5 | 1.4848 | 1.4510 | 78.2 | 17.0 | 36 |
| 6 | 1.4800 | 1.4486 | 70.0 | 12.8 | 33 |
| 7 | 1.4732 | 1.4446 | 58.0 | 5.2 | 33 |
| | | | | | Average...34 |

[a] The number of theoretical plates was determined to the nearest one-half plate.

The refractive indices shown in table 2 are the average values for two samples, one taken from the still 10 minutes after the other. The individual values of refractive index differed only by amounts ranging from 0.0000 to 0.0004, which indicated that equilibrium had been established. There was an increase from 20 to 36.5 in the value of $(n-1)$ plates when the diameter of the balls decreased from about 4 to about 2 mm. The locket chain and the 2-mm lead balls gave the greatest number of theoretical plates.[7]

The values of the number of theoretical plates obtained for various regions of the phase diagram show the extreme deviations to be as follows: for locket chain, about 10 percent, and for balls, about 5 percent. The greatest mean deviation, however, is about 3 percent. These variations may be due to the fact that channeling differed from time to time. While the absolute magnitude of the number of theoretical plates may be in error by an appreciable amount, the authors believe that, relative to one another, the values are quite reliable. The balls would be expected to be more evenly distributed, and hence exhibit less channeling, than packings with a less symmetrical form. This may account for the smaller deviations obtained with the ball type of packing. An excellent discussion and tabulation of the values of hetp obtained with columns of different size and with various packings is given by Fenske, Tongberg, and Quiggle [6].

### 3. DETERMINATION OF HOLD-UP

The amount of material held in the rectifying column as vapor and as liquid together with the vapor in the pot is the quantity determined as the hold-up under operating conditions.

In order to determine the hold-up when operating the still at the optimum back pressure, the two-component mixture of benzene and dibutyl phthalate was employed [7]. The dibutyl phthalate was first distilled in a molecular still and the head fractions were rejected. The boiling point of the dibutyl phthalate was about 340° C. The benzene had the constants given in section III.

A mixture of benzene and dibutyl phthalate of a known weight relationship was added to the pot of a dry still. On distillation, the vapor in the pot and the vapor and liquid in the column consisted essentially of pure benzene, because the very much higher-boiling dibutyl phthalate remained in the still pot [8]. A sample of the liquid in the pot was withdrawn while the still was operating under total reflux. The new weight relationship of benzene to dibutyl phthalate was determined by first weighing the sample, and then weighing again after distilling off the benzene. The weight of benzene associated with the total weight of dibutyl phthalate before and after distillation represents the hold-up of benzene. To prevent a loss of benzene during the removal of the sample from the hot still pot, the receiver *I* was surrounded with a slush of solid carbon dioxide in a 50:50 solution of chloroform and carbon tetrachloride. This mixture maintains a temperature of approximately −75° C.

[7] For the highest efficiency of separation obtainable with single-turn helices, see Tongberg, Lawroski, and Fenske [5]; for glass bubbling-cap columns, see Bruun and Faulconer [9].

The ball packings in table 4 show a change in hold-up of 56 to 74 ml for a decrease in diameter of 4.05 to 2.05 mm. The locket chain gave the largest hold-up.

## 4. DETERMINATION OF VAPOR VELOCITY

The vapor velocity of the packings was determined from the values of through-put [8] and free space. The through-put was determined at the optimum back pressure by distilling benzene through the column with no reflux to the still. This was done by keeping the glass-jacketed tube *B* (fig. 1) hot and condenser *C* cold. The rate of collection of distillate in receiver *E* was timed with a stop watch. A correction was applied for the partial condensation at *B*.

The free space offered by the packings was obtained by measuring the amount of kerosene necessary to fill the interstices. The mean deviation between determinations was of the order of 1 to 2 percent. The free space of the ball packings was nearly constant, the deviation being 4 percent. For the packings investigated, table 3 shows the comparison of free space, vapor velocity, through-put, and the computed rate of distillation with a given reflux ratio.

TABLE 3.—*Comparison of different packings*

| Type of packing | Vapor velocity | Free space | Through-put | Calculated rate of distillation | | Height equivalent to one theoretical plate (under total reflux) |
|---|---|---|---|---|---|---|
| | | | | Reflux ratio 9:1 | Reflux ratio 19:1 | |
| | m/min | cm³ | ml (liq)/min | ml (liq)/min | ml (liq)/min | cm |
| Glass balls (3.80 mm diam) | 32.0 | 238 | 20 | 2.0 | 1.0 | 5.5 |
| Copper balls (4.00 mm diam) | 28.0 | 244 | 18 | 1.8 | 0.9 | 5.8 |
| Glass balls plus copper balls (50:50 mixture; glass, 3.8 mm diam; copper, 4.0 mm diam) | | | 21 | 2.1 | 1.1 | 6.0 |
| Glass balls (2.95 mm diam) | 25.7 | 233 | 15.5 | 1.5 | .7 | 4.2 |
| Lead balls (2.05 mm diam) | 24.5 | 238 | 15 | 1.5 | .7 | 3.2 |
| Locket chain | 20.3 | 413 | 21.5 | 2.1 | 1.0 | 3.5 |

The results shown in table 3 indicate that it is possible to obtain higher vapor velocities with the ball type of packing than with the locket chain. However, the smaller free space in ball packing reduces the amount of through-put that can be realized. The results indicate that locket chain is superior from the standpoint of ample free space, whereas balls are better from the standpoint of vapor velocity. These two factors govern the through-put of a column. It appears, however, that the speed with which vapor can travel through packing, without loss in efficiency of rectification, is governed by the way in which the free space is distributed. The ideal type of packing appears to be one that combines the uniform distribution of free space offered by ball packings and the greater amount of free space in relation to surface offered by chain packings. Equal distribution would permit higher vapor velocities without loss in efficiency of separation by partial flooding, channeling, entrainment, or passage of vapor without rectification. Furthermore, it is desirable to have

[8] The amount of distillate collected in a given time.

the maximum surface for separation that is compatible with the free space necessary for the desired through-put.

## 5. DETERMINATION OF THE SURFACE AREA OF PACKING

The surface area of the packings was calculated from the following: the total weight of units as packing in the tube, the weight of an individual unit, and the volume of the total number of units. The surface area of the ball packings was computed from their radii, considering the units to be spheres. The values of the radii, computed from the volume of an individual unit, differed from those obtained by direct measurement by about 2 percent. In the case of the chain packing the surface area was calculated by assuming each unit to have the shape of a cylindrical rod. Their radii were determined by direct measurement and their length was computed from their volume. The calculated length of each unit was checked by measuring its circumference and the two values were found to agree within 7 percent. The estimated total error in the area calculated for the chain packing was about 10 percent. The values in table 4 show the calculated surface areas of the amounts of different packings required to fill a tube 2.58 cm in diameter and 120 cm long. The effective surface area of the packing is less than the calculated area by the amount lost by contact of the units in packing. Of the total calculated area, that percentage which is effective for separation would be expected to be smallest for the locket chain packing and greatest for the ball packings.

TABLE 4.—*Summary of data obtained on the various packings*

[Column used had an inside diam of 25.8 mm; packing occupied 120 cm of length in each case except for the copper balls.] [a]

| Type of packing | Diameter | Back pressure (optimum) | Column hold-up (operating conditions) | Free space | Vapor velocity | Number of theoretical plates, less one $n-1$ | Height equivalent to one theoretical plate | Calculated surface area of packing [c] | Area per theoretical plate |
|---|---|---|---|---|---|---|---|---|---|
| | mm | mm Hg | ml | cm³ | m/min | | cm | cm² | cm² |
| Lead balls | [b](4.05) 4.05 | 10 | -------- | 242 | -------- | 20 | 6.0$_0$ | 5,660 | 283 |
| Copper balls [a] | (4.00) 3.96 | 10 | [a] 56 | 244 | 28.0 | [a] 20½ | 5.8$_8$ | 5,730 | 280 |
| Glass balls | (3.76) 3.79 | 10 | 59 | 238 | 32.0 | 21½ | 5.5$_8$ | 6,330 | 295 |
| Glass balls plus copper balls: | | | | | | | | | |
| Glass balls | 3.79 | 10 | -------- | -------- | -------- | 20 | 6.0$_0$ | -------- | -------- |
| Copper balls | 3.96 | | | | | | | | |
| Glass balls | (2.97) 2.92 | 12 | 64 | 233 | 25.7 | 28 | 4.2$_8$ | 7,890 | 282 |
| Lead balls | (2.03) 2.08 | 15 | 74 | 238 | 24.5 | 36½ | 3.2$_9$ | 11,400 | 312 |
| Locket chain (diam of rod 0.33 mm; circumference of link 6.2 mm) | -------- | 10 | 81 | 413 | 20.3 | 34 | 3.5$_6$ | (24,200) | (712) |

[a] In the case of the copper balls, the length of packing was 115 cm. Where appropriate, the observed values of hold-up and theoretical plates have been multiplied by the factor 120/115 to obtain the value for the standard length of 120 cm.

[b] The values in parentheses were obtained by direct measurement; the others were calculated as described in the text on p. 600.

[c] The total surface area exposed in the packed column is obtained by adding 1,130 cm², the area of the walls of the column, to the surface area of the packing.

## VI. DISCUSSION OF RESULTS

With respect to packing composed of uniformly sized spherical balls 0.2 to 0.4 cm in diameter in a column 2.6 cm in diameter, the following conclusions are made on the basis of the data obtained in the present investigation:

1. The efficiency of separation, the vapor velocity, and the hold-up are substantially independent of the heat conductivity of the packing. Table 4 shows the values obtained with lead, copper, and glass balls approximately 4 mm in diameter.

2. The efficiency of separation is substantially directly proportional to the total surface area exposed in the packed column. This relationship for the given column and given sized balls shown in figure 2, is represented by the equation

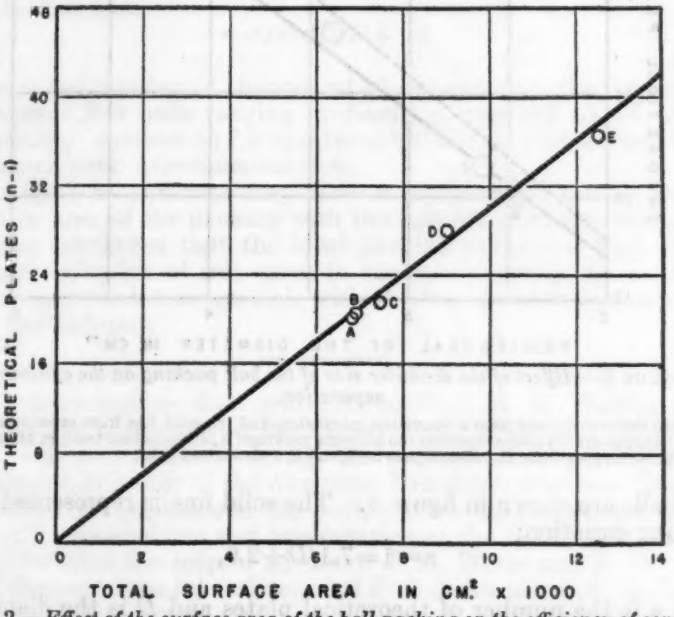


FIGURE 2.—*Effect of the surface area of the ball packing on the efficiency of separation.*

The letters opposite the circles represent the following packings: *A*, 4.05-mm lead balls; *B*, 4.00-mm copper balls; *C*, 3.8-mm glass balls; *D*, 2.95-mm glass balls; and *E*, 2.05-mm lead balls.

$$n-1=0.0030\ (S+s), \tag{1}$$

where $n$ is the number of theoretical plates and $(S+s)$ is the total surface area exposed in the packed column in square centimeters, $S$ being the total surface area of the balls and $s$ being the internal surface area of the column.

3. The hold-up is approximately linear with the total surface area of the balls, the relation being

$$H=0.0032\ S+38, \tag{2}$$

where $H$ is the hold-up in milliliters.

Since, in a large container filled with small balls of a uniform diameter, the volume of the void space and the volume occupied by

the material of the balls are each substantially constant and independent of the diameter of the balls, it follows that the surface area of the balls is substantially inversely proportional to the diameter[9] of the balls. The experimental data for the given column and given

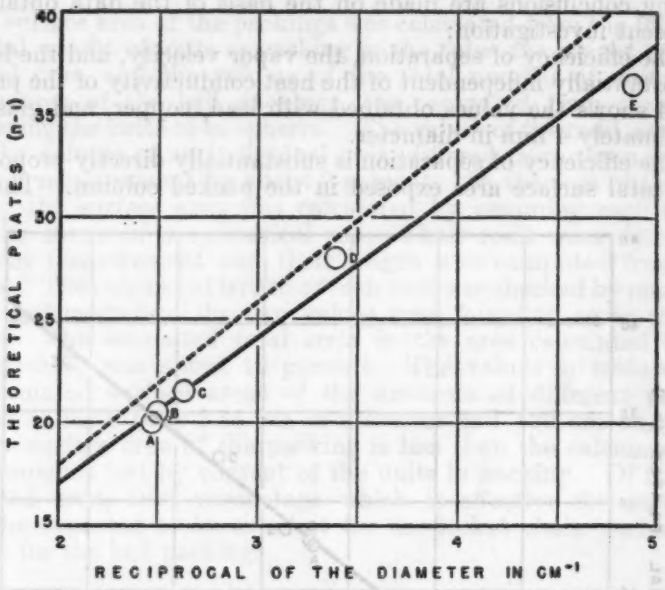


FIGURE 3.—*Effect of the diameter size of the ball packing on the efficiency of separation.*

The broken line was derived from a theoretical calculation, and the solid line from experimental values. The letters opposite the circles represent the following packings: *A*, 4.05-mm lead balls; *B*, 4.00-mm copper balls; *C*, 3.8-mm glass balls; *D*, 2.95-mm glass balls; and *E*, 2.05-mm lead balls.

sized balls are shown in figure 3. The solid line is represented by the following equation:

$$n-1=7.1/D+2.9, \tag{3}$$

where $n$ is the number of theoretical plates and $D$ is the diameter of the balls in centimeters.

For a container in which the size of the balls is not infinitesimal in comparison with the dimensions of the container, a simple approximate calculation can be made of the relation between the total volume of the container, the free or void space, the volume actually occupied by the material of the balls, and the total surface area of the balls. Assuming, for simplicity, a rectangular parallelopiped of cross section and length equivalent to that of the column actually used in the present investigation, and taking cognizance of the extra free space occurring near the walls of the container, with the balls in the center being packed ideally so that each ball touches twelve others, the following relationships may be obtained:

$$N=V/(0.707D^3)-292/D^2 \tag{4}$$

[9] For an individual ball the surface area is proportional to the diameter squared, and the total number of balls is inversely proportional to the diameter cubed. The net result is that the surface area of the ball packing is inversely proportional to the diameter.

$$F=0.259V+153D \quad (5)$$

$$S=4.45V/D-918 \quad (6)$$

where $N$ is the total number of balls, $V$ is the volume of the container in cubic centimeters, $D$ is the diameter of each ball in centimeters, $F$ is the free or void space in cubic centimeters, and $S$ is the total surface area of the balls.

The substitution of the value of $S$ from eq 6 above and the value of $s$, the area of the inner walls of the rectifying tube (1130 cm$^2$), into the previously determined eq 1 yields the following equation for the number of theoretical plates in relation to the diameter of the balls in the given column, the equation being represented in figure 3 by the broken line:

$$n-1=8.3/D+1.6, \quad (7)$$

where $n$ is the number of theoretical plates and $D$ is the diameter in centimeters. For balls ranging in diameter from 0.2 to 0.4 cm, the "theoretically" derived eq 7 is in substantial accord with the analogous eq 3 derived from experimental data.

Other types of packings may show a similar relationship between the surface area of the packing with the number of theoretical plates. It may be concluded that the ideal packing is the one that gives a uniform distribution of free space in the column, with the maximum surface for separation compatible with the free space necessary for the desired through-put.

---

The authors express their gratitude to Prof. M. M. Haring of the Department of Chemistry at the University of Maryland, for his kind interest, aid, and criticism during the present investigation, and to F. D. Rossini, Director of the American Petroleum Institute Research Project 6, for his guidance in the work and for his suggestions in connection with the analyses and presentation of the data. The authors also acknowledge the helpful advice of J. D. White and F. W. Rose, Jr., and the experimental assistance of P. E. Schoonover, C. L. Miller, and F. W. Melpolder.

## VII. REFERENCES

[1] J. H. Bruun and S. T. Schicktanz, BS J. Research **1**, 851 (1931) RP379.
[2] E. Pahlavauni, Bul. soc. chim. Belg. **36**, 533 (1927).
[3] W. L. McCabe and E. W. Thiele, Ind. Eng. Chem. **17**, 605 (1925).
[4] Arthur Rose, Ind. Eng. Chem. **28**, 1210 (1936).
[5] C. O. Tongberg, S. Lawroski, and M. R. Fenske. Ind. Eng. Chem. **29**, 957 (1937).
[6] M. R. Fenske, C. O. Tongberg, and D. Quiggle. Ind. Eng. Chem. **26**, 1169 (1934).
[7] C. O. Tongberg, D. Quiggle, and M. R. Fenske. Ind. Eng. Chem. **26**, 1213 (1934).
[8] E. W. Washburn and J. W. Read. J. Am. Chem. Soc. **41**, 729 (1919).
[9] J. H. Bruun and W. B. M. Faulconer. Ind. Eng. Chem., Anal. Ed. **9**, 192 (1937).

WASHINGTON, September 11, 1937.